



This is to certify that the

dissertation entitled

THE CHARACTERIZATION OF NYLON OPEN-TUBULAR IMMOBILIZED ENZYME REACTORS INCORPORATED IN STOPPED-FLOW AND CONTINUOUS FLOW SYSTEMS

presented by

Robert Q. Thompson

has been accepted towards fulfillment of the requirements for

Ph.D. degree in Chemistry

Date __August 2, 1982



RETURNING MATERIALS:
Place in book drop to remove this checkout from your record. FINES will be charged if book is returned after the date stamped below.

THE CHARACTERIZATION OF NYLON OPEN-TUBULAR IMMOBILIZED ENZYME REACTORS INCORPORATED IN STOPPED-FLOW AND CONTINUOUS FLOW SYSTEMS

Ву

Robert Q. Thompson

A DISSERTATION

Submitted to
Michigan State University
in partial fulfillment of the requirements
for the degree of

DOCTOR OF PHILOSOPHY

Department of Chemistry

1982

ABSTRACT

THE CHARACTERIZATION OF NYLON OPEN-TUBULAR IMMOBILIZED ENZYME REACTORS INCORPORATED IN STOPPED-FLOW AND CONTINUOUS FLOW SYSTEMS

By

Robert Q. Thompson

Open-tubular immobilized enzyme reactors are becoming widely useful in the clinical laboratory for specific and sensitive substrate determinations. However, the dependence of apparent enzyme activity on reactor design and mass transport effects has not been well documented. Several open-tubular immobilized enzyme reactors, prepared from 0.1 cm i.d. O-alkylated nylon tubing, were incorporated into flow systems and characterized. The apparent activity of an immobilized glucose oxidase reactor, used in a miniature, 1.0 mm i.d., continuous flow system to determine glucose, was found to be independent of coiling diameter and ionic strength, but was affected by temperature, segmentation gas composition, and the amount of co-immobilized catalase. Sodium azide was found to inhibit catalase, thereby improving the assay sensitivity, and to

inhibit glucose oxidase at higher concentrations.

To investigate the influence of mass transport on immobilized enzyme kinetics, a novel stopped-flow instrument was developed. The enzyme reactor was employed as a photometric observation cell to allow direct and continuous monitoring of the enzyme reaction. The kinetics, as measured under static conditions, are simpler than in other flow systems because only molecular diffusion and/or coulombic forces contribute to mass transport. Kinetics constants for immobilized lactate dehydrogenase are shown to be influenced by radial diffusion in the stopped-flow instrument. The method is also applicable to clinical substrate determinations. Glucose, in the range of 1-10 mM, and lactate, in the range of 5-50 μ M, were determined by reaction-rate methods with the instrument.

A new enzyme reactor for use in flow-injection analysis was also developed. Glucose oxidase was immobilized on non-porous glass beads and the beads, 0.5 mm in diameter, were packed into a 0.8 mm i.d. Teflon tube. The resulting reactor was incorporated into a flow-injection manifold for the determination of glucose. Calibration curves were very linear over the range of 0.0-2.5 mM glucose, and at least 60 samples/hour could be processed.

То

Mom and Dad and Jan

and all my other teachers

ACKNOWLEDGMENTS

I would first like to thank Dr. Stanley R. Crouch for his helpful advice and help with this and other manuscripts. He also has good taste in baseball teams. Special thanks also go to Dr. Gerald Babcock for serving as my Second Reader, and Dr. Enke and Dr. Wood for being members of my Guidance Committee.

Charlie Patton deserves a lot of credit. The "Bubble King" taught me about continuous flow analysis and shared with me a lot of ideas. He was a friend and helpmate in the laboratory. Thanks Chas, I couldn't have done it without you.

Thanks also go to Frank Curran for his friendship in and out of the chemistry building (inspite of his poor taste in baseball teams), and Gene Ratzlaff for loaned equipment and the gift of helpful advice. All the Crouch group members who lent a helping hand deserve thanks.

The times of play were also very valuable. I thank all my basketball buddies, my golf partners-- Steve M., Steve B., and Pete, my tennis nemesis-- John Leckey, and my good friends-- Rich and Jane Farmer.

Several support people deserve hearty thanks: Tom
Atkinson for MULPLOT, Dick Menke and Deak Waters, and the
graphics artists-- Katherine, Bev, and Jo. Thank you.

Finally, I thank my wife, Jan, for everything else.

TABLE OF CONTENTS

INTRO	DUC	TION 1
CHAPT		l tion to Immobilized Enzymes
	Α.	Immobilized Enzyme Characteristics 3
	В.	The Uses of Immobilized Enzymes in Analytical Chemistry 6
CHAPT Chemi		2 Bonding of Glucose Oxidase to Nylon Tubing 14
	Α.	Nylon Activation
	В.	Addition of Spacer Molecules 25
	С.	Attachment of Glucose Oxidase 31
CHAPT Kinet		of Open-Tubular Reactors
	Α.	Kinetics Properties of Open-Tubular Reactors
		 Electrostatic and environmental effects
	В.	Experimental Considerations 51
	C.	The Determination of Michaelis Constants. 57
		 Introduction
		genase
	D.	Analytical Determinations 70
		1. Introduction

	3. 4. 5.	Enzyme immobilization	72 73
	6.	determination	73
	•	determination	77
Ε.	A N	ew Cell / Reactor Design	81
CHAPTER			
		Determination of Glucose Based on Glucose Oxidase	90
2	LECU	orucose onruuse	00
Α.	The	Method and Instrumentation	97
	1.	The glucose oxidase reaction	97
	2.	The Trinder/peroxidase reaction	98
	3. 4.	The continuous flow manifold The continuous flow instrument	99 105
	4.	The continuous flow instrument	105
В.	Expe	erimental Studies of the Trinder	
	Read	ction	107
С.	Read	ction Characteristics	114
	1.	Segmentation gas composition	114
	2.	The effect of ionic strength	
	3.	The specificity of glucose oxidase	
	4.	Mutarotation kinetics	121
D.	Read	ctor Design Characteristics	124
	1.	Coiling diameter	124
	2.	Coil temperature	
_			
Ε.		Characterization and Elimination of Effect of Catalase	197
	the	Effect of Catalase	141
	1.	The nature of the interference	127
	2.	The reagents and continuous flow	
	0	instrument	130
	3. 4.	Enzyme immobilization Effect of azide on aqueous peroxidase	131 131
	5.	Effect of azide on immobilized	131
	•	catalase	133
	6.	Effect of azide on immobilized	.
	7	glucose oxidase	137
	7.	preparations of glucose oxidase	140
	8.	A method to determine the presence	_ 10
		of catalase	141
	9.	Conclusions	143

Enzyme Immobiliza	tion on Non-porous Glass	147
	zation of Glucose Oxidase Tubing	148
B. Glucose	Oxidase Bead String Reactor	150
CHAPTER 6 Future Plans	• • • • • • • • • • • • • • • • • • • •	161
APPENDICES		
Appendix A.	Derivation of Diffusion-control Rate Equation	164
Appendix B.	Derivation of the Absorbance of a Solution with a Radial Concentration Gradient	165
LIST OF REFERENCES	S	166

LIST OF TABLES

Table 1.1. Recent Examples of Enzyme Electrodes	8
Table 1.2. Recent Examples of Open-Tubular Reactors	11
Table 1.3. Packed-Bed and Other Reactors	12
Table 2.1. The Results of the Spacer Molecule Studies	26
Table 2.2. The Activities of Nylon Tubular Reactors Resulting From the Incorporation of Various Spacer Molecules	29
Table 2.3. Immobilization Procedure	35
Table 2.4. Various Enzymes Bonded to Nylon Tubing and Their Approximate Half-lives	36
Table 3.1. Reviews of Immobilized Enzyme Kinetics	38
Table 3.2. Kinetics Values for Aqueous and Immobilized Lactate Dehydrogenase	68
Table 3.3. Results of Serum Assays for Glucose	76
Table 3.4. Results of Serum Assays for Lactate	80
Table 4.1. Chromogens for Reaction with Hydrogen Peroxide	95
Table 4.2. Specificity of Glucose	120

Table 4.3. Solutions Used to Prepare the Immobilized Enzyme Reactors	132
Table 4.4. Glucose Concentrations Found in Control Sera With and Without Added Azide	146
Table 5.1. Immobilization Procedure for Glass Beads	152

LIST OF FIGURES

Figure 1.1. Schematic of an instrument employing an open-tubular reactor	9
Figure 2.1. The immobilization scheme	15
Figure 2.2. Reactor activity versus TOTFB reaction time	20
Figure 2.3. Reactor activity versus reactor length for different TOTFB concentrations. The concentrations were 0.1 M (A), 0.05 M (B), 0.01 M (C), and 0.005 M (D)	22
Figure 2.4. The precision of the immobilization procedure	24
Figure 2.5. The storage stability of reactors prepared with different spacer molecules	27
Figure 2.6. Fluorescamine determination of 1,6-diaminohexane	30
Figure 2.7. The effect of initial glucose oxidase concentration on the reactor activity	33
Figure 3.1. Immobilized enzyme kinetics	39
Figure 3.2. Influence of slow mass transport on enzyme kinetics	45
Figure 3.3. Concentration gradients in an open-tubular reactor	47
Figure 3.4. Bolus flow pattern	50

Figure 3.5. Cross-sectional view of the GCA McPherson stopped-flow mixer/observa-	
tion cell unit. The outer aluminum housing	
(a), quartz windows (b), and the main KEL-F	
body (c) are press fit with three bolts.	
Mixing occurs at (e), where the two reagent	
flow streams meet at 90° to each other	
one stream is in the plane of the figure	
and the other is perpendicular to it.	
The immobilized enzyme reactor is placed	
inside the observation cell (d). The	
dashed arrow represents the light path	
inside the cell	55
Figure 3.6. Stopped-flow colorimeter	56
Figure 3.7. Typical progress curves ob-	
tained with the instrument. The dotted	
lines represent the initial reaction rates	
calculated from these curves. The reactions	
represented were of 2.00 mM lactate with	
0.425 mM (A), 0.850 mM (B), and 2.12 mM (C)	ca
β-NAD	63
Figure 3.8. Lineweaver-Burk plot of	
1/Rate versus 1/[Lactate] at four differ-	
ent β -NAD concentrations: 0.26mM (A),	
0.43 mM (B), 0.85 mM (C), and 2.12 mM	
(D)	64
Figure 3.9. Lineweaver-Burk plot of	
1/Rate versus 1/[β-NAD] at three differ-	
ent lactate concentrations: 0.80 mM (A),	
2.00 mM (B), and 4.00 mM (C)	65
Figure 3.10. Plot of y-intercepts from	
Figures 3.8 and 3.9 versus 1/[Substrate]	
for different β -NAD and lactate concen-	
trations. The y-intercept equals $1/V_m$, and the x-intercepts yield the two K_m	
values	67
Figure 2 11 Calibration curve for	
Figure 3.11. Calibration curve for glucose	75
glucose	13
Figure 3.12. Calibration curve for	
lactate	78

Figure 3.13. Design of the new cell/ reactor. Two pneumatically actuated pistons (A) were used to push the slider (B) back and forth between the fill posi- tion (P1) and the viewing position (P2). Quartz windows were used (C) to contain the solution in the viewing position	82
Figure 3.14. Reproducibility of cell positioning. Distilled water was pumped through the cell at 0.46 mL/min. Each trial represents movement of the cell from the viewing position to the fill position and back again	84
Figure 3.15. The results of five progress curve determinations with 0.44 mM glucose as the sample. The 1 mm i.d. reactor was used	86
Figure 3.16. Progress curves obtained with the 1 mm i.d. reactor. The glucose concentrations (mg/L) which were used are written at the end of each curve	87
Figure 3.17. Progress curves obtained with the 2 mm i.d. reactor. The glucose concentrations (mg/L) which were used are written at the end of each curve	88
Figure 4.1. The three forms of D-glucose	91
Figure 4.2. The reactions involved in the enzymatic assays for glucose	93
Figure 4.3. The continuous flow reaction manifold. The pump speed setting which gave nominal flow rates was 42	101
Figure 4.4. The pH dependence of the glucose assay. A 0.1 M phosphate buffer was used to control the pH. The dotted line indicates the approximate relationship in the absence of many data points	103
Figure 4.5. Diagram of the continuous flow instrument	

Figure 4.5. Progress curves for the reaction of hydrogen peroxide and the Trinder reagent. The peroxide concentrations were 50 μ M (A), 25 μ M (B), 10 μ M (C), 5 μ M (D)	9
Figure 4.7. The effect of ascorbate concentration on the assay sensitivity 11	.2
Figure 4.8. First order plots of data for the hydrogen peroxide-Trinder reaction in the presence of ascorbate. The ascorbate concentrations were 10 μ M (A), 20 μ M (B), 40 μ M (C). A was the absorbance at equilibrium, and A was the absorbance at any time, t	.3
Figure 4.9. Calibration curves for a series of glucose standards using three different segmentation gases: N ₂ , Air, O ₂	.6
Figure 4.10. The output from the continuous flow instrument using three different segmentation gases. The glucose concentrations were 0.44 mM, 1.44 mM, 2.22 mM, and 4.44 mM. Only the first three concentrations were sampled using 0_2	.7
Figure 4.11. The effect of ionic strength on the glucose oxidase reaction	.9
Figure 4.12 First order plot of data for the mutarotation of 4.44 mM β -D-glucose solution at 22°C. The results of two independent experiments are presented. [β] is the concentration of the β -form of D-glucose at any time, t, while [β] is the initial β -form concentration	:3
Figure 4.13. The effect of coiling diameter on the calibration slope (0) and wash ()	6

Figure 4.14. The dependence of the assay sensitivity on temperature	128
Figure 4.15. The effect of azide on the amount of hydrogen peroxide that was converted to product. A 79 µM H ₂ O ₂ solution was sampled without an enzyme reactor (□) and with a 30 cm catalase reactor (O) in the manifold	134
Figure 4.16. Lineweaver-Burk plot of the data which exhibited azide inhibition of immobilized catalase. The azide concentrations ranged from 0.0 (A) to 1.5 mM (B)	136
Figure 4.17. The effect of azide on three glucose oxidase reactors, type B (Δ), type C (0), and type D (\square), containing various amounts of catalase (refer to Table 4.3)	138
Figure 4.18. Dixon plot of data from Figure 4.17, curve B. Three glucose concentrations were used: 0.44 mM (1), 0.22 mM (2), and 0.11 mM (3)	139
Figure 4.19. The effect of azide on three commercial preparations of glucose oxidase, reactor types G, E, and F (refer to Table 4.3)	142
Figure 4.20. The change in calibration slope with different lengths of reactors B, C, and D (refer to Table 4.3). No azide was added	144
Figure 4.21. The change in calibration slope with different lengths of reactors B, C, and D (refer to Table 4.3). The reactions occurred in the presence of 0.8 mM azide	145
Figure 5.1. View of the immobilized enzyme single bead string reactor	153
Figure 5.2. Schematic diagram of the flow-injection instrument	155

Figure 5.3. The degree of incomplete mixing at various sample volumes. Four pump speeds were used: 8.3, 12.3, 25.0, and 33.3 µL/sec	157
and dotte par sections.	20.
Figure 5.4. Flow-injection instrument	
response. The four glucose concentra-	
tions were: 0.44 (A), 0.88 (B), 1.33	
(C), and 2.22 (D) mM	159
Figure 5.5. Calibration curve for the	
flow-injection determination of glucose	160

LIST OF SYMBOLS

```
AU - Absorbance units
A - initial absorbance (AU)
A_{\infty} - equilibrium absorbance (AU)
b - wash value (seconds)
c - ratio of mean ionic activity coefficients (unitless)
C - a constant (unitless)
d - reactor diameter (cm)
D - substrate diffusion coefficient (cm<sup>2</sup>/sec)
e - charge on the electron (coulombs)
[E] - total enzyme concentration (Molar)
h - mass transport rate constant (second<sup>-1</sup>)
H(ss) - height of CF peak at flat portion (AU)
H(t) - height of CF peak at any time, t (AU)
j_s - Bessel functions (unitless)
k - Boltzmann constant (joules {}^{\circ}K^{-1})
k_{e} - an enzyme rate constant (second<sup>-1</sup>)
K, - enzyme interaction constant (Molar)
K_{T} - enzyme inhibition constant (Molar)
K_{m} - Michaelis constant (Molar)
L - reactor length (cm)
N<sub>11</sub> - Nusselt number
[P]<sub>h</sub> - bulk product concentration (Molar)
\left[ \mathbf{P} \right]_{\mathbf{w}} - product concentration at the reactor wall (Molar)
r - reactor radius
[S]<sub>b</sub> - bulk substrate concentration (Molar)
[S]_w - substrate concentration at reactor wall (Molar)
t - time (seconds)
T - temperature (°K)
v - initial reaction rate (Molar second<sup>-1</sup>)
V - volume of a single liquid segment (cm<sup>3</sup>)
V_{m} - maximum rate of an enzyme reaction (Molar second<sup>-1</sup>)
```

- z electrovalency of the substrate (unitless)
- Z effective concentration of charges on the carrier (M)
- ε molar absorptivity (AU Molar $^{-1}$ cm $^{-1}$)
- ξ ratio of the mass transport rate constants times the ratio of Michaelis constants of the two substrates for the same enzyme (unitless)
- η liquid viscosity (poise)
- γ surface tension of a liquid (dyne cm⁻¹)
- ψ electrostatic potential between the carrier and the substrate (volts)
- σ diffusion layer thickness (centimeters)
- μ ratio of the enzyme rate constant (V $_m/K_m$) to the mass transport rate constant (h) (unitless)
- v -liquid flow rate (cm sec⁻¹)

INTRODUCTION

The concept of passing a reagent solution through an open tube to which an enzyme is attached has led to specific, sensitive, and fast determinations of clinically important compounds. The use of immobilized enzymes with continuous flow instruments is an important and growing area. This research is a part of the effort to improve such systems. The goals were to optimize the procedure for binding enzymes to nylon tubing and then to characterize the resulting reactors in terms of their physical and chemical properties.

Glucose oxidase was chosen as the major enzyme of study, because it is relatively inexpensive, highly active, and bonds well to nylon. Lactate dehydrogenase, catalase, and other enzymes were used in immobilized form to a lesser extent.

The enzyme activities were measured by incorporating the open-tubular reactors into a continuous flow or stopped-flow system. The continuous flow technique involves a flowing liquid stream in which the sample is injected, mixed with reagents, and detected. When gas bubbles are added to the liquid stream the technique is termed gassegmented, continuous flow analysis (CF) [1-3]. Without gas segments, the technique is called flow-injection analysis (FI) [4-6]. The major interest in this research

has been with CF systems. The stopped-flow (SF) technique [7-9] involves the rapid mixing of reagents and sample, followed by the rapid cessation of the flow. The reaction mixture is most often monitored by spectrophotometry. These flow techniques are not discussed in detail; only important points pertinent to this research are mentioned. Informative discussions can be found in the references given above.

After a brief introduction to immobilized enzymes (Chapter 1), the optimization of the nylon immobilization procedure is presented (Chapter 2). The kinetics properties of enzyme reactors are discussed in Chapter 3. A novel stopped-flow instrument is described which should help in learning more about the inherent properties of immobilized enzymes. In Chapter 4, a glucose oxidase reactor, incorporated into a CF manifold, is characterized. The influence of catalase impurities on the determination of glucose was studied. In Chapter 5, the possibility of replacing nylon with non-porous glass is explored, and finally, suggestions for future projects are given (Chapter 6).

This research project has provided several surprises and many interesting results. The work is mostly experimental and practical. Further work should provide a more mathematical description of the open-tubular immobilized enzyme reactors (OTIMERS).

CHAPTER 1

Introduction to Immobilized Enzymes

The interest and activity in the field of immobilized enzymes has been high for the past fifteen years. Hundreds of papers have appeared in the literature extolling the use of enzymes attached to an insoluble support. Many excellent reviews of the theory and practice of immobilized enzyme technology are available. At least nine books have been published in this area [10-18], with two of them appearing in 1980; several other books have chapters dealing with immobilized enzymes [19,20]. Furthermore, many reviews on the uses of immobilized enzymes have appeared in the scientific literature [21-25].

Since the research in this area has been well-documented, only the fundamental concepts are presented here. Section A introduces bound enzymes and the factors which may alter the properties of the enzyme. Section B reviews the uses of the immobilized enzymes in analytical chemistry and introduces the concept of open-tubular reactors in flow systems.

A. Immobilized Enzyme Characteristics

An enzyme is a protein which can catalyze one or a small set of reactions. Thus, the enzyme is specific and very sensitive toward a few compounds and is useful as an analytical probe. Confining an enzyme to an insoluble

support provides the further advantages of longer lifetime and easier manipulation. The enzyme reactor can be used again and again. Thus, immobilized enzymes lower the time and costs of employing biological catalysts.

The enzyme can be confined or attached to a carrier in four basic ways. (1) Adsorption [13] occurs to some extent in all immobilization procedures. This method includes attachment by coulombic attraction and other short range forces. The procedure is the mildest and results in the highest percentage of active bound enzyme. However, the bond is weak, and the enzyme is gradually lost from the carrier with use. This method is not frequently used for analytical applications.

- (2) Encapsulation is really an indirect method of immobilization. A solution or slurry containing the enzyme is simply contained inside a semipermeable membrane. The technique is widely used to prepare enzyme electrodes [22] (See Section B). Substrate molecules must diffuse through the membrane in order for the reaction to occur. Thus, the membrane barrier limits the size of molecules that can react and limits the rate at which the enzyme can function.
- (3) Entrapment occurs when a gel is made to polymerize in the presence of an enzyme [13]. The enzyme molecule is trapped inside the empty spaces of the gel. Similarly, a fiber stretched in a solution of enzyme will retain some of the enzyme in between the layers of fiber. Like

encapsulated enzymes, enzymes trapped in a matrix are limited by substrate transport.

(4) Covalent bonding of the enzyme to a carrier is the most widely used immobilization technique in analytical chemistry [12]. A chemical bond is formed between the carrier surface and the enzyme molecule. The reactor that results shows good temperature and time stability. The enzyme is not easily stripped from the carrier by a flowing liquid, so the technique is chosen in preparing open-tubular reactors. However, the percentage of active, bound enzyme is low. The reason for this is that no technique has yet been developed to single out a site on the enzyme for attachment. Thus, enzyme bound at the active site becomes inactive. Likewise, multiple bonds to the same enzyme molecule can change its tertiary structure, affecting its activity. Covalent bonding of enzymes is still rather empirical and not yet based on solid fundamental grounds.

An enzyme covalently bound to a carrier experiences much of the carrier environment in addition to that of the bulk solution. The hydrophilicity or hydrophobicity, charge, and chemical reactivity of the support all influence the enzyme properties. The substrate affinity for the carrier and the enzyme is also affected. The enzyme is not always in intimate contact with the substrate as it is in solution; thus, substrate transport from the bulk solution to the carrier surface influences the reaction rate. Changes in

pH optima and enzyme kinetics are discussed in more detail in Chapter 3. Thus, it is expected that the attached enzyme would display different properties from those of an enzyme in aqueous solution.

B. The Use of Immobilized Enzymes in Analytical Chemistry
Enzymes in aqueous solution have been used for
thousands of years to produce beer, cheese, and other
products. Similarly, industrial processes were among the
first to use immobilized enzymes. Several reviews of the
use of enzymes in industry have been written [26-29]. The
lower costs that result are making bound enzymes popular.

In analytical chemistry, enzymes have been transformed from aqueous reagents to integral parts of chemical instrumentation. The immobilized enzyme is usually a part of the transducer or manifold of the instrument. The chemist does not need to prepare enzyme solutions each day, but instead must maintain the activity of the enzyme. Storage of the enzyme at reduced temperature, in the dark, and immersed in a buffer at neutral pH is usually all that is required. The job of the chemist is simplified by using immobilized enzymes.

Immobilized enzyme instrumentation can be divided into three major areas: enzyme electrodes, open-tubular reactors, and miscellaneous methods. Enzyme electrodes are prepared by confining an enzyme solution or suspension to an area adjacent to the surface of an ion-selective electrode.

A semipermeable membrane, stretched over the enzyme layer and the electrode, separates the enzyme from the reagent solution. Substrate molecules diffuse into the catalytic layer, the reaction occurs, and the product concentration is sensed by the electrode. Potentiometric and amperometric sensing are the usual means of detection. Enzyme electrodes do not include systems in which the electrochemical detector is separated from and subsequent to the immobilized enzyme reaction. The general reviews mentioned previously and several specific reviews [30-32] show the wide use of enzyme electrodes. Recent reports, listed in Table 1.1, are further evidence of the importance of these methods.

Open-tubular reactors are even more widely used. A general schematic of a typical instrument is displayed in Figure 1.1. Open tubes allow low pressure pumping and preserve the integrity of the flow profile which are required in the analytical flow methods. Delivery of the reagents is usually performed by a peristaltic pump (CF and FI) or a pneumatically-driven syringe (SF). The mixed reagents are pushed into the reactor, where they are allowed to react for a short period of time. The reaction time is a compromise between sample throughput and acceptable instrumental response. The reaction products are usually measured by absorption spectroscopy, but can also be monitored electrochemically, thermometrically, or by luminescence spectroscopy.

Table 1.1. Recent Examples of Enzyme Electrodes

Enz	Enzyme(s)	Enzyme Matrix	<u>Analyte</u>	Detector	Ref.
+	 Alcohol dehydrogenase 	Aqueous solution	Ethanol	Amperometric	33
	2. Bienzyme- glucose oxidase hexokinase	Polyacrylamide gel	АТР	Amperometric	34
ဗိ	3. Alcohol dehydrogenase	Sepharose gel	Ethanol	Amperometric	35
4.	4. Amino acid oxidase	Covalent bond to graphite electrode	L-amino acids	Potentiometric	36
သ	5. Trienzyme- glucose oxidase peroxidase catalase	Gelatin	Bilirubin	Amperometric	37

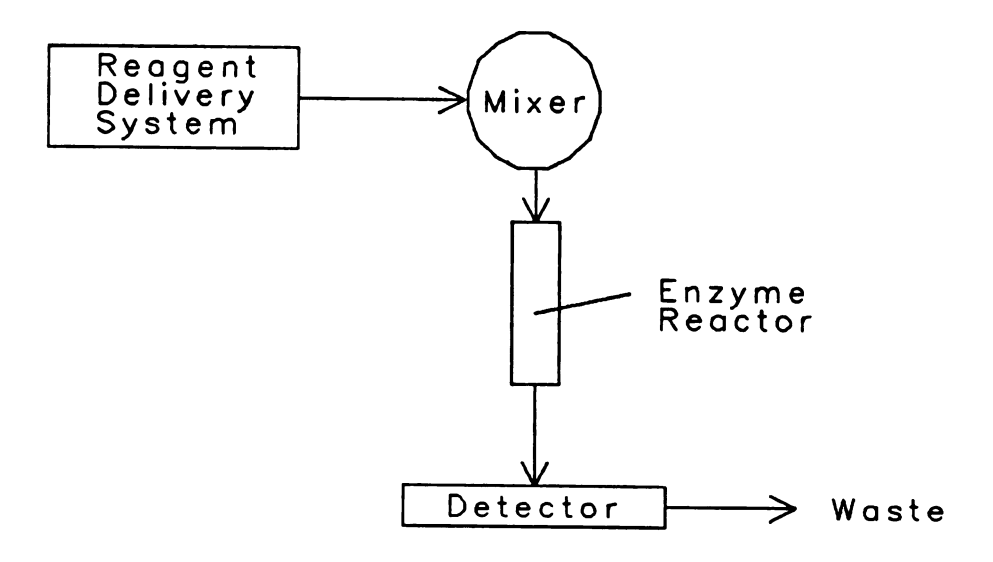


Figure 1.1. Schematic of an instrument employing an open-tubular reactor.

In most cases, nylon tubing has been used as the carrier. It is inert, sturdy, easily molded into a helix, and readily activated for subsequent enzyme immobilization. The only disadvantages are that it has a small surface area (few sites for enzyme attachment), and it tends to adsorb organic compounds, making sample carryover a problem. Despite these problems, no other carrier has replaced nylon for analytical use. Table 1.2 lists some of the more recent uses of nylon open-tubular reactors.

Several other analytical reactors have been reported in the literature. A few of these are listed in Table 1.3. The most common type is a packed bed reactor. The enzyme is covalently bound to porous glass beads, and the beads are packed into a tube. Thermometric detection is common with these systems. More unusual instrumentation includes a nylon tubular reactor connected to a pipette tip and a stirring bar coated with an enzyme.

Immobilized enzymes have been termed a "solution in search of a problem". Indeed, the potential usefulness of immobilized enzymes has not been reached. Only a few enzymes of high inherent activity have been used successfully. In order for more and better enzyme reactors to be developed, the following needs must be met. The carrier environment needs to be modified so that it is more conducive to enzyme attachment. Also, the chemist needs to be able to choose the site of attachment on the

Recent Examples of Open-Tubular Reactors Table 1.2.

Enzyme(s)	Activation	<u>Analyte</u>	Detector	Reference
1. Alcohol oxidase	Hydrolysis	Ethanol	Oxygen electrode	38
2. Bienzyme- uricase aldehyde dehyd	TOTFB alkylation 1.	Uric acid	UV absorbance	39
3. Creatininase		Creatinine	Ammonia electrode	40
4. Glycerol dehydrogenase	TOTFB alkylation	Triglyceride	UV absorbance	41
5. Glycerol dehydrogenase	TOTFB alkylation	Glycerol	UV absorbance	42

Table 1.3. Packed-Bed and Other Reactors

Carrier	Enzyme	<u>Detector</u>	Reference
1. Porous glass packed in a column	Urease Glucose oxidase cholesterol oxidase	Thermometric	43-45
2. Same as 1.	Urease	Coulometric	46
3. Same as 1.	Alcohol dehydrogenase Lactate dehydrogenase	e Amperometric e	47
4. Same as 1.	Nitrate reductase	Potentiometric	48
5. Stirring bar	Alcohol dehydrogenase	e Spectrophotometric	49
6. Nylon tube attached to a pipette tip	Urease	Spectrophotometric	20

enzyme. Furthermore, if diffusional limitations and electrostatic effects could be eliminated, the use of immobilized enzymes would be simpler since the large body of soluble enzyme data would be directly applicable.

CHAPTER 2

Chemical Bonding of Glucose Oxidase to Nylon Tubing

The goal of immobilization is to produce an enzyme reactor with the highest possible activity. This means that many sites on the carrier must be available for attachment, and that the enzyme must be bonded in its most active form. With nylon, four chemical steps are employed to produce the desired results, as shown in Figure 2.1. First, the inert, amide polymer is treated so that a reactive group is formed. Three different activators have been used, and these are discussed in Section A. Next, a bifunctional compound is added. This "spacer" molecule increases the distance between the nylon surface and the enzyme. Therefore, the enzyme experiences less of the carrier environment and more of the bulk solution properties. Diffusional and steric limitations are reduced to some extent by adding the spacer. In Section B, the use of diamines as spacers is described.

Third, enzyme attachment is accomplished, usually via free amino groups (lysine residues or N-terminus) or free carboxyl groups (aspartic acid, glutamic acid, or C-terminus). In most cases, bonding through amino groups yields higher activities than bonding to other sites. This may be due to participation of carboxyl groups in the active site. Thus, glutaraldehyde is often used to link the amine group

Step 1:
$$(C - N)_x + (C_2 H_5)_3 O^+ BF_4^- + (C = N)_x + BF_4^- + (C_2 H_5)_2 O$$

NYLON

Step 2: $OC_2 H_5 + H_2 N - (CH_2)_n - NH_2 + (NYLON) + C_2 H_5 OH$

Step 3: $(SPACER) + HC - (CH_2)_3 - C - H + (NYLON) + (NYLON) + HOH$

Step 4: $(SPACER) + HC - (CH_2)_3 - C - H + (NYLON) + HOH$

Step 4: $(SPACER) + HC - (CH_2)_3 - C - H + (NYLON) + HOH$

Step 4: $(SPACER) + HC - (CH_2)_3 - C - H + H_2 N - ENZYME + HOH$

Step 4: $(SPACER) + H_2 N - ENZYME + HOH$

GLUTARALDEHYDE)

Figure 2.1. The immobilization scheme.

on the spacer molecule and the enzyme. Such procedures are examined in Section C. Since glucose oxidase and other enzymes are glycoproteins, Zaborsky and Ogletree [51] have suggested that attachment can be performed via the carbohydrate residues. This method may prevent loss of activity due to bonding at the active site. Another suggestion for improving the activity of the reactor is to bond the enzyme in the presence of its substrate or a reversible inhibitor. Again the active site should be protected from chemical bonding. In spite of their theoretical merits, these latter two methods have not gained wide acceptance.

The immobilization of glucose oxidase is examined here. Activity measurements were made by incorporating the reactor in a continuous flow manifold and monitoring the amount of product formed. Glucose standards were reacted with the enzyme and a calibration curve was prepared. The slope of the calibration curve was used as the measure of reactor activity. Details of the instrumental method are given in Chapter 4.

A. Nylon Activation

A few years ago, hydrolysis of the amide linkage of nylon was the major means of activation [52]. Free amine groups were produced for subsequent bonding. First, a calcium chloride solution was pushed through the tubing to remove amorphous nylon and to etch the inner wall. Then a dilute (about 4 M) solution of HCl was allowed to react

in the tube at 45 °C for 40 minutes. Washing with water prepared the tube for subsequent reactions. The advantages of this method were that a carrier surface free of charges was prepared and the surface was well pitted to increase the number of attachment sites. The major disadvantage was that conditions had to be carefully controlled in order to prevent the loss of tube wall strength. If the reaction times were too long or acid concentrations too high, holes could form in the tubing. The procedure required the use of strong acids and was messy. The tubing often became clogged with nylon particles, released by the hydrolysis treatment. In conclusion, this procedure was expensive in terms of time and materials.

In 1975, Morris, et.al. [53] first described the activation of nylon by O-alkylation. Two compounds, dimethylsulfate (DMS) and triethyloxonium tetrafluoroborate (TOTFB), were introduced as reagents that formed secondary imidate groups with the amide groups on nylon. The resulting structure was very reactive toward amines. Thus, spacer molecules were easily added to the nylon.

The procedure employing dimethylsulfate has several severe disadvantages. First, the reagent gives off poisonous vapors and causes burns; it must be used in undiluted form. Second, the reaction must be carried out at 100 °C. Third, the amount of enzyme immobilized with this reagent is small. Despite these disadvantages, this method of

activation is still widely used.

The advantage of the TOTFB method is its simplicity.

The reagent is commercially available (Aldrich Chemical Co.), and although it should be stored under nitrogen, it can be used safely in the laboratory atmosphere. The diluted reagent is perfused through the nylon tubing for several minutes at room temperature, and then the tube is washed with cold methanol and water. Clogging is rarely a problem. Excess TOTFB can be neutralized with water, which yields ethanol and other harmless products. The procedure does impart to the nylon a positive charge, which may affect the enzyme properties. Also, only a small surface area is produced due to the mild conditions. Nevertheless, this is the method of choice in many cases, because it preserves the integrity of the tubing and the number of active sites is adequate to produce analytically useful reactors.

The complete immobilization scheme is shown in Figure 2.1. The first two steps are of concern here. A 0.1 M solution of TOTFB in methylene chloride is usually employed. The amide is converted to an imidate, with the concomitant development of a positive charge on the amide nitrogen. The amide bond is not broken, however, and this preserves the nylon structure. The reaction of an amine group with the activated nylon (step 2) is rapid, and a C-N bond is formed between the amide carbon atom and a free amine nitrogen on the spacer molecule.

The amidine formation from the nylon backbone has been examined closely by Sundaram [54]. He determined that the stability of the C-N bond is rather poor. Exchange with proteins as well as small nucleophiles occurs readily.

Also, attempts to improve the stability of the bond by reduction of the C=N amide bond and concomitant removal of the positive charge with sodium borohydride was unsuccessful. Thus, nylon reactors prepared in the above fashion should not be used as extracorporeal shunts in clinical applications. The slow loss of enzyme from such reactors could be due to the lability of the amidine bond. The lifetime of most reactors, nevertheless, is long.

A study of the TOTFB reaction with nylon was performed with the help of an undergraduate, Michael A. Schneider.

We studied the precision of the method as well as the effects of reaction time and reagent concentration on the resulting activity. The reactors were prepared in identical fashion in steps two, three, and four, but the treatment in step 1 was varied. The volume of TOTFB solution used was 10 mL, and the treatment was performed at room temperature. The nylon tubing (Type '6', 1 mm i.d., Portex Ltd., Hythe, Kent, U.K.) was all taken from the same lot.

Using a 0.06 M solution of TOTFB in dichloromethane, the reaction time was varied from five minutes to thirteen minutes. Figure 2.2 shows the effect of reaction time on the activity of 25 cm reactors. No trend was apparent,

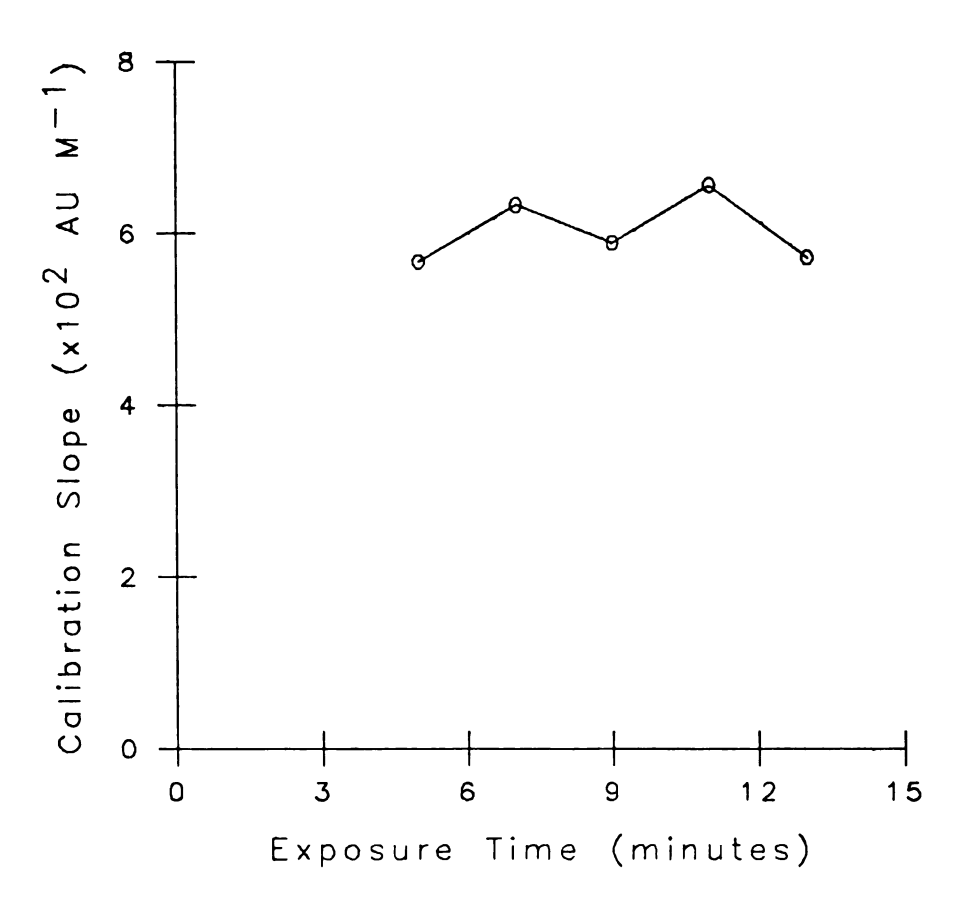


Figure 2.2. Reactor activity versus TOTFB reaction time.

and the treatments for five and thirteen minutes yielded the same activities. Since the total amount of TOTFB was constant, it appears that the reaction occurred rapidly and was limited by either the amount of TOTFB or the number of sites on the nylon. With a 0.06 M solution, the duration of the treatment was not critical. The use of the shortest possible reaction time, about five minutes, is desirable.

In the next study, the optimum concentration of TOTFB was determined. Coiled, 100 cm lengths of nylon tubing were treated for 5 minutes with TOTFB solutions in the concentration range, 0.005 M - 0.1 M. The tubing was then cut into four 25 cm segments, and each coil was assayed with the continuous flow instrument. Figure 2.3 displays the results. The x-axis represents the distance along the nylon tube with zero being the end in which the TOTFB solution entered and 100 representing the exit end. Each curve contains four data points, representing the four segments of tubing. The first segment's data are plotted at 12.5 cm, the second's at 37.5 cm, and so on, displaying the mean activity over that 25 cm of reactor.

For the lowest concentration, Figure 2.3 shows that almost all of the TOTFB was reacted with the first 50 cm of nylon; the TOTFB was the limiting reagent. With a concentration of 0.01 M, the TOTFB reacted beyond 75 cm, while the 0.05 M solution provided similar numbers of active sites along the entire length of tubing. Thus, with reactors up

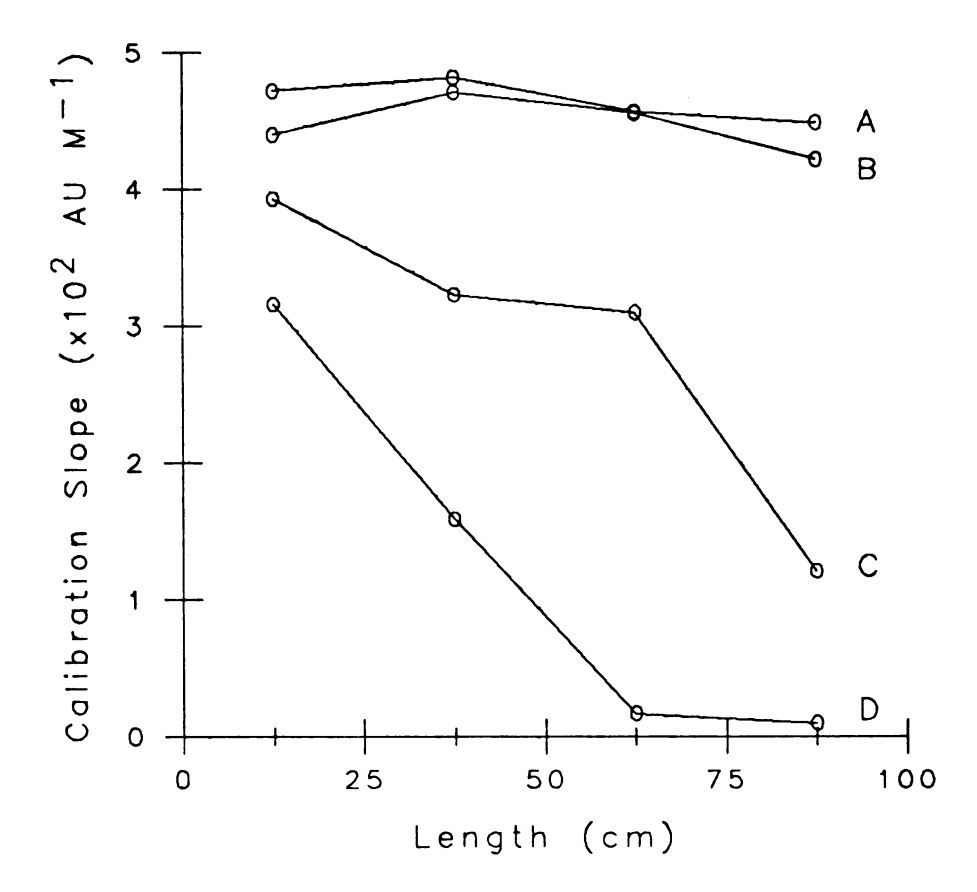


Figure 2.3. Reactor activity versus reactor length for different TOTFB concentrations. The concentrations were 0.1 M (A), 0.05 M (B), 0.01 M (C), and 0.005 M (D).

to one meter in length, the TOTFB concentration should be at least 0.05 M. An increase to 0.1 M did not improve the final reactor activity very much. This could have resulted from nylon becoming the limiting reagent. A second explanation is that more reactive sites were developed on the nylon, but the enzyme bonding in active form was limited by steric or other factors. Since lengths longer than 100 cm were often used in our studies, a concentration of 0.1 M was chosen. This required that the reaction time be limited to 3-4 minutes to prevent clogging of the tube. Likewise, it is recommended that the nylon tubing be kept under 1.5 meters in length. With higher concentrations of TOTFB, one end will be over-reacted and clog, while the other end of the tubing will not be activated enough.

Using a concentration of 0.1 M and a reaction time of three minutes, the precision of the method was tested. Again, a 100 cm length of tubing was treated, cut into 25 cm segments, and tested. The results of two independent experiments are shown in Figure 2.4. The variation in activity along the reactor length was found to be 2.9% and 4.8% (relative standard deviation). The variation between immobilization experiments was 6.4%. Similar results are also shown in Figure 2.3 for the highest two concentrations of TOTFB. Thus, the precision of the step 1 procedure is good. Another interesting fact was that for the experiments mentioned above, the second 25 cm segment always showed the

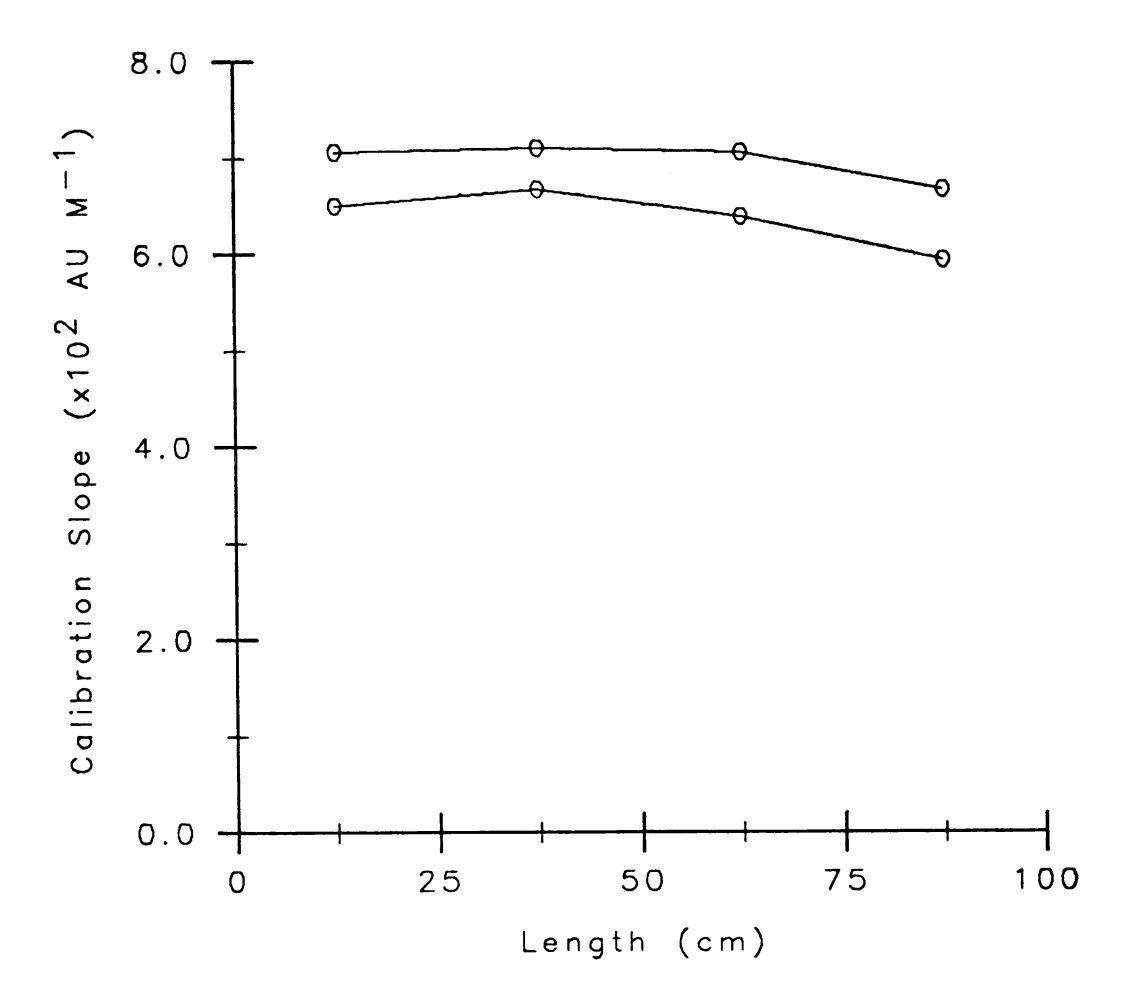


Figure 2.4. The precision of the immobilization procedure.

highest activity. The reason for this peculiar trait is not known.

B. Addition of Spacer Molecules

Several diamines of the formula, $H_2N-(CH_2)_N-NH_2$, were tested as spacer molecules. A diamine concentration of 0.1 M in a sodium bicarbonate buffer (0.1 M, pH 9.4) was used in all experiments. The effects of amine concentration and solution pH on the reactor activity were not examined. After activation of the nylon, the tubing was cut into 25 cm segments and filled with the appropriate diamine. After reaction for 4-5 hours at room temperature, the tubes were treated identically during the remainder of the immobilization. Thus, differences in activity should be due to differences in the spacer molecule only. The spacers are abbreviated S-N, where N is the number of carbon atoms in the molecule.

Three studies were performed, and the results of the first two are listed in Table 2.1. Bonding of the enzyme directly to the activated nylon gave relatively low activities. Ethylenediamine and 1,8-diaminooctane yielded the best reactors. Study 3, however, gave different results as shown in Figure 2.5. The S-O reactor had a much higher activity than the S-2 reactor, in contrast to the previous studies. The S-4 reactor showed the best properties. Though all the reactors lost enzyme activity during storage, the S-4 tube had the highest stability. Thus, 1,4-diaminobutane

Table 2.1. The Results of the Spacer Molecule Studies

Spacer	Calibration Slope (100 AU M ⁻¹)	Relative Activity	
Study #1			
S-0	0.54	0.09	
S-2	6.05	1.00	
S-6	5.79	0.96	
Study #2			
S-0	0.27	0.27	
S-2	1.01	1.00	
S-6	0.72	0.71	
S-8	1.86	1.84	

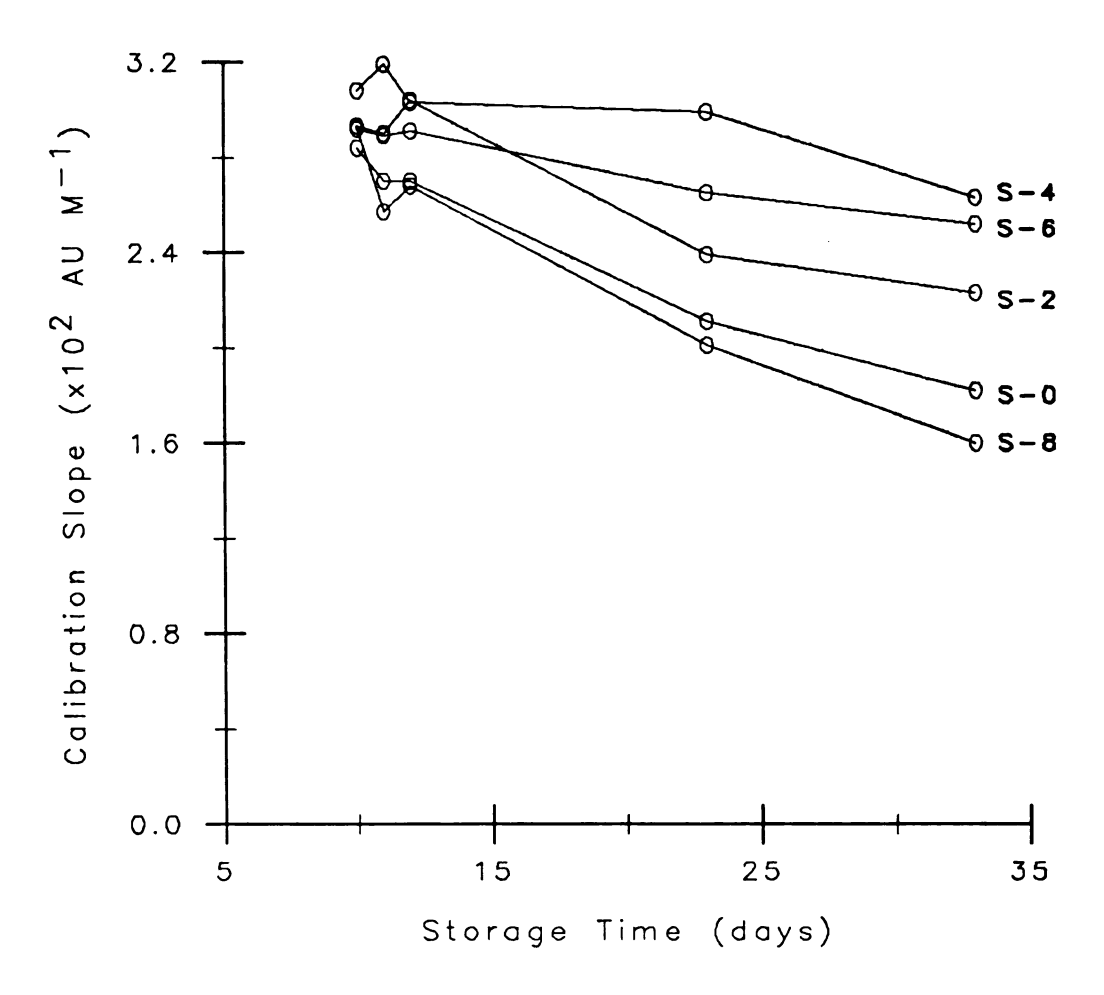


Figure 2.5. The storage stability of reactors prepared with different spacer molecules.

was used in all subsequent studies.

The very inconsistent results shown here are not atypical. Table 2.2 shows some of the spacer molecule experiments which have been described in the literature. Various spacers have been used, including aminated starch and pectin, polyethyleneimine (PEI), diamines, and lysine. When more than one spacer was used, the spacers are ranked (1=highest) according to the activities that they produced. One can see many inconsistencies, possibly due to the use of different enzymes. Only a rough estimate of the best spacer molecule can be ascertained from the current data.

An attempt to calculate the amount of amine bound to nylon was made. The diamine was determined by reaction with fluorescamine [61] and measurement of the product absorbance at 390 nm. The fluorescamine, 15 mg per 50 mL of acetone, was mixed with an equal volume of diamine in pH 8 phosphate buffer in a stopped-flow instrument. The reaction rate over the first 0.5 second was directly proportional to the diamine concentration. A calibration curve for 1,6-diaminohexane is shown in Figure 2.6. The other diamines also gave linear plots with similar (±10%) slopes.

The amount of diamine used in the immobilization and the amount washed form the tubing after the reaction were determined. The difference between these two values should be the amount bonded to the tubing. However, because of imprecision in the method, no significant differences were

Table 2.2. The Activities of Nylon Tubular Reactors Resulting From the Incorporation of Various Spacer Molecules

Step 1 Reagent	Enzyme	<u>S-2</u>	<u>S-6</u>	PEI	<u>Lysine</u>	Ref.
DMS	NAD kinase		2	1		55
TOTFB	Creatininase			1		56
DMS	Invertase	1	2	4	3	57
TOTFB	Lactate dehydrogenase	1				58
DMS	Urease		2		1	59
DMS	Glucose oxidase		1	3	2	60
TOTFB	Glycerol dehydrogenase			1		41

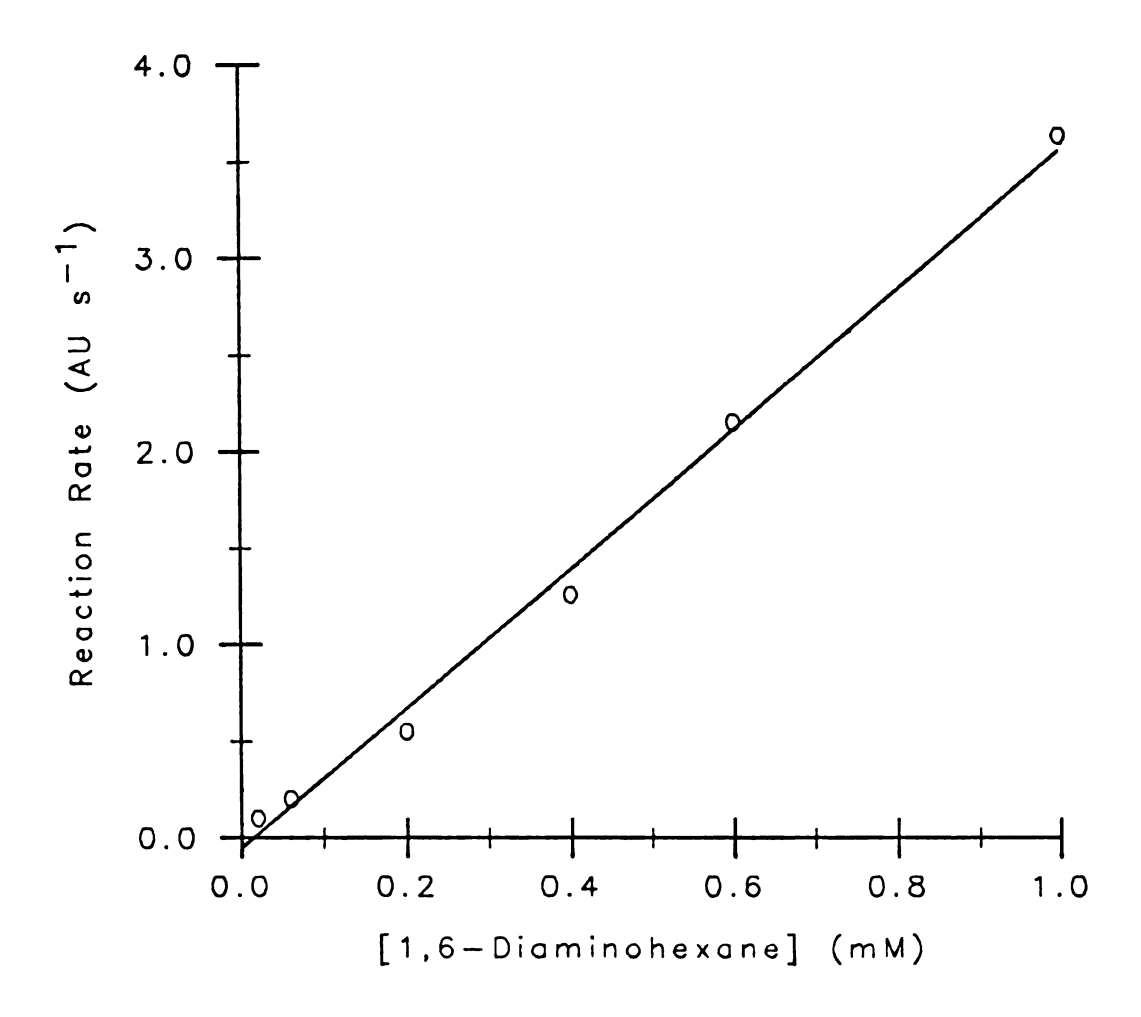


Figure 2.6. Fluorescamine determination of 1,6-diaminohexane.

found. Thus, the amount of amine bound to the tubing was not determined. Perhaps a direct method in which the bonded diamine was stripped from the tube and measured by fluorescence would have been better.

C. Attachment of Glucose Oxidase

In order to bond the enzyme through a free amine group, glutaraldehyde was reacted first with the spacer molecule. A Schiff's base formed, and a reactive carbonyl group was established on the carrier. Most researchers have employed a dilute solution of the glutaraldehyde in a basic medium. Our procedure was to fill the nylon tube with a 5% w/v solution of glutaraldehyde in pH 8.0 phosphate buffer (0.1 M) for about 1.5 hours at room temperature. The parameters involved in this immobilization step were not investigated.

Free amine groups on the enzyme were coupled to the glutaraldehyde through a second Schiff's base reaction. The coupling was performed at the optimal pH for enzyme activity, so that the enzyme was bonded in its most active form. Also, the reaction occurred at 4 °C to prevent loss of the enzyme activity in solution. The duration of the reaction was 18 hours to allow the bonding to go to completion.

The concentration of the glucose oxidase solution used in step 4 of the immobilization procedure was varied to discover the effect on the resulting reactor activity. An undergraduate, Brenda Kaufmann, performed these studies.

With the conditions of the first three steps held constant, different solutions of glucose oxidase were added to 30 cm segments of the same tubing and reacted for 18 hours. Subsequently, the reactors were incorporated into the CF manifold and their activities (calibration curve slopes) were determined. The results are presented in Figure 2.7.

The attachment sites on the nylon were not saturated until the glucose oxidase concentration exceeded 4 mg/mL. A nearly linear relationship between activity and added glucose oxidase was found at lower concentrations. The non-zero intercept may not be significant in light of experimental errors. Further experiments need to be done to confirm these results. One conclusion that can be drawn, however, is that a 5 mg/mL solution is optimal. This ensures the highest activity with the least amount of enzyme. The value was also used in work with other enzymes, though the optimal concentration may change.

The amount of glucose oxidase bonded to the nylon was not successfully determined. Difference methods were used in which the amount of protein added to the reactor and the amount washed from the tube after the reaction were determined. The difference in the two values should be the amount bonded. First, the biuret method [62] for proteins was employed. No significant difference between the two solutions was found. Next, UV absorbance at 280 nm was monitored. Aromatic amino acid residues absorb strongly

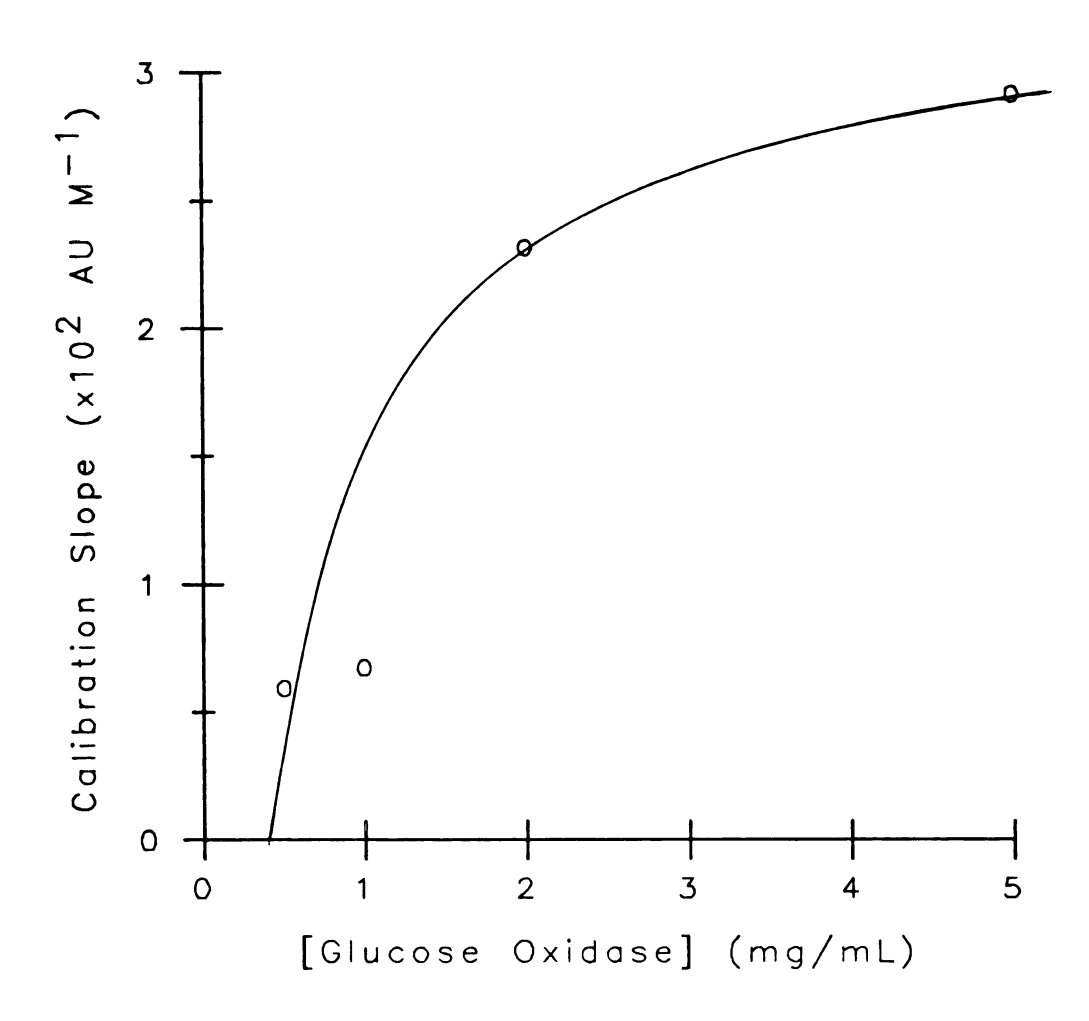


Figure 2.7. The effect of initial glucose oxidase concentration on the reactor activity.

at that wavelength [63]. Very linear calibration curves were obtained, but the method frequently gave negative results. Finally, the ability of glucose oxidase to catalyze the oxidation of glucose was utilized. A linear relationship between enzyme concentration and initial reaction rate was established. Positive results for the amount of enzyme bonded were obtained, but the precision of the method was poor. No definitive results were found. In the future, direct methods should be attempted. The completed reactor could be cut into pieces and treated with dilute HCl at high temperatures to strip the enzyme from the tube and to cleave the protein into amino acids. Then the amount of aromatic amino acids could be measured by UV absorbance.

The immobilization procedure selected for this work is listed in Table 2.3. The reactors were washed with distilled, deionized water between all steps. Cold methanol was used to wash unreacted triethyloxonium tetrafluoroborate from the tubes after step 1. Many enzymes can be immobilized using this method. Table 2.4 lists the enzymes with which we have experimented and gives their approximate half-lives, when the activity drops to 50% of the activity on day one. The TOTFB procedure for the covalent attachment of enzymes to nylon tubing is versatile and easy to perform.

Table 2.3. Immobilization Procedure

Step	Reagent	Duration	Temp (°C)
1	0.1 M TOTFB in $\mathrm{CH_2Cl}_2$	3 min.	22
2	0.1 M Diaminobutane in pH 9.4 HCO ₃ Buffer	4.5 hr.	22
3	5% w/v Glutaraldehyde in pH 8.0 HPO3 ²⁻ Buffer	1.5 hr.	22
4	Enzyme in pH 6.85 Phosphate Buffer	18 hr.	4

Table 2.4. Various Enzymes Bonded to Nylon Tubing and Their Approximate Half-lives

- Half-life -

Enzyme		E.C. Number	<u>Days</u>	Weeks	Months	?
Alcohol dehydrog	enase	1.1.1.1	x			
Peroxidase		1.11.1.7	X			
Carbonic anhydra	se	4.2.1.1		X		
Catalase		1.11.1.6		x		
Glutamate dehydr	ogenase	1.4.1.2		x		
Lactate dehydrog	enase	1.1.1.27		X		
Glucose oxidase		1.1.3.4			X	
Amino acid oxida	se	1.4.3.2				X
Malate dehydroge	nase	1.1.1.38				X

CHAPTER 3

Kinetics of Open-Tubular Reactors

The study of the kinetics properties of immobilized enzymes is important because these properties are often very different from those of enzymes in aqueous solution. While several compilations of soluble enzyme properties are available [64-66], relatively little is known about the kinetics of immobilized enzymes. Most of the current information can be found in the references listed in Table 3.1 and in many general reviews of immobilized enzymes.

The reason for the lack of data is that immobilized enzyme properties depend on reactor design and the type of immobilization used. Figure 3.1 shows the factors that can change the properties of an enzyme when attached to a carrier. Environmental and electrostatic effects vary according to the chemical nature of the carrier and the linkage to the enzyme. Similarly, the physical structure of the carrier determines whether internal and/or external mass transport will be present and the extent that mass transport influences the overall reaction rate. External mass transport is the transfer of material from the bulk solution to the enzyme environment, while internal mass transport concerns the movement in the enzymic matrix, such as a gel layer, membrane, or fiber. The kinetics constants of immobilized enzymes are defined in terms of the

Table 3.1. Reviews of Immobilized Enzyme Kinetics

- 1. K.J. Laidler and P.S. Bunting, Meth. Enzymol. <u>64</u>, 227 (1980).
- 2. J.-M. Engasser and C. Horvath, Applied Biochemistry and Bioengineering, Volume 1, Academic Press, NY (1976), pp 127-220.
- 3. G.P. Royer, <u>Immobilized Enzymes</u>, <u>Antigens</u>, <u>Antibodies</u>, <u>and Peptides</u>, <u>Marcel Dekker</u>, <u>Inc.</u>, NY (1975), pp 49-91.
- 4. W.R. Vieth and K. Venkatasubramanian, Chem. Technol. (1974), 303.
- 5. T. Kobayashi and K.J. Laidler, Biotech. Bioeng. 16, 99 (1974).
- 6. K.J. Laidler and P.S. Bunting, <u>The Chemical Kinetics</u> of Enzyme Action, Clarendon Press, Oxford, England (1973), pp 383-412.
- 7. C. Horvath and B.A. Solomon, Biotech. Bioeng. 14, 885 (1973).
- 8. G.J.H. Melrose, Rev. Pure Appl. Chem. 21, 83 (1971).
- 9. R. Goldman, L. Goldstein, and E. Katchalski, <u>Biochemical</u>
 <u>Aspects of Reactions on Solid Supports</u>, Academic Press,
 NY (1971), pp 1-78.
- 10. P.V. Sundaram and K.J. Laidler, <u>Chemistry of the Cell Interface</u>, Part A, Academic Press, NY (1971), <u>Chapter V.</u>

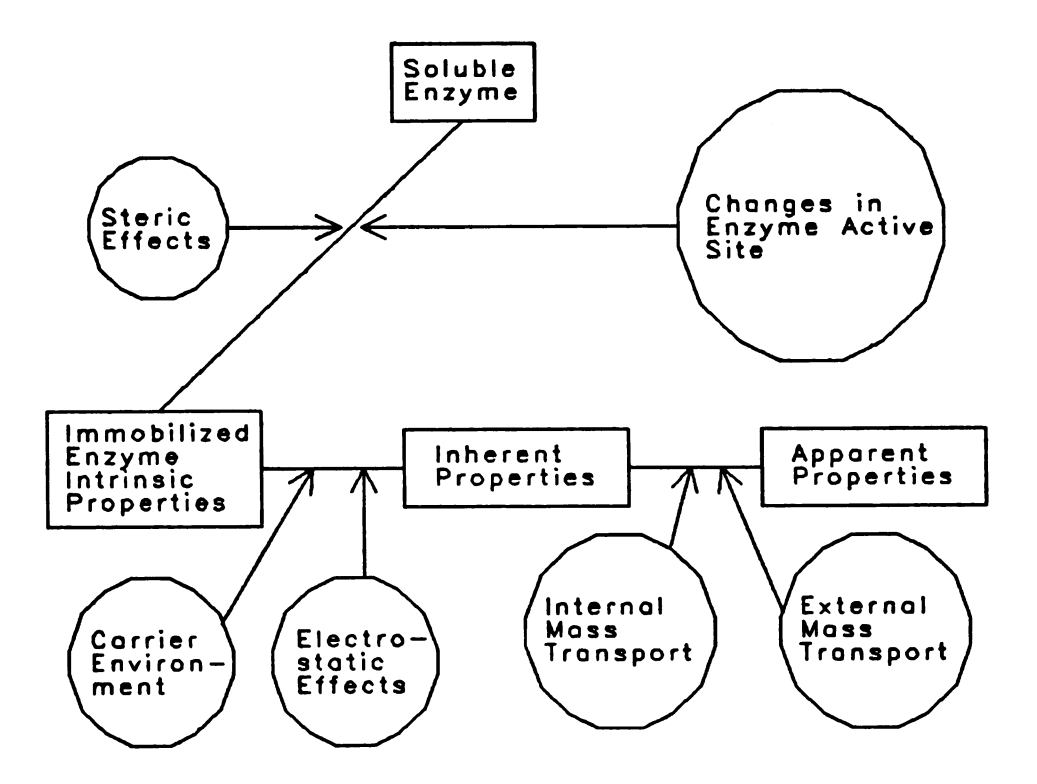


Figure 3.1. Immobilized enzyme kinetics.

conditions under which they were determined. Thus, there are three different Michaelis constants -- K_m (intrinsic), K_m (inherent) which accounts for electrostatic and environmental effects, and K_m (apparent) which also accounts for slow mass transfer.

The aim of much of the research on immobilized enzyme kinetics is to decouple transport effects from enzyme kinetics in the overall reaction rate. In other words, it is important to know the properties inherent to the immobilized enzyme in order to design the carriers and immobilization procedures better. The inherent properties are often masked by slow mass transport, and only the apparent enzyme kinetics are measurable. A new instrument has been developed which should allow the inherent properties to be seen indirectly. Testing of this instrument is the focus of this chapter.

Because fine reviews on immobilized enzyme kinetics are available, Section A serves only to review the major theoretical findings of researchers in the field. The kinetic processes which occur inside open-tubular immobilized enzyme reactors (OTIMER) integrated in three different flow systems are explained in more detail. Section B describes the experimental requirements in monitoring the kinetics of immobilized enzymes in open tubes and presents our novel method. The design of the stopped-flow instrument is detailed. Experimental results show that the

instrument is valuable in determining Michaelis constant (K_m) values (Section C), in performing clinical determinations (Section D), and for investigating more fundamental kinetics properties (Section E). Section E also describes an improved design for the instrument.

- A. Kinetics Properties of Open-Tubular Reactors
- 1. Electrostatic and environmental effects

The enzyme reaction rate for a single substrate reaction that obeys Michaelis-Menten kinetics is given in equation 3.1.

$$v = (k_e[E]_o[S]_w)/(K_m(intrinsic) + [S]_w)$$
 (3.1)

The rate, v, depends on an enzyme rate constant, k_e , the enzyme concentration, $[E]_o$, the substrate concentration at the reactor wall, $[S]_w$, and the intrinsic Michaelis constant, K_m . Differences in the immobilized enzyme rate from that of the enzyme in aqueous solution are usually shown by modifying the K_m term in equation 3.1. This is sensible since the Michaelis constant indicates the degree of enzyme affinity for a substrate, and electrostatic and other environmental effects can change this affinity.

If both the carrier and substrate are charged, then the affinity of the substrate toward the enzyme will be altered. Equation 3.2 shows the change which occurs [67].

$$K_{m}(inherent) = K_{m}(intrinsic)exp(-ze\psi/kT)$$
 (3.2)

In equation 3.2, z is the electrovalency of the substrate, e is the charge on the electron, ψ is the electrostatic potential between the carrier and substrate (if the carrier and substrate are of like charge, then ψ is negative), k is the Boltzmann constant, and T is temperature in °K. If like charges are present, the Michaelis constant is larger than the intrinsic value, while the opposite is true if unlike charges are present. Wharton, et.al. considered the effect of ionic strength on the K_m value and derived the following equation [68].

$$K_{m}(inherent) = K_{m}(intrinsic)(2cI)/(Z+2I)$$
 (3.3)

The term, I, is the ionic strength, Z is the effective concentration of fixed charges on the support, and c is the ratio of the mean ionic activity coefficients for the carrier and the bulk solution.

Electrostatics also change the pH optima and substrate migration rates in carriers which have a surface charge.

The pH optimum changes according to the following mathematical description [67].

$$pH(inherent) = pH(intrinsic) + 0.43e\psi/kT$$
 (3.4)

The substrates are attracted to the reactor wall if the carrier is of opposite charge and repelled if of like charge. This effect on the substrate transport can be described again by modifying the Michaelis constant term [69].

$$K_{m}(inherent)=K_{m}(intrinsic)/(1-\sigma zeC(grad \psi)/kT)$$
 (3.5)

Here σ is the diffusion layer thickness, C is a constant, and the other variables are defined above. In summary, many factors can change the intrinsic kinetics properties of an immobilized enzyme. The resulting properties are termed the inherent properties.

2. Mass transport effects

Inside an OTIMER, the chemical reaction occurs at the tube wall, catalyzed by the attached enzyme. Simultaneously, the substrate molecules migrate under the influence of a radial concentration gradient or convection from the bulk solution to the reactor wall. The enzyme reaction rate is given in equation 3.1, and the mass transport rate is described below [70].

$$v = h([S]_b - [S]_w)$$
 (3.6)

The reaction rate, v, is influenced by the mass transport rate constant, h, the bulk substrate concentration, [S]_b, and the substrate concentration at the reactor wall. These two rate processes contribute to the overall reactor performance. In most cases, both processes influence the reaction rate, although at the extremes of enzyme and/or substrate concentration one process may dominate.

At steady-state, when $d[S]_w/dt = 0$, the rates of the enzyme reaction (eqn. 3.1) and mass transport (eqn. 3.6) are equal. If the two equations are set equal to each

other, the equations are solved for $[S]_w$, and then $[S]_w$ is substituted into the reaction rate equation (3.1), the following equation results.

$$\frac{v}{k_{e}[E]_{o}} = \frac{\left[S\right]_{b}/K_{m} - (1+\mu) + ((1+\mu)^{2} + 2\left[S\right]_{b}(1-\mu)/K_{m} + (\left[S\right]_{b}/K_{m})^{2})}{1+\left[S\right]_{b}/K_{m} - \mu + ((1+\mu)^{2} + 2\left[S\right]_{b}(1-\mu)/K_{m} + (\left[S\right]_{b}/K_{m})^{2})} \frac{1/2}{172}$$

The above equation is equation 3.7. The term, K_m is the inherent Michaelis constant for the enzyme, and μ is equal to $k_e[E]_O/K_m(\text{inherent})(h)$, the ratio of the enzyme rate constant to the mass transport rate constant. The effect of slow mass transport on the apparent Michaelis constant can be seen in Figure 3.2. The plots were produced by substituting different values for $[S]_b/K_m(\text{inherent})$ and μ into equation 3.7. The value of K_m is increased over the inherent value as described in the equation shown below [71].

$$K_m(apparent) = K_m(inherent)(1 + 0.5\mu)$$
 (3.8)

As mass transfer limitations become larger (μ increases), the analytical range for substrate determinations widens. Thus, the ideal conditions for analytical methods are high enzyme activity and substrate transport control of the reaction rate inside the OTIMER.

With two substrate reactions, mass transport has a very interesting effect on the two ${\rm K_m}({\rm inherent})$ values. If the inherent affinity of the enzyme toward the two substrates is very different, then substrate transfer tends to raise the ${\rm K_m}$ of the higher affinity substrate while

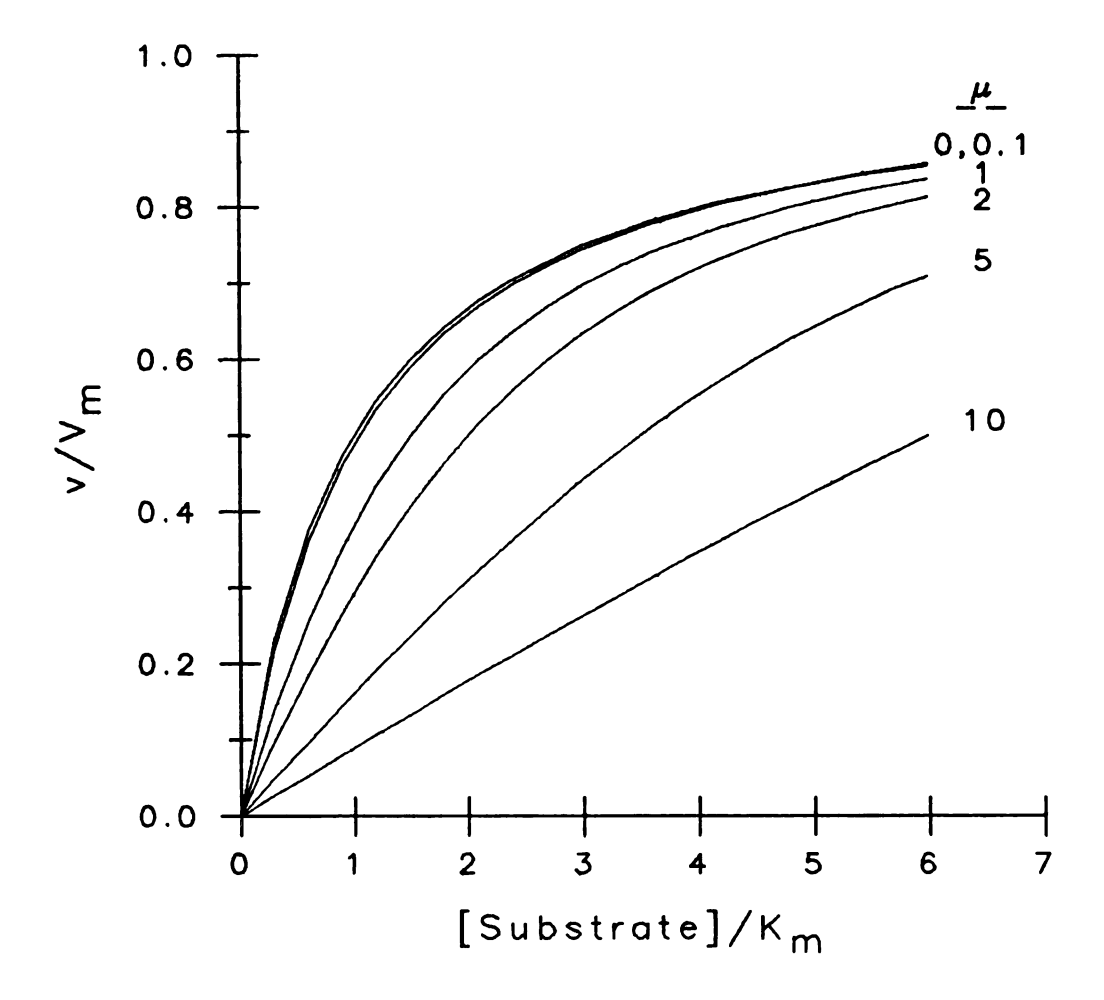


Figure 3.2. Influence of slow mass transport on enzyme kinetics.

lowering the constant of the other substrate [72,73]. This see-saw effect has been confirmed in several immobilized enzyme studies [74-76]. Under other conditions, the apparent K_m values can both be higher or lower (see Engasser's paper for details [72]).

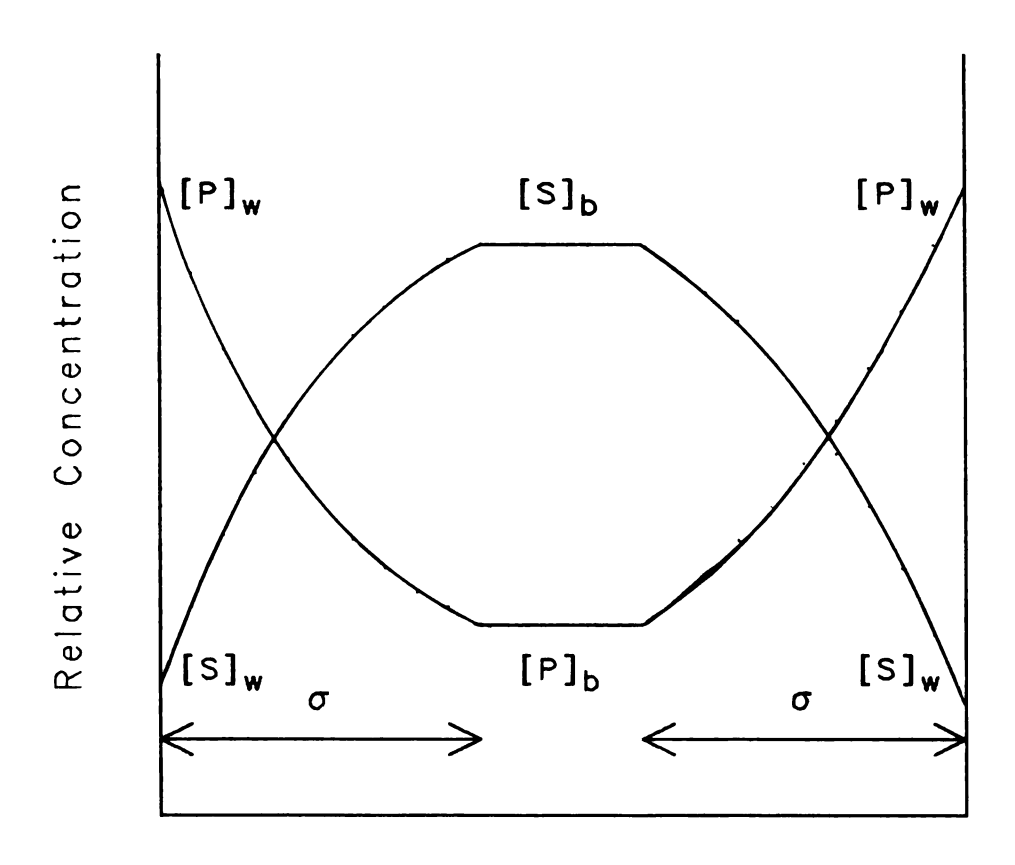
The type of mass transport in open-tubular reactors depends on the system being considered. These reactors are used almost entirely in three flow system types: stopped-flow, flow-injection, and continuous flow. The mass transport processes and kinetics of each of these are discussed in turn. Only external mass transport needs to be examined, since the enzyme is bound essentially to a non-porous wall in a very thin layer.

The reaction in the stopped-flow system occurs under static conditions. In the simplest mass transfer model, only molecular diffusion is considered. Once the enzyme reaction begins, concentration gradients in both substrate and product are established as shown in Figure 3.3. The mass transport rate constant under static conditions may be given by the following equation [70].

$$h = N_{U}D/(2r\sigma)$$
 (3.9)

Here $N_{\mathbf{u}}$ is the Nusselt number, D is the molecular diffusion coefficient for the substrate, and r is the reactor radius.

Under conditions of high enzyme binding and activity, molecular diffusion may totally control the overall reaction



Distance along Reactor Diameter

Figure 3.3. Concentration gradients in an open-tubular reactor.

rate. A mathematical description has been derived and is given below. Details of the model are described in Appendix A.

$$[P]_{b} = [S]_{b}(1 - 4 \sum_{s=1}^{3} \exp(-Dj_{s}^{2}t/r^{2})/j_{s}^{2})$$
 (3.10)

where $[P]_b$ is the product concentration in the bulk solution at time t, r is the reactor radius, j_s is a Bessel function, and t is the time in seconds.

When a flowing liquid passes through an OTIMER, convection becomes the primary means of transport. Enzyme reactors used in flow-injection analysis [4-6] are examples of this system. Laidler and coworkers have been the major contributors to the theory of mass transport in such systems [77-80]. Equation 3.11 is a mathematical description of the transport rate constant [77].

$$h = 1.29 \sigma^{-1} (D^2 v/rL)^{1/3}$$
 (3.11)

where ν is the linear (cm/s) flow rate, and σ is the diffusion layer thickness. The inherent Michaelis constant is transformed into the following [77].

$$K_{m}(apparent)=K_{m}(inherent)+0.39\sigma k_{e}[E]_{o}(rL/D^{2}v)^{1/3}$$
 (3.12)

Since mass transport is faster in flowing systems than under static conditions, the enzyme reaction rate should have a greater influence on the overall kinetics in flowing systems.

Similar interplay between the enzyme and mass transport is expected in air-segmented continuous flow systems [21-23], but the mass transport rate has not been described mathematically. A thin film of liquid which moves only slowly along the reactor wall and secondary, bolus, flow which is established in each liquid segment complicate the fluid dynamics. Therefore, primary flow, secondary flow, and mass transport in the thin film all contribute to the mass transfer of the system. Snyder has described the effect of incomplete mixing in the liquid segments on the sample dispersion [82,83]. One should be able to relate the extent of dispersion to the rate of radial mass transport, since it is known that mixing along the direction of flow is fast while mixing across adjacent streamlines is the limiting factor. Figure 3.4 shows the pattern of bolus flow.

One can assume that the rate of mass transport is inversely proportional to the sample dispersion due to incomplete mixing. From Snyder's theory, the following equation may be a good estimate of mixing in OTIMERs in segmented-flow systems.

$$h = (1.25\gamma^{2/3}VD^{1/2})/(v^{7/6}\eta^{2/3}L^{1/2}d^3)$$
 (3.13)

Here γ is the surface tension of the liquid, V is the volume of a single liquid segment, η is the solution viscosity, ν is the linear flow rate, L is the reactor

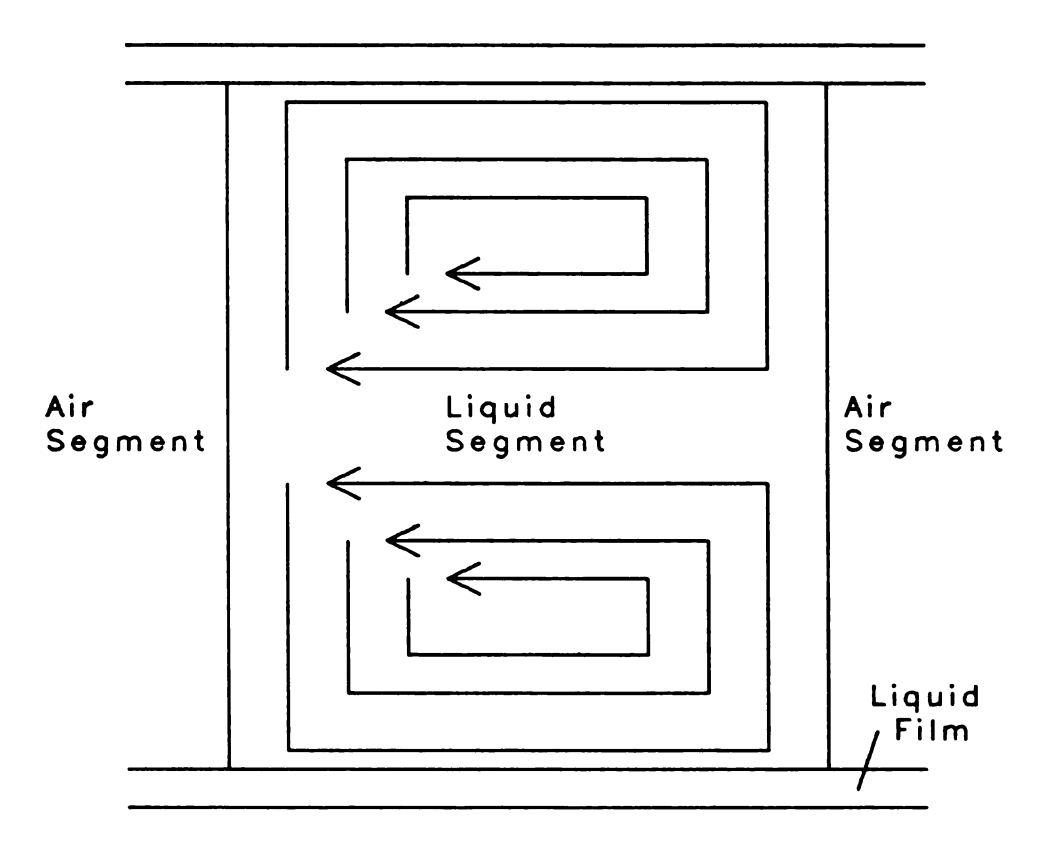


Figure 3.4. Bolus flow pattern.

length, and d is the reactor diameter. Further theoretical and experimental work on this system is needed.

B. Experimental Considerations

The kinetics of open-tubular immobilized enzyme reactors are difficult to monitor. In all systems, the reagents are pushed into the reactor, allowed to react for a time, and then the substrates or products are monitored as they exit the tube. Thus, the reaction rate obtained is the result of a fixed-time measurement, with the initial time (t_1) being zero and the final time (t_2) being the moment that the substrate solution exits the reactor. While t_2 can be varied, t_1 is usually restricted to a value of zero. Enzyme lag phases, therefore, are included in the rate measurements, which introduces error.

Continuous flow methods are used widely in conjunction with immobilized enzymes. Yet few kinetics experiments have been performed because data at early reaction times are impossible to obtain and entire progress curves would require many experiments under varying conditions. For example, a change in pump speed to change the reaction time might also alter the mass transport rate. Bi-directional flow, continuous flow methods [84] and other designs are possible ways of reducing the number of required experiments, but the instrumentation and procedures are complicated. A stopped-flow method using OTIMERs has been described [85], but again many experiments are required in

order to draw a complete progress curve of the enzyme reaction.

Ideally, one would like to monitor the reaction directly and continuously. We have developed an instrument that is ideal in its concept, and only a little less so in its function. A tubular reactor, containing an immobilized enzyme, is fitted inside the observation cell of a stopped-flow instrument. With the reagents mixed and pushed into the observation cell, the reaction begins. The light path of the photometer passes through the reactor and reacting solution; thus, the formation of product or depletion of substrate can be monitored directly and continuously by absorption spectroscopy.

The advantages of the instrument are numerous. Early reaction times are obtainable since the injection of the mixed reagents is performed quickly by the stopped-flow. The time window can be varied so as to exclude lag periods and other error-prone regions. Also, initial reaction rates can be calculated more accurately by the linear regression slope method rather than by the fixed-time method. Only diffusion and/or electrostatic effects contribute to mass transport in the reactor so that fundamental studies of the kinetics can be done more easily. The only disadvantage is that one of the substrates or products must have a unique absorbance maximum in the range of the monochromator. If not, a follow-up reaction can be

used, but only if its reaction rate is much faster than that of the analytical reaction rate.

The requirements for the instrument described above are somewhat different from those of a conventional stoppedflow instrument. First, fast mixing is not essential since the reaction does not begin until the reagents enter the observation cell. Even manual mixing is possible. However, the injection time, the time taken to push the solution through the cell, must be small so that the reaction extent prior to the first data point is negligible. These requirements can be provided by simply employing a T-mixer and a strong syringe push. Second, downstream stopping is not required since typical enzyme reactions are monitored on the order of seconds rather than milliseconds. Third, mixing between reagents and the reaction volume inside the observation cell should be minimized. Unlike standard stopped-flow experiments, products are only formed in the observation cell/reactor; diffusion of product into the reagent solution at the entrance and exit of the cell will cause errors in the rate measurement. Any siphoning or solution leakage will lead to drastic errors. design of an instrument which minimizes this mixing is a difficult problem. A prototype instrument which eliminates the reaction volume/reagent solution interface was built, and preliminary test results are given in Section E.

A modified GCA McPherson stopped-flow module was used

in most of the kinetics studies. A 1.75 cm immobilized enzyme reactor, 1 mm i.d., was fit tightly inside the observation cell of the module. Figure 3.5 shows the location of the reactor in the cell housing. A T-mixer was employed, along with upstream stopping. The remainder of the instrument was constructed from commercial components as shown in Figure 3.6. Data acquisition was performed by a microcomputer [86], linked to a PDP-8/e minicomputer (Digital Equipment Corporation). Further details of the instrument and its use are given in Section C.

One other important consideration in the use of this method is that the absorbance measurement is atypical. Because a product (and substrate) concentration gradient exists radially across the tube, the relationship between absorbance and concentration does not depend only on the molar absorptivity, ε , and the reactor length, but also upon reactor radius and the "steepness" of the concentration gradient. A mathematical model of the time-independent absorbance versus reactor design relationship is described in Appendix B. The time dependent case is complicated by the rate of product formation and mass transport and has not been considered. The final result of the mathematical treatment is given in equation 3.14.

Absorbance =
$$\varepsilon L([P]_b + \sigma([P]_w - [P]_b)/2r)$$
 (3.14)

Here $[P]_b$ is the concentration of the product in the bulk

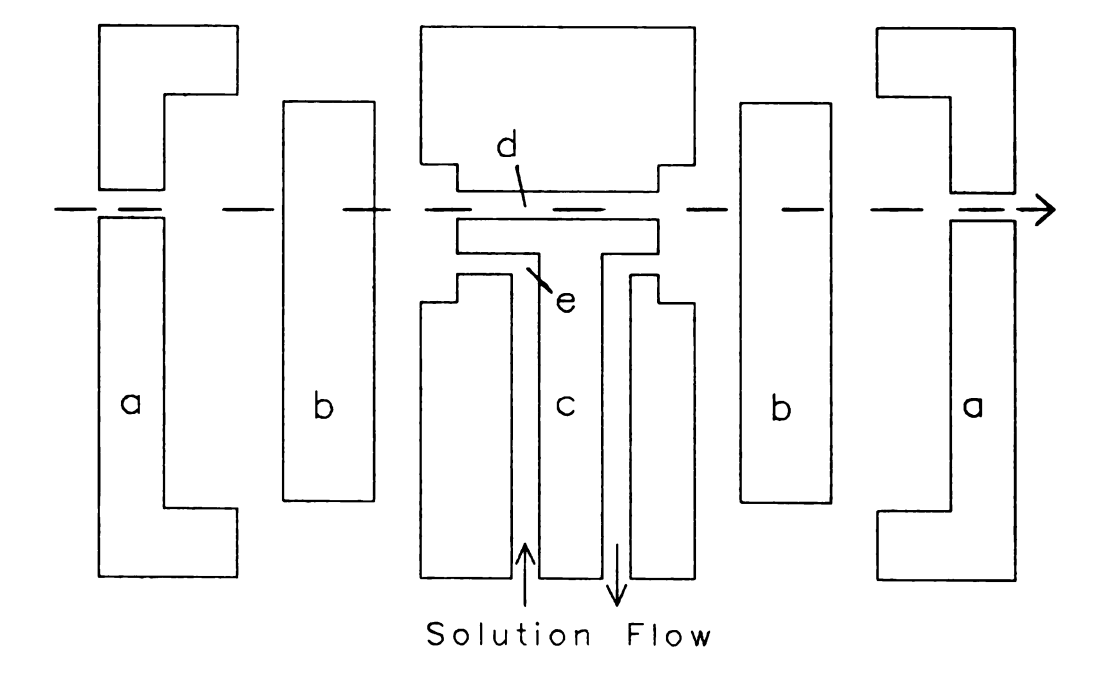


Figure 3.5. Cross-sectional view of the GCA McPherson stopped-flow mixer/observation cell unit. The outer aluminum housing (a), quartz windows (b), and the main KEL-F body (c) are press fit with three bolts. Mixing occurs at (e), where the two reagent flow streams meet at 90° to each other— one stream is in the plane of the figure and the other is perpendicular to it. The immobilized enzyme reactor is placed inside the observation cell (d). The dashed arrow represents the light path inside the cell.

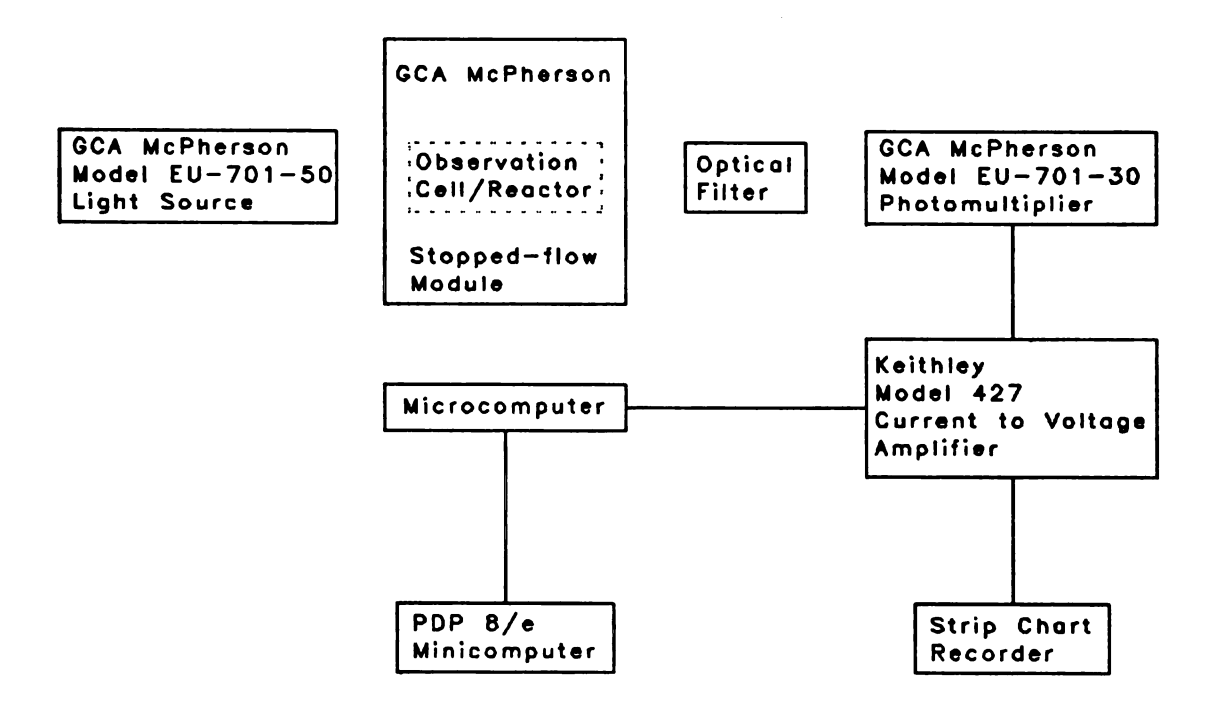


Figure 3.6. Stopped-flow colorimeter.

solution, and $[P]_W$ is the concentration of product at the reactor wall. The absorbance can vary with reactor diameter. However, during a single experiment, the reactor diameter is a constant and the absorbance depends on the diffusion layer thickness, σ . Changes in this factor during an experiment are expected to occur until steady-state between the enzyme reaction rate and mass transport is established. If steady-state conditions are established quickly, then most of the data will be free of mass transport influence on the absorbance measurement. More definitive experiments are needed to establish when steady-state is attained and to verify equation 3.12.

C. The Determination of Michaelis Constants

1. Introduction

We report here a study of the kinetics of L(+)-lactate dehydrogenase, LDH (E.C. 1.1.1.27). This enzyme converts L-lactic acid and β -nicotinamide adenine dinucleotide (β -NAD) to pyruvic acid and β -NADH, the reduced form of β -NAD. The reaction goes by a compulsory order bi-bi mechanism [87]:

$$E_1 + \beta - NAD \neq E_2$$

 $E_2 + Lactate \neq E_3$
 $E_3 \rightarrow E_1 + Pyruvate + \beta - NADH + H^+$

Here \mathbf{E}_1 represents the free enzyme, and \mathbf{E}_2 and \mathbf{E}_3 represent

the bimolecular and termolecular enzyme-substrate complexes respectively. The initial reaction rate for such a mechanism is given in equation 3.15.

$$v=k_{e}[E]_{O}/(1+K_{m}^{N}/[NAD]+K_{m}^{L}/[Lac]+K_{i}K_{m}^{L}/([NAD][Lac]))$$
 (3.15)

The term, K_i , represents the degree of interaction between the two substrates on the enzyme; the value is zero for a ping-pong type mechanism.

Lactate dehydrogenase is a tetrameric molecule, composed of heart (H) or skeletal muscle (M) type monomers [87]. Thus, five different isozymes exist— H_4 , MH_3 , M_2H_2 , M_3H , and M_4 , and their relative proportion varies among different species and tissues. The preparation used in this study was obtained from beef muscle, and so it contained mostly the M_4 and M_3H tetramers. The molecular weight of the enzyme is about 140,000. Each subunit contains a β -NAD binding site, but these sites are independent of one another. High concentrations of pyruvate and lactate inhibit the enzyme. The K_I value, the inhibition constant, for lactate varies from 26 mM for the H_4 isozyme to 130 mM for the M_4 tetramer.

In this section, the three kinetics constants and V_m , which equals $k_e[E]_o$, are reported for aqueous and nylon-immobilized LDH, and the values are compared. Partial diffusion control of the reaction rates is evident.

2. Reagent preparation

Tris Buffer. The following quantities of materials were dissolved in distilled, deionized water (DDW): 10.0 g trishydroxyaminomethane, 13.0 g hydrazine sulfate, and 2.0 g ethylenediaminetetracetic acid. The solution was diluted to one liter with DDW and then the pH of the solution was adjusted to 9.6 with NaOH. The buffer was stable for one week.

 β -NAD Solutions. The desired amount of β -NAD (Grade III, molecular weight=706, Sigma Chemical Company) was dissolved in buffer and diluted to 50.0 mL with buffer to give a stock solution. The working solutions were prepared by appropriate dilution of this stock with buffer. The stock solution and working standards were prepared daily.

Lactate Solutions. Purified L-lactic acid (0.960 g, Grade L-X, Sigma) and 0.125 mL of concentrated sulfuric acid were added to 500 mL of DDW. The resulting solution was diluted to 1.00 L with DDW. This stock was diluted appropriately with DDW to give the desired standard solutions. The stock solution was stable for two weeks, and the standards were prepared daily.

Soluble Enzyme Reagent. Eighty to one hundred microliters of a suspension of beef muscle LDH (Type X, 8800 Units/mL suspension, Sigma) were dissolved in Tris buffer, and then diluted to 0.200 L with buffer. This reagent was then substituted for the Tris buffer in the β -NAD solution

preparations described above. The $\beta\text{-NAD/enzyme}$ solutions were used within two hours.

3. Immobilization of lactate dehydrogenase

Lactate dehydrogenase was covalently bonded to straight, 20 cm lengths of nylon tubing (Portex Ltd., 1 mm i.d.). The immobilization procedure is given in Chapter 2, Table 2.3. The lactate dehydrogenase suspension obtained from Sigma was used directly in the immobilization.

4. The instrumentation

The stopped-flow system was assembled from commercially available components. The stopped-flow module (GCA Mc-Pherson) was modified for upstream stopping by removal of the stop syringe. The two push syringes had volumes of 370 µL. A filter photometer was employed for absorbance measurements. The radiation source was a deuterium lamp housed in a commercial light source module (GCA McPherson). A 340 nm interference filter (bandwidth = 12 nm) was mounted between the stopped-flow unit and a photomultiplier module (GCA McPherson). The photocurrents from the photomultiplier were converted to voltages (Kiethley model 427 current amplifier), digitized, and the digital voltages stored in RAM with a microcomputer data acquisition system [86]. Data were acquired at 1.0 Hz. At the end of each trial, the data were shipped serially to a PDP-8/e minicomputer (Digital Equipment Corporation) for processing and analysis. The initial reaction rates were computed as

the linear regression slopes over the time period from 10 to 20 seconds after the final reagent push.

The instrument was operated in the following manner. The two syringes were filled with DDW, the water was pushed through the observation cell, and the flow was stopped. This procedure was repeated six times to wash out the reactor completely. Next, the syringes were filled with the reagents, the reagents were pushed through the mixer and cell, and the flow was stopped. This second procedure was repeated five times in order to ensure quantitative 1+1 mixing of the β -NAD and lactate solutions. After the final reagent push, the microcomputer data-taking routine was started. These steps were repeated for each experiment. The blank consisted of the β -NAD working solution mixed with distilled deionized water.

For the soluble LDH studies, the instrument was used as described above. After the soluble enzyme studies were completed, the observation cell of the stopped-flow module was disassembled, and a 1.75 cm section of the immobilized LDH tube was fitted tightly inside the cell. The cell was reassembled, and the study was repeated. Between trials, the IME tube was filled with pH 6.85 phosphate buffer, 0.05 M. A room temperature water bath kept the reagents at a constant temperature, between 18 and 20 °C, during all experiments.

5. Results and discussion

The precision of the rate measurement was determined by repetitively montoring the immobilized LDH catalyzed reaction of 0.50 mM lactate and 1.35 mM β -NAD. The relative standard deviation was found to be 4%. The enzyme activity declined rapidly during the first two days of use and, thereafter, only slowly. Even after seven days at room temperature and about 175 experiments, 60% of the original enzyme activity remained.

Typical progress curves obtained with our instrument are shown in Figure 3.7. The immobilized LDH displays a sigmoid-shaped curve, that is similar to the one produced by the aqueous LDH. No odd reaction kinetics are apparent. Also, a short lag phase is noticeable. These facts are quickly and easily shown, in contrast to other indirect kinetics methods.

The K_m values were determined by the method of Florini and Vestling [88]. The mean values of the initial reaction rates for each pair of substrate concentrations were fit to equation 3.15 by a computer regression program. The experimental and regression results are shown as Lineweaver-Burk plots in Figures 3.8 and 3.9. Because the lines in the double reciprocal plots intersect at a common point below the x-axis, the formation of a ternary complex is confirmed.

A small concave curvature exists in the experimental

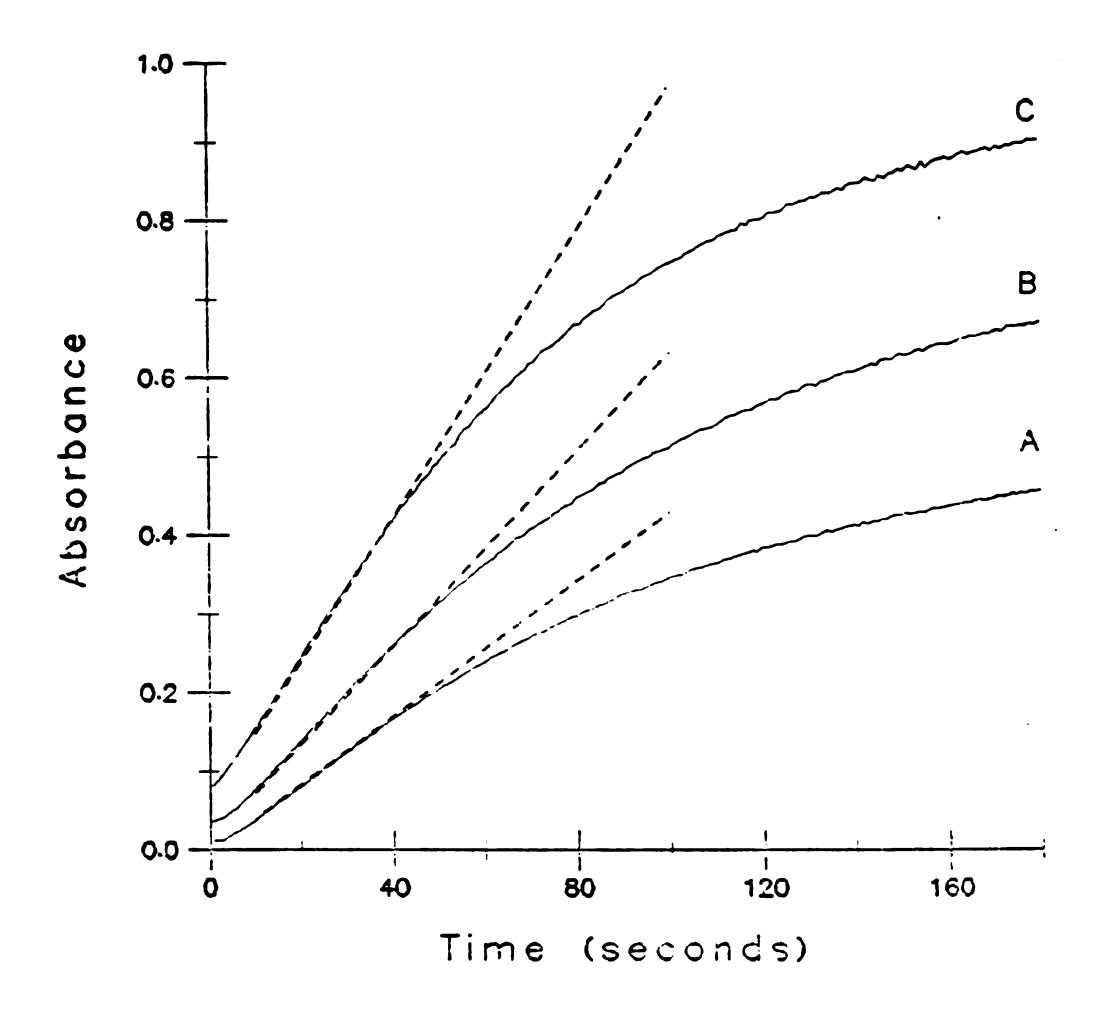


Figure 3.7. Typical progress curves obtained with the instrument. The dotted lines represent the initial reaction rates calculated from these curves. The reactions represented were of 2.00 mM lactate with 0.425 mM (A), 0.850 mM (B), and 2.12 mM (C) β -NAD.

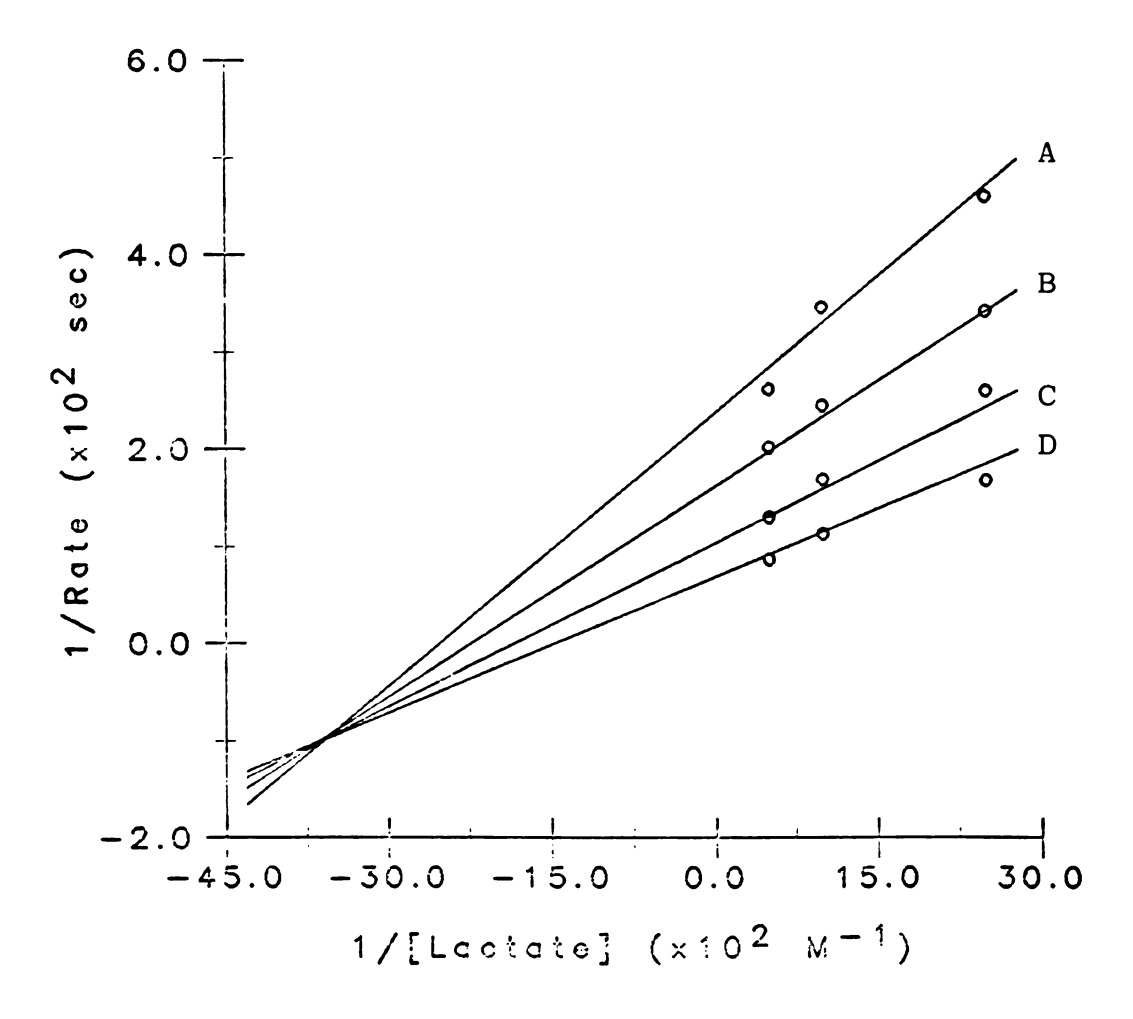


Figure 3.8. Lineweaver-Burk plot of 1/Rate versus 1/[Lactate] at four different β -NAD concentrations: 0.26 mM (A), 0.43 mM (B), 0.85 mM (C), and 2.12 mM (D).

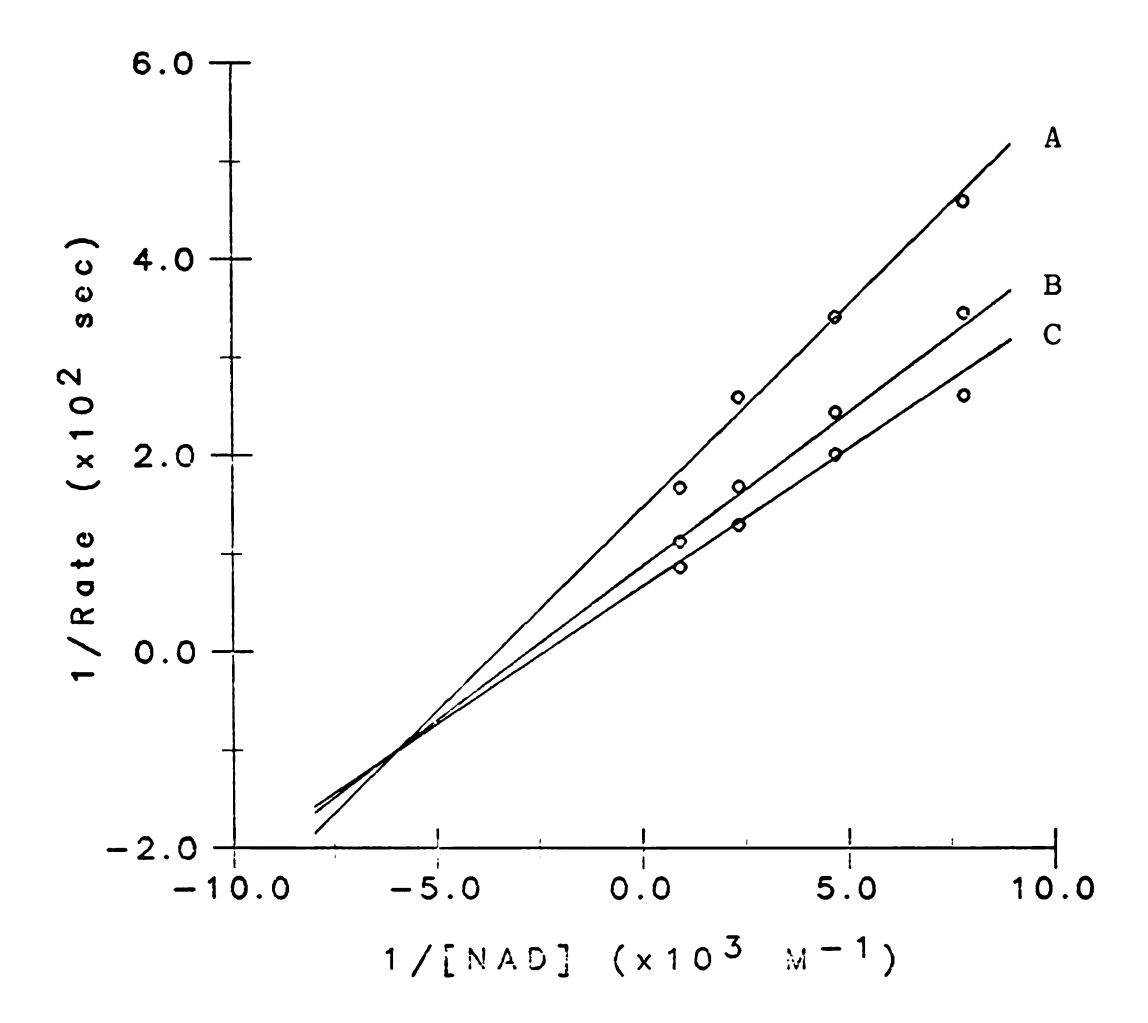


Figure 3.9. Lineweaver-Burk plot of 1/Rate versus $1/[\beta-NAD]$ at three different lactate concentrations: 0.80 mM (A), 2.00 mM (B), and 4.00 mM (C).

values. Such curvature is not apparent in the aqueous enzyme data. Sundaram and Igloi also reported such curved plots in a multi-enzyme system bound inside nylon tubing [56]. Diffusional resistance or the presence of several isozymes may be the cause of this effect, but no realistic mathematical model has been found.

The y-intercepts of the Lineweaver-Burk plots represent the reaction rate at infinite lactate or $\beta\text{-NAD}$ concentrations. A second Lineweaver-Burk plot of these rates yields the desired K_m and V_m values, as shown in Figure 3.10. The results of five independent trials were weighted and averaged to give final values for the kinetics constants. The values found for soluble and immobilized LDH by this method are given in Table 3.2.

The K_m of β -NAD increases and the K_m of lactate decreases upon immobilization. Intuitively, K_m values of bound enzymes should not be lower than those of soluble enzymes, unless a conformational change occurs upon immobilization. However, Engasser, et.al. [72] recently explained that if the K_m values and diffusion rate constants (h_S) of the enzyme substrates differ greatly, then the tendency is to increase the K_m of the higher affinity substrate and decrease the K_m of the lower affinity substrate. This is due to diffusional limitations on the reaction rate.

Engasser, et.al. restricted the model to ping-pong

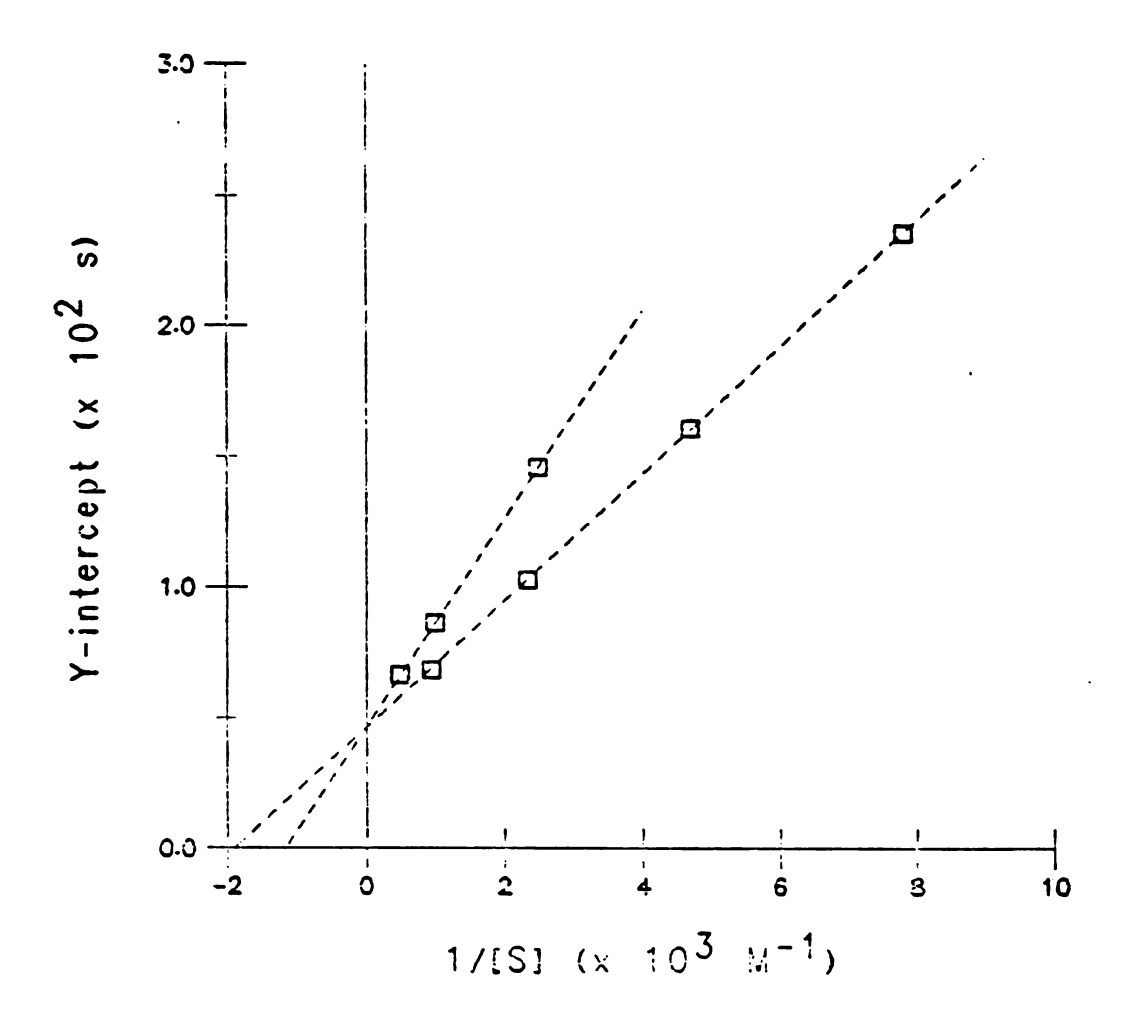


Figure 3.10. Plot of y-intercepts from Figures 3.8 and 3.9 versus 1/[Substrate] for different $\beta\text{-NAD}$ and lactate concentrations. The y-intercept equals 1/V , and the x-intercepts yield the two K_m values.

Table 3.2. Kinetics Values for Aqueous and Immobilized Lactate Dehydrogenase

	Aqueous	Immobilized
$V_{\rm m} (10^{-6} {\rm Ms}^{-1})$	2.0 ± 0.1	2.1 ± 0.1
K_m^N (10 ⁻⁴ M)	2.5 ± 0.3	4.3 ± 0.5
K_{m}^{L} (10 ⁻⁴ M)	19 ± 4	9 ± 1
$K_{i} (10^{-4} M)$	5.8 ± 1.6	1.9 ± 0.5

type reactions, but we believe that the same effect should occur with compulsory order mechanisms. In the case of LDH, the important dimensionless factor, $\xi = (h_N^R K_m^N)/(h_L^K K_m^L)$, equals approximately 0.07. Since this is very much different from 1, it may be expected that the see-saw effect on the K_m values will occur. Using Figures 1 a,b, e, and f of reference 72 and interpolating to approximate the conditions of this experiment, we estimated that the enzyme reaction rate was about five times faster than the diffusion rate.

A second explanation of the $\mathbf{K}_{\mathbf{m}}$ changes is based on electrostatic effects. The immobilization procedure imparts a positive charge to the nylon surface. Since lactate has a negative charge and β -NAD has a positive charge, the apparent K_{m} values could decrease and increase respectively, because the surface concentrations of the two substrates differ from those in the bulk solution. The kinetics values found here are relevant to other methods in which a reagent solution is allowed to react inside an OTIMER under static Sundaram's impette method [50] and stoppedconditions. flow, flow-injection methods employing OTIMERs should benefit directly. The method is very useful in determining the apparent Michaelis constant values for enzymes immobilized inside open tubes. A variety of enzymes can be tested in this manner.

D. Analytical Determinations

1. Introduction

Direct reaction rate methods for two clinically important substrates, glucose and lactate, are reported here. The glucose determination was performed under fixed-time conditions, while the lactate results were obtained from rates calculated by linear regression analysis of the absorbance-time data. The instrument allows calculation of the initial reaction rate by the fixed-time, variable-time, or the slope approach [89].

The Trinder method [90,91] for the determination of glucose with glucose oxidase was adopted here. The two reactions involved are given below.

$$β-D-glucose + O_2 + H_2O \rightarrow δ-gluconolactone + H_2O_2$$

2 $H_2O_2 + DCPS + AAP \rightarrow Dye + 3 H_2O + H_2SO_4$

Glucose oxidase (GO) catalyzes the first reaction, while peroxidase (PO) does the same for the second reaction. DCPS is 2,4-dichlorophenolsulfonate and AAP is 4-amino-antipyrine. The absorbance of the dye product at 505 nm was monitored.

Lactate was determined by measuring the absorbance of $\beta\text{-NADH}$ produced in the following reaction.

Lactate +
$$\beta$$
-NAD + Pyruvate + β -NADH

Lactate dehydrogenase (LDH) catalyzes this reaction.

The spectroscopic measurement was done at 340 nm. A basic solution and hydrazine were used to drive the reaction toward completion. The results of several control serum assays for glucose and lactate are also reported.

2. Reagent preparation

Glucose Standards. The glucose stock solution was prepared by dissolving 2.000 g of anhydrous α -D-glucose and 0.50 g of benzoic acid in about 0.75 L of distilled deionized water (DDW). The solution was then diluted to exactly 1.00 L with DDW. The standard solutions were prepared by appropriate dilution of the stock with DDW. The stock was stable for a month at 4 °C.

Trinder/Peroxidase Reagent. The method of Barham and Trinder [91] was used to prepare a solution of 2,4-dichlorophenolsulfonate. Two mL of this solution (about 0.2 mmoles), 10 mg (1,670 Units) of peroxidase (Type II, Sigma), and 10 mg (about 0.05 mmoles) of 4-aminoantipyrine were dissolved in 75 mL of pH 6.4 phosphate buffer, 0.1 M. The solution was then diluted to exactly 0.100 L with the pH 6.4 buffer. This reagent was prepared daily.

Lactate Standards. Purified L-lactic acid (0.960 g, Grade L-X, Sigma) and 0.125 mL of concentrated sulfuric acid were added to 500 mL of DDW. The resulting solution was diluted to exactly 1.00 L with DDW. This stock was diluted appropriately with DDW to give the desired standard solutions. The stock was stable for two weeks; standards

were prepared daily.

 β -NAD Reagent. The following quantities of materials were dissolved in DDW: 10.0 g of trishydroxyaminomethane, 13.0 g hydrazine sulfate, and 2.0 g ethylenediaminetetraacetic acid. The pH of the solution was adjusted to 9.6 with NaOH after dilution to exactly 1.0 L with DDW. The buffer was stable for one week. In 40 mL of this buffer, 0.300 g of β -NAD (Grade III, Sigma) were dissolved. The resulting solution was diluted to exactly 50.0 mL to give a 8.5 mM β -NAD solution. This reagent was prepared daily.

Serum Samples. The control sera (Monitrol and Pathotrol, Dade Division, American Hospital Supply) were reconstituted according to the manufacturer's instructions. For the glucose determination, 1.00 mL of the serum, 1.50 mL of a 20 g/L solution of Ba(OH)2, and 1.40 mL of a 20 g/L solution of ZnSO4, in that order, were added to a centrifuge tube. The solution was thoroughly mixed and then centrifuged for three minutes. The supernatant fluid was used directly for the determination. No protein precipitation was involved in sample preparation for the lactate determination. One millilter of the control serum was diluted to exactly 0.100 L with DDW, and the resulting solution was used in the analysis.

3. Enzyme immobilization

The enzymes, glucose oxidase (Type II, Sigma) and beef muscle lactate dehydrogenase (Type X, Sigma), were

immobilized on Type '6' nylon tubing (0.1 cm i.d., Portex Ltd.) by a procedure described in Chapter 2, Table 2.3. A 10 mg/mL solution of glucose oxidase was prepared for use in step 4 of the procedure, while the lactate dehydrogenase suspension was used directly as sold by Sigma. The completed reactor was filled with buffer (pH 6.4, phosphate) and stored at 4 °C when not in use. Short, 1.75 cm, segments of the tubing were cut for use in the stopped-flow observation cell when required.

4. The instrumentation

The instrument has been described in detail in Section C. For the fixed-time measurements, a monostable timer circuit was built to cause a sample-and-hold device to hold light intensity values obtained thirty seconds (I_1) and sixty seconds (I_2) after the reaction began. The change in absorbance was taken to be $\log(I_1/I_2)$. This assumes no drift in the 100% T setting over the 30 second time interval. The light source was very stable, so this was probably a good (< 2% error) assumption. The time range was chosen as an optimum between sample throughput and errors due to mixing effects and enzyme lag periods. The lactate data were taken and processed by computer as described in Section C.

5. The results of the glucose determination

Glucose standards and the Trinder/peroxidase reagent were mixed rapidly and pushed into the observation cell/immobilized enzyme reactor by the stopped-flow instrument.

The decrease in light intensity reaching the detector was monitored and the change in absorbance was calculated as described above. A blank was tested between each sample, because the Trinder reagents and product adsorbed strongly to the nylon, producing some carryover. Thus, the sample throughput was limited to a maximum of thirty samples per hour.

The results of five separate experiments over a four day period using the same glucose oxidase reactor are shown in Figure 3.11. A very linear calibration plot with a slope of $8.3 \pm 0.2 \times 10^{-2}$ and a y-intercept of $-3.4 \pm 0.1 \times 10^{-3}$ was obtained. The error in the absorbance measurements was mostly due to a decline in the enzyme activity with time. The reactor, stored at room temperatrue for five days, dropped in activity by only 8%. The linear range of the method, 1-10 mM, covered the normal levels found in human blood serum (3.8-5.9 mM [92]).

Three control serum samples were assayed with the instrument. During the protein precipitation treatment, the samples were diluted 1:3.9; the resulting concentrations were still within the linear range. Table 3.3 compares the concentrations found in our laboratory with those given on the data sheets accompanying the samples. The accuracy of the method was good, with the greatest deviations occurring with samples of low glucose content. This

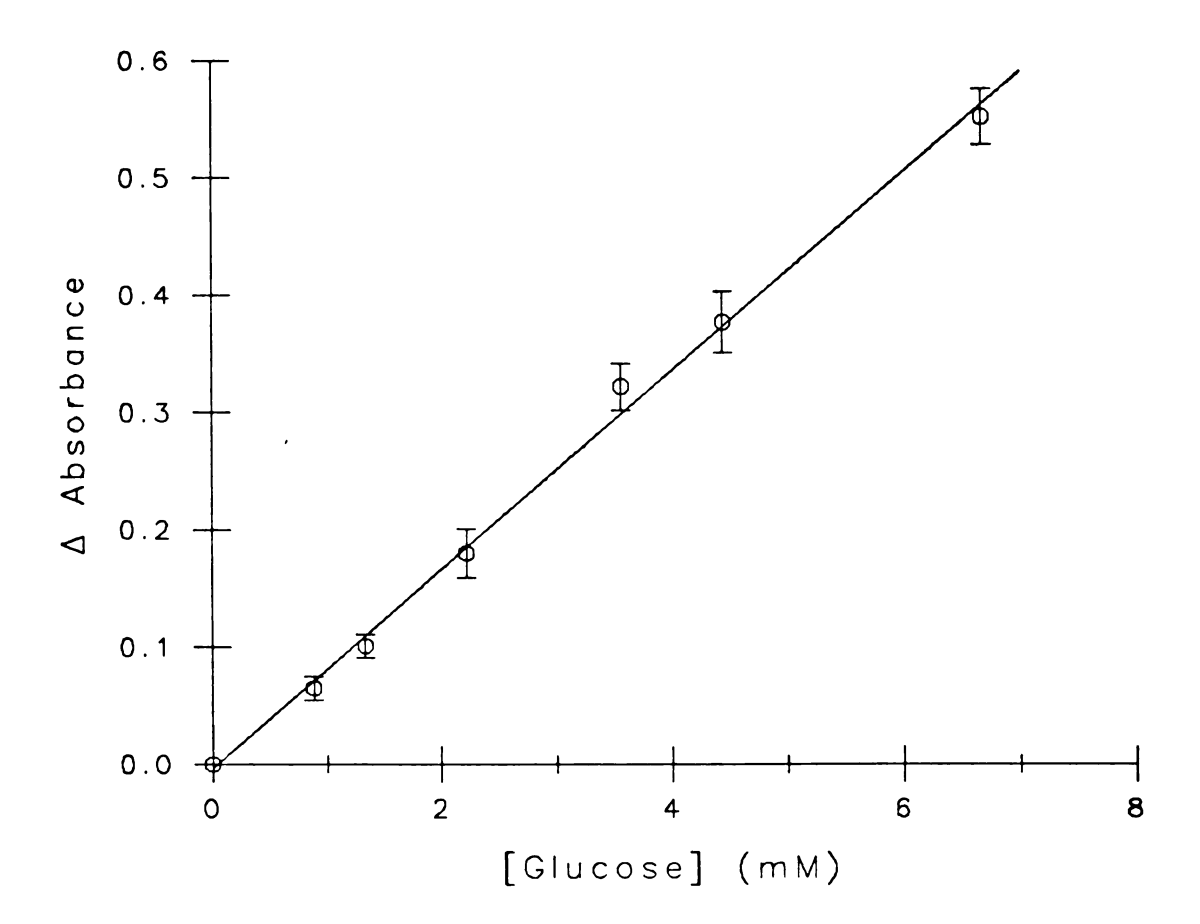


Figure 3.11. Calibration curve for glucose.

Table 3.3. Results of Serum Assays for Glucose

Serum	No. Detns.	<pre>Expected(mM)</pre>	Found(mM)
Monitrol I	5	5.67	4 ± 1
Pathotrol	6	12.8	13.3 ± 0.3
Monitrol II	9	13.4	13.2 ± 0.5

deviation was probably due to the presence of ascorbic acid, gentisic acid, and other reducing agents, which can interfere with peroxidase-catalyzed reactions [93,94].

More details of this problem are given in Chapter 4,

Section B.

6. The results of the lactate determination

Initial reaction rates for the reaction of lactate and β -NAD were determined between 10 and 20 seconds after the final reagent push, with a computer linear regression program. Sets of standards were tested with a blank run at the end of each set. Sample carryover was small with this system, apparently because little adsorption of reagents or products on the nylon occurred. Thus, the processing of 90 samples per hour was possible.

Reaction rates obtained from five experiments over a four day period are plotted versus lactate concentrations in Figure 3.12. The same lactate dehydrogenase reactor was used in all of the experiments. The linearity is excellent, but a small positive intercept is apparent. This intercept may have been caused by a slow non-enzymatic reaction between the reagents. The blank, which consisted of DDW and the β -NAD reagent, would not correct for this. The slope of the calibration curve was $4.3 \pm 0.3 \times 10^{-3}$, and the y-intercept was $1.0 \pm 0.1 \times 10^{-10}$.

The errors in the reaction rate data were mostly due to fluctuations in the reactor activity. Sixty percent

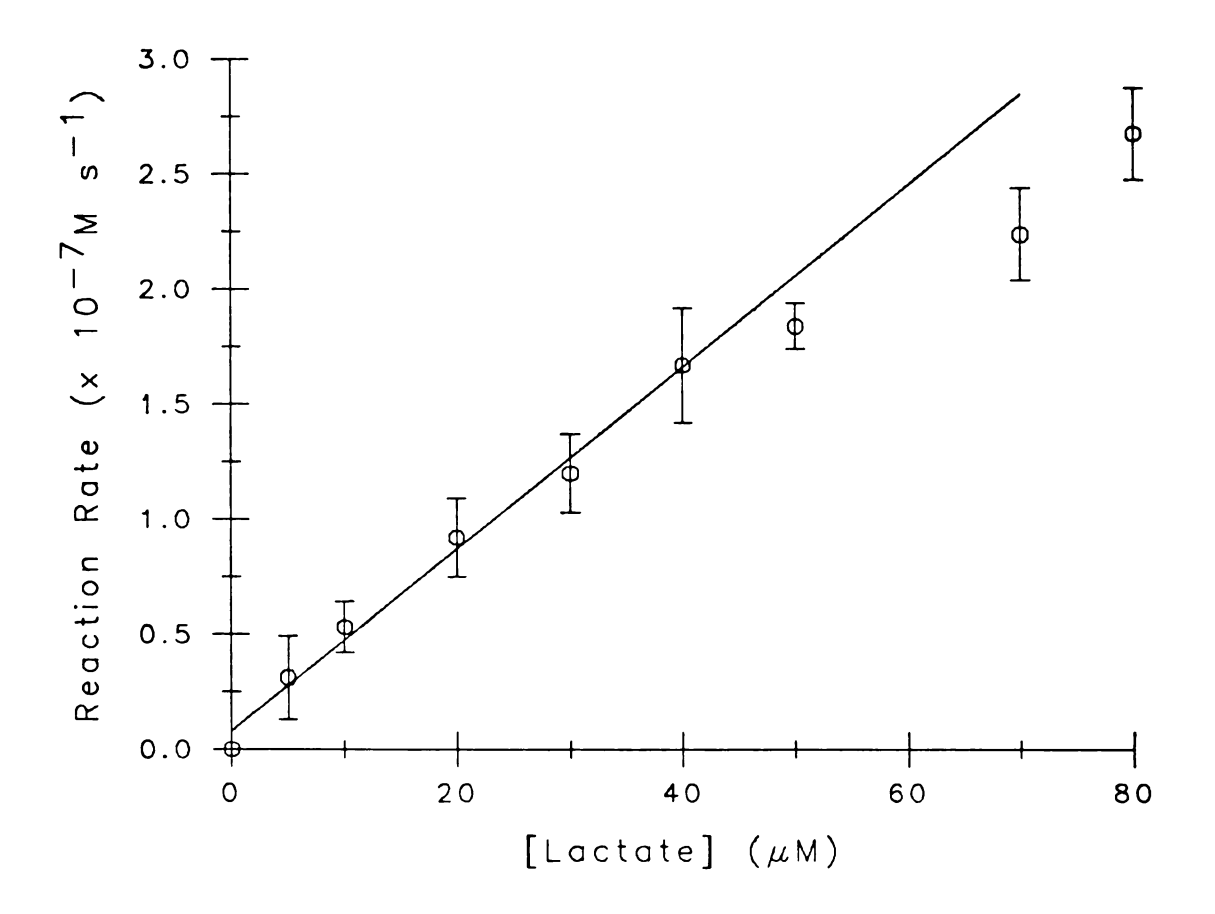


Figure 3.12. Calibration curve for lactate.

of the original enzyme activity remained after seven days of heavy use at room temperature. The linear range of the method, 5-50 μM , is limited at the high end by the following requirement: [Lactate] < 0.05 K_m^L . The K_m^L of immobilized LDH was determined to be 9 mM in Section C of this chapter. Thus, the calibration curve should bend off near 45 μM and it does.

Serum assays were performed on 1:100 dilutions of the reconstituted controls with DDW in order to adjust the sample concentrations to the linear range of the method. This was quite advantageous, since the sample preparation was simplified and interfering substances should have a much smaller effect. Table 3.4 shows that the lactate concentrations in all three samples were accurately determined. However, the average values were slightly higher than those expected. The reason for this was that a small amount of aqueous lactate dehydrogenase was present in the sera, and the soluble enzyme reaction also occurred inside the reactor. Nevertheless, the method is very sensitive and the accuracy is within the limits of error.

Since the sensitivity and accuracy are good, but the sample throughput is low, this stopped-flow instrument should be suitable for method development and substrate determinations in small clinical laboratories. Many other enzymes can be immobilized inside nylon tubing and used in the instrument to determine a wide variety of compounds.

Table 3.4. Results of Serum Assays for Lactate

Serum	No. Detns.	<pre>Expected(mM)</pre>	Found(mM)
Monitrol I	6	1.8	2.1 ± 0.2
Monitrol I	5	2.2	2.2 ± 0.4
MOHITTOI I	3	2.2	2.2 1 0.1
Monitrol I	6	3.1	3.2 ± 0.6

The calculation of reaction rates is direct, and lag periods can be avoided. With greater automation and the use of more inert supports, such as glass or Teflon, higher throughput is likely, and the method should become more advantageous. The instrument is versatile in that it can function as a device which determines kinetics values for assay development and also performs the actual determination.

E. A New Cell / Reactor Design

In order to eliminate any error due to mixing between reacting and unreacted solutions in the stopped-flow instrument, the cell/reactor was redesigned. Figure 3.13 is a diagram of the new instrument, built around two Altex slider valves. The cell was moved between positions 1 and 2 with a pneumatic valve and applied gas pressure. Typically, the cell was filled while in position 1 and then was moved quickly into position 2 for spectrophotometric monitoring. In this way, the interface between the reaction volume and the mixed reagents was eliminated. Errors due to undesirable mixing were prevented.

The slider, shown in Figure 3.13, was constructed of nylon to allow direct immobilization of enzymes to the walls of the observation cell. In the previous design, slight movements of the nylon tube at early reaction times often caused large fluctuations in the instrumental output. This problem was eliminated. Another advantage of

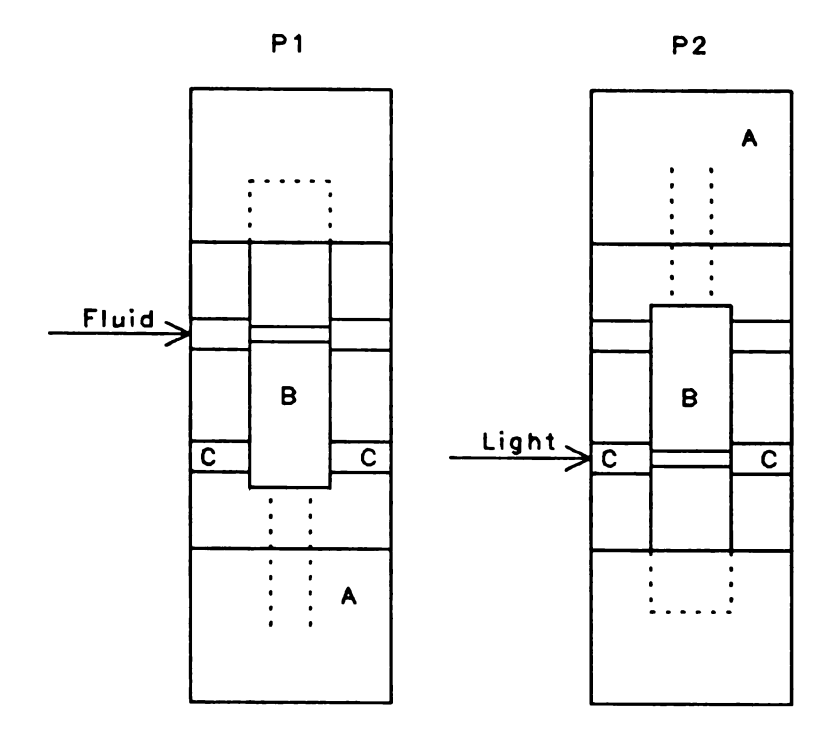


Figure 3.13. Design of the new cell/reactor. Two pneumatically actuated pistons (A) were used to push the slider (B) back and forth between the fill position (P1) and the viewing position (P2). Quartz windows were used (C) to contain the solution in the viewing position.

using nylon sliders was that various reactor diameters could easily be implemented by simply changing sliders.

One obvious disadvantage of this new method was the increase in cost of materials and time. While nylon tubing is fairly cheap, it is expensive to machine a new nylon block for each experiment. Also, more difficulty and time is involved in immobilizing enzymes on these blocks with high precision. The greatest disadvantage was found to be that the movement of the slider sometimes caused bubbles to form in the observation cell, because the solution was lost from the ends of the cell during changes in position. The development of bubbles was infrequent and was detected by a large drop in instrumental Several stopped-flow pushes usually restored the output. original output. The results of a series of experiments with distilled water are displayed in Figure 3.14, and they show fairly good reproducibility in the cell positioning.

The use of the instrument was demonstrated by determining glucose with immobilized glucose oxidase. The enzyme was bonded on two sliders— one with a 1 mm i.d. cell and one with a 2 mm i.d. cell. The immobilization procedure was identical to that described above (Chapter 2). A stopped—flow unit employing a T—mixer and upstream stopping was used with the cell assembly. Each syringe held 0.16 mL. Four reagent pushes and

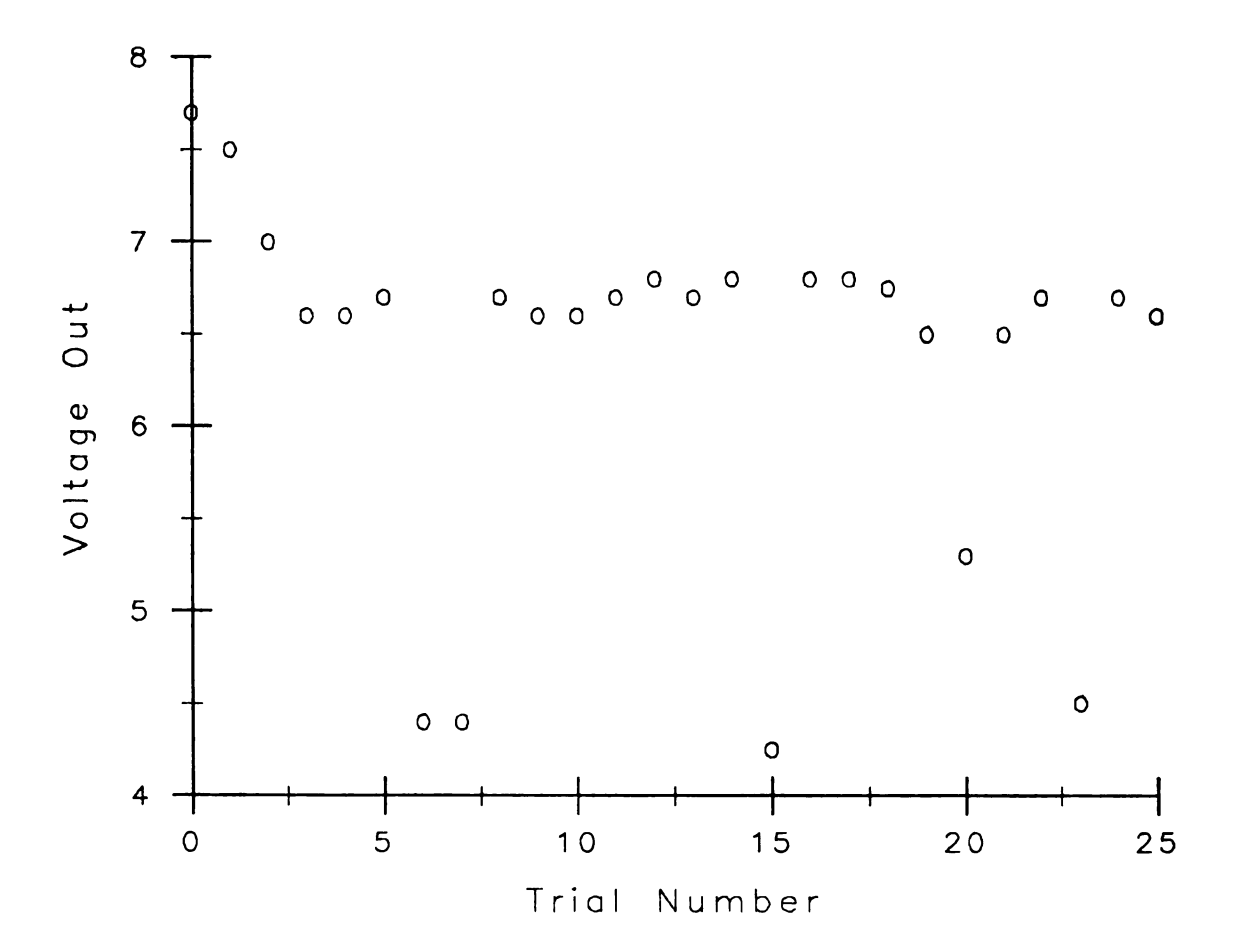


Figure 3.14. Reproducibility of cell positioning.

Distilled water was pumped through the cell at 0.46 mL/min. Each trial represents movement of the cell from the viewing position to the fill position and back again.

four wash pushes were employed to reduce sample carryover. One reagent was the glucose standards, while the
Trinder/peroxidase reagent filled the other syringe. The
Trinder reagent was composed of the following: 4 mg
peroxidase, 2 mM AAP, and 2 mM DCPS made up to 25.0 mL
with a pH 6.85 phosphate buffer, 0.05 M.

The precision of the progress curve determination is shown in Figure 3.15. Both reactors displayed very good precision. The determination of initial reaction rates from repetitive experiments with three different glucose concentrations gave an average relative standard deviation of 7%.

A preliminary study of the effect of reactor diameter on overall reaction progress displayed some interesting results. Figure 3.16 displays the data for the 1 mm i.d. reactor and Figure 3.17 for the 2 mm i.d. reactor. The enzyme reactors were not prepared at the same time, nor were the absorbances corrected for the effect of reactor diameter (equation 3.14). Despite these possible errors, it appears that the reaction was much slower in the larger diameter reactor. The reaction in the 2 mm i.d. reactor is about five times slower than that in the other reactor. Equation 3.8 predicts about a three-fold change in the reaction rate with this change in reactor diameter. However, the diffusion-control model does not predict the absolute reaction rate very well.

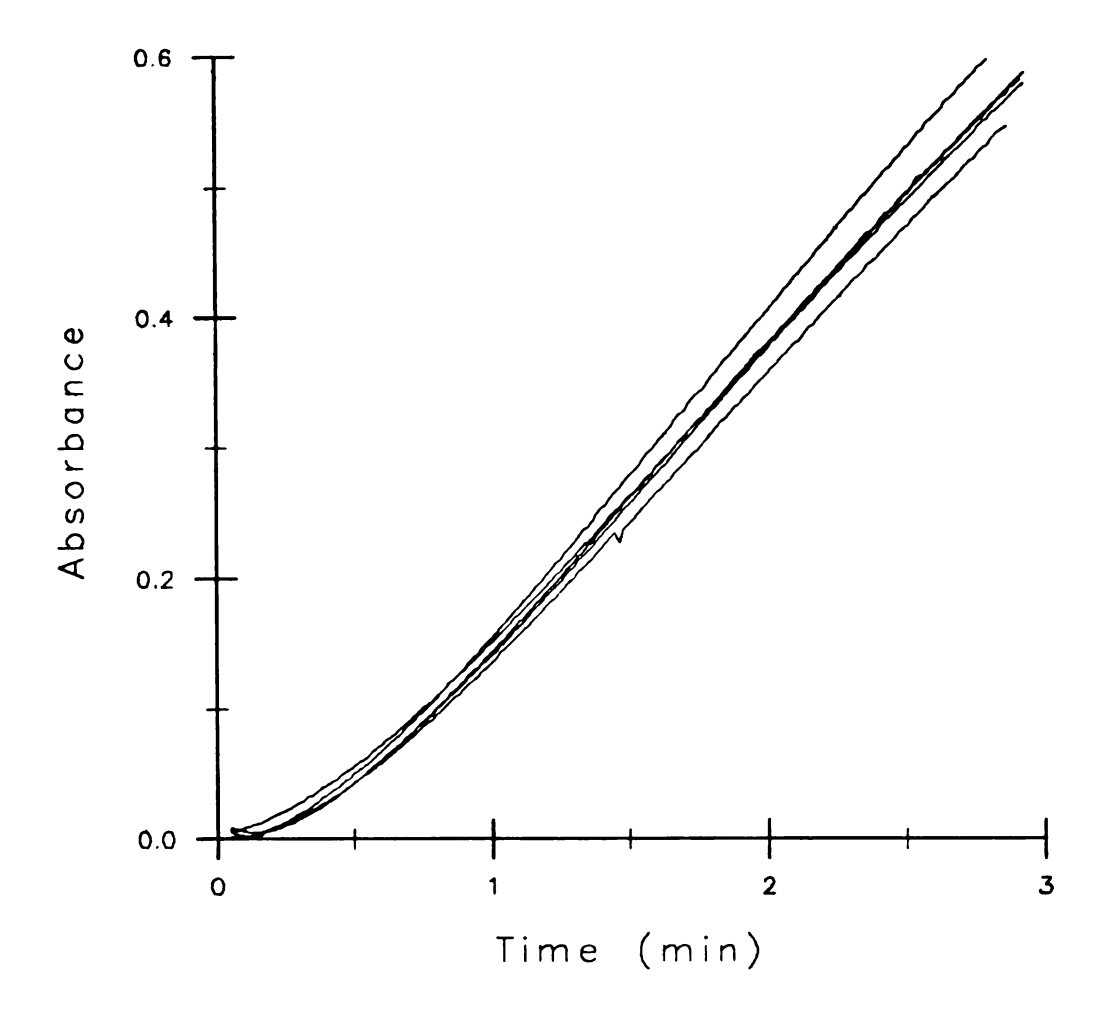


Figure 3.15. The results of five progress curve determinations with 0.44 mM glucose as the sample. The 1 mm i.d. reactor was used.

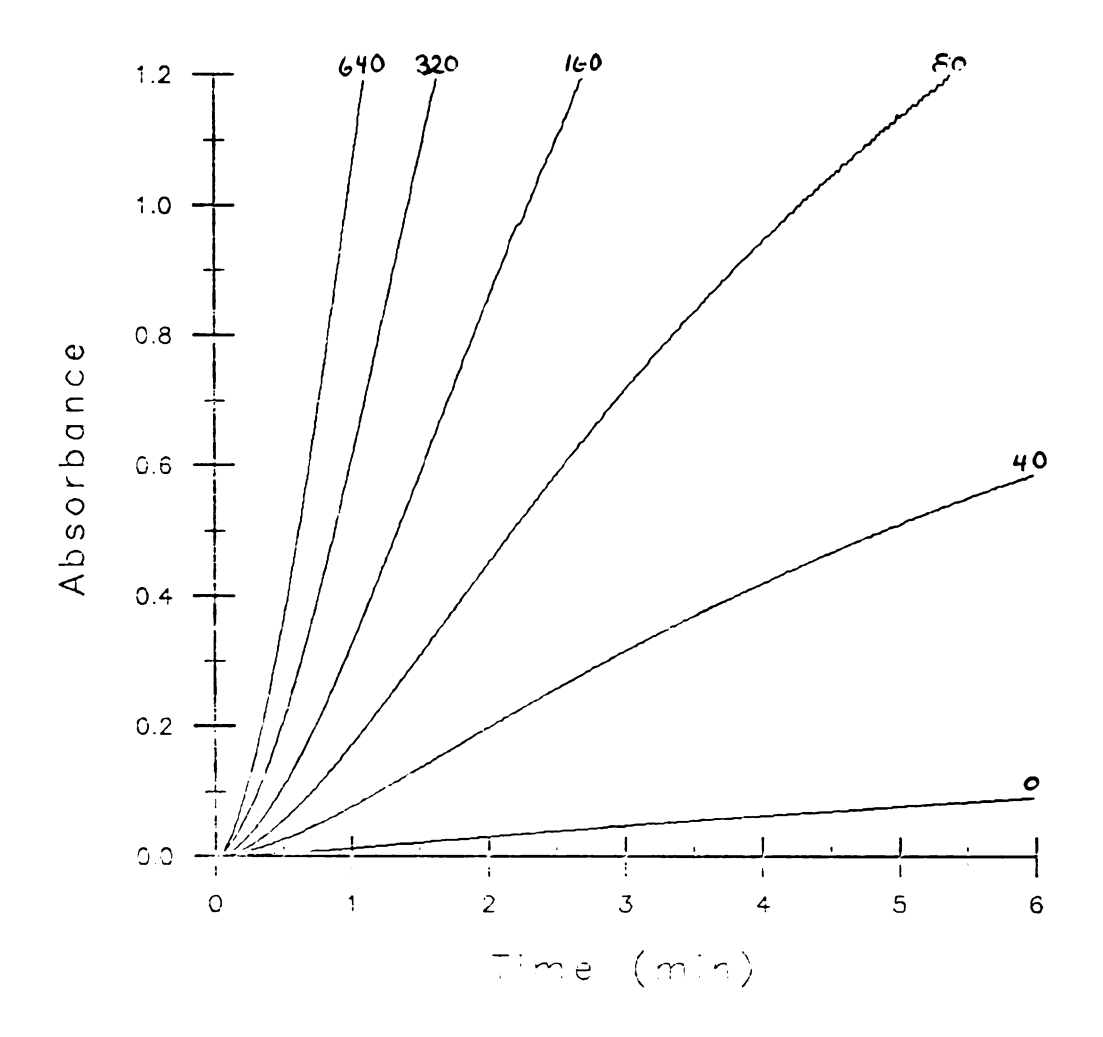


Figure 3.16. Progress curves obtained with the 1 mm i.d. reactor. The glucose concentrations (mg/L) which were used are written at the end of each curve.

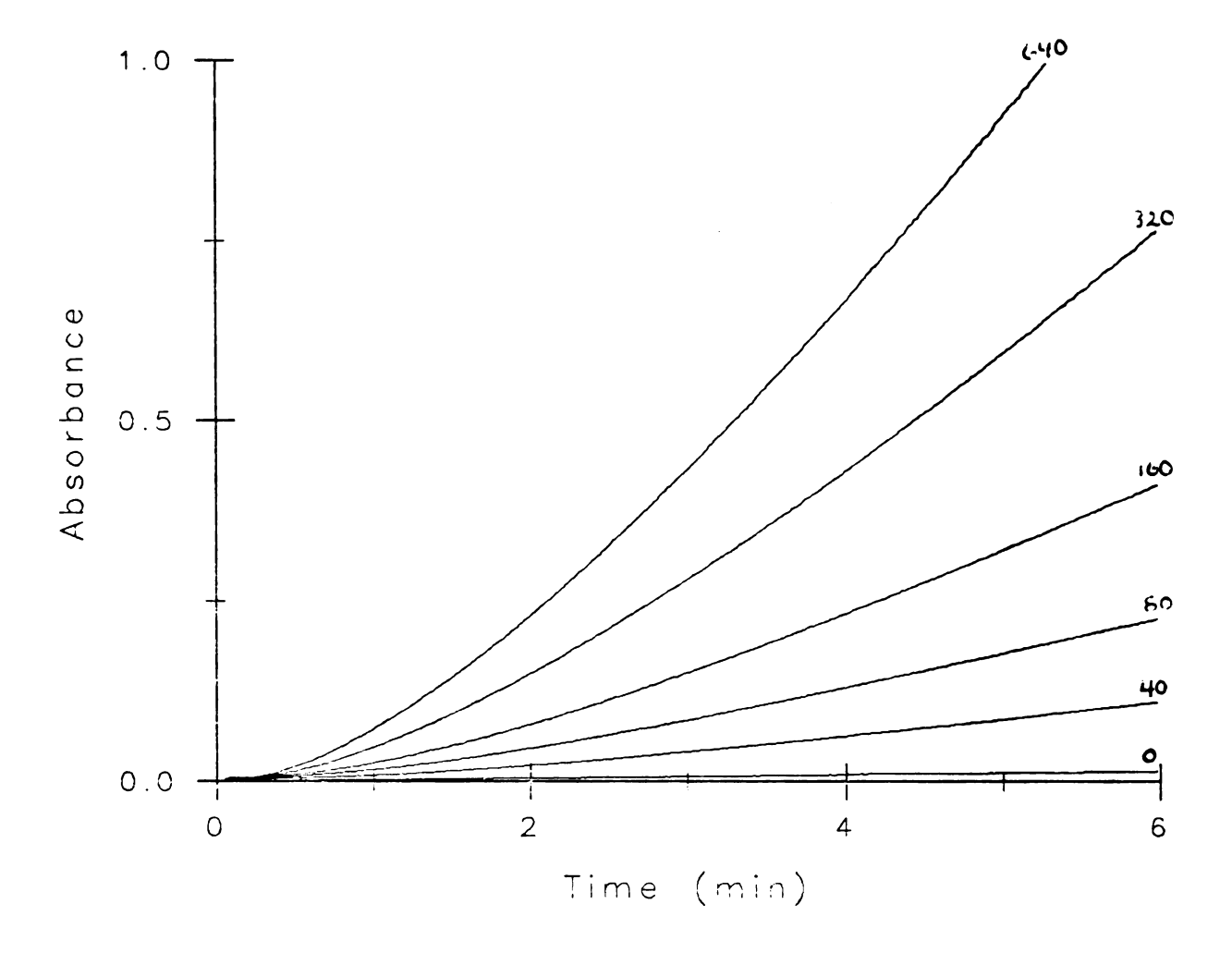


Figure 3.17. Progress curves obtained with the 2 mm i.d. reactor. The glucose concentrations (mg/L) which were used are written at the end of each curve.

The enzyme concentration also changes with the reactor radius. The concentration is directly dependent on the surface-to-volume ratio or 1/r. The increase in reactor radius from 0.5 mm to 1.0 mm could decrease the reaction rate and also change the ratio of the enzyme rate constant to the diffusion rate constant. In these ways, variation in reactor radius can change the kinetics indirectly. To keep the enzyme concentration constant with changes in reactor radius, additional enzyme should be bound to tubes of larger diameter.

The stopped-flow instrument should provide a fairly direct route to the determination of inherent enzyme properties. By varying the reactor diameter and enzyme concentration, information about the enzyme reaction and diffusional influences should be obtainable. Reactors from these studies under static conditions can then be incorporated into a continuous flow manifold. Differences in kinetics between the two systems can be attributed to the change in mass transport, from diffusion to primary and secondary flow. Thus, definitive information concerning continuous flow systems with integrated opentubular immobilized enzyme reactors should be forthcoming. Much more research on the kinetics of such reactors is needed.

CHAPTER 4

Colorimetric Determination of Glucose Based on Immobilized Glucose Oxidase

The determination of blood glucose is the most frequently performed test in clinical laboratories. Because glucose is the major energy source for living cells, any variation in the concentration of this sugar has a large effect on cell function. The most common disease related to carbohydrate metabolism is diabetes mellitus; nearly two percent of the U.S. population has this disease [95]. Glucose assays can reveal such abnormalities, and then treatment of the illness can begin.

Glucose is a monosaccharide, containing six carbon atoms. The structure of D-glucose, the form that is found in nature, is shown in Figure 4.1. The D-form has the hydroxyl group on carbon #5 on the right side of the carbon chain. The aldehyde group and the hydroxyl group on carbon #5 react to form a hemiacetal and a six-membered ring. The carbon #1 atom becomes asymmetric and, thus, can exist in two anomeric forms, α and β , shown in Figure 4.1. Mutarotation of glucose occurs slowly in aqueous solution [96,97]. At equilibrium, the D-glucose exists as 64% α -form, 36% β -form, and traces of the free aldehyde form [95,98,99]. The normal range of blood glucose concentrations is 70-105 mg/dL or 3.9-5.8 mM [95].

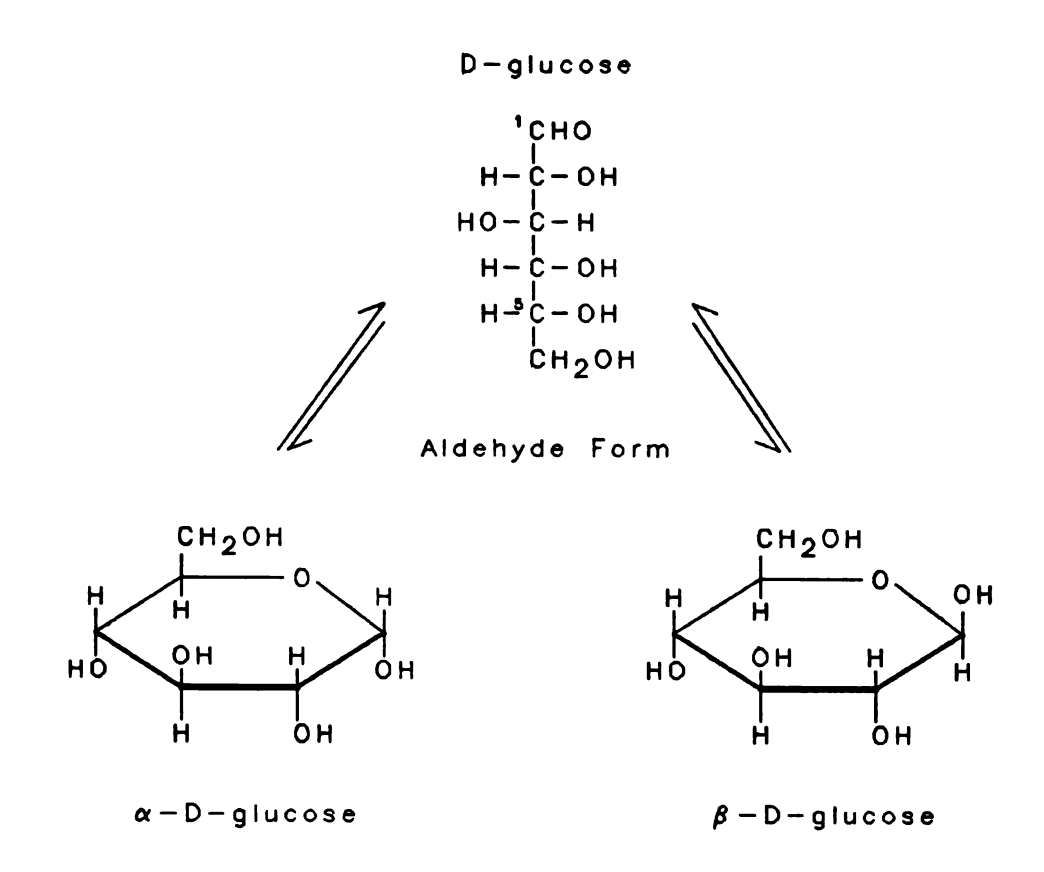


Figure 4.1. The three forms of D-glucose.

Because the determination of glucose has been so important for so many years, a large number of methods have been used. Non-enzymatic methods are based on the reducing nature of D-glucose and include reactions with ferricyanide ion, cupric ion, and o-toluidine [95]. These methods are sensitive but relatively non-specific. The enzymatic methods are much more selective. A list of the three common enzymatic systems is given in Figure 4.2. These systems have been used in immobilized forms. The hexokinase/glucose-6-phosphate dehydrogenase method has been adopted for use in the Technicon SMAC instrument, the major clinical analyzer in hospital laboratories.

In this study, the glucose oxidase method was used for several reasons. First, the enzyme has a high K_m value for glucose. This property ensures a large analytical range of glucose concentrations. Second, the enzyme and other reagents necessary for the assay are relatively inexpensive. The hexokinase and glucose dehydrogenase methods require β -NAD, which is expensive. Furthermore, commercial preparations of the enzymes are more than fifty times as expensive as glucose oxidase [103]. The reason that these other methods are used is that they are somewhat less susceptible to chemical interferences. Another reason glucose oxidase was chosen is its high specific activity (up to 150,000 Units/g) and the fact that it bonds well to nylon tubing. Therefore, glucose oxidase is well-suited

1) β -D-glucose + β -NAD - $\frac{GLDH}{-}$ δ -D-gluconolactone + β -NADH

pH optimum = 7.6 [100] Measure β -NADH absorbance at 340 nm

2) D-glucose + PO $_4^{3-}$ -- $_{---}^{HK}$ D-glucose-6-phosphate

D-glucose-6-phosphate+ β -NAD GL-6-PDH \rightarrow 6-phospho-D-gluconate + β -NADH

pH optimum = 8.5 [101] Measure β -NADH absorbance at 340 nm

3) β -D-glucose + H_2O + O_2 --GO δ -D-gluconolactore + H_2O_2

pH optimum = 6.0 [102] Measure hydrogen peroxide conc.

GLDH: glucose dehydrogenase (E.C. 1.1.1.47)

HK: hexokinase (E.C. 2.7.1.1)

GL-6-PDH: glucose-6-phosphate dehydrogenase (E.C. 1.1.1.49)

GO: glucose oxidase (E.C. 1.1.3.4)

Figure 4.2. The reactions involved in the enzymatic assays for glucose.

for use in immobilized form.

Most assays using glucose oxidase are based on the increase in concentration of peroxide or the depletion of dissolved oxygen. Electrochemical methods have involved an alternate oxidizing agent, p-benzoquinone [102,104], the measurement of the decrease in oxygen concentration with an oxygen electrode [105,106], and amperometric sensing of the production of hydrogen peroxide [107-109]. Luminescence methods include the reaction of peroxide to give chemiluminescence [110], the reaction of peroxide and homovanillic acid to yield a fluorescent compound [111], and the measurement of oxygen via its ability to quench the fluorescence of pyrene [112]. A novel method based on the absorbance or fluorescence of β -NADH using additional enzymes, catalase and aldehyde dehydrogenase, has also been described [113].

Most often, colorimetric methods are used. Hydrogen peroxide, in the presence of peroxidase, can oxidize many aromatic compounds to give colored products. Under the proper conditions, the absorbance of these molecules is proportional to the initial D-glucose concentration. A variety of color-forming reactions have been used; some are listed in Table 4.1. Note that two of the methods do not require peroxidase, making then less costly and less susceptible to chemical interferences. A recent study presented several more water-soluble reagents for reaction with

Table 4.1. Chromogens for Reaction with Hydrogen Peroxide

Chemical System	λ _{max} ε	c(AU M ⁻¹ cm ⁻¹)	Reference
AAP-DCPS	510	5 x 10 ⁴	94,114,115
AAP-HB	500	-	116
DPAS	465	~3 x 10 ¹	117
MBTH-CTA	572	-	118
MBTH-DMA	590	-	101,119,120
o-Dianisidine	410	-	121
o-Toluidine	630	-	93
KI/MoO_4^{2-*}	365	2 x 10 ⁴	85
Xylenol orange*	582	2.5 x 10 ⁴	122

AAP: 4-aminoantipyrine CTA: Chromotropic acid

DCPS: 2,4-dichlorophenol sulfonate

DMA: N-N-dimethylaniline DPAS: p-diphenylamine sulfonate

HB: p-hydroxybenzoate

MBTH: 3-methyl-2-benzothiazolinone hydrazone

^{* -} peroxidase is not required

hydrogen peroxide [123]. The multitude of available chromogenic agents reveals the fact that no one method is significantly better than the others.

The 4-aminoantipyrine (AAP) - 2,4-dichlorophenol sulfonate (DCPS) system was chosen for this study. The product has a high molar absorptivity, the reaction occurs rapidly, and the reagents are readily available and water soluble. A comparative study of eight chromogens showed that systems involving AAP were most suitable [124]. Also, a variety of phenolic compounds are acceptable coupling agents for AAP [125]. Trinder and coworkers first reported the use of AAP-DCPS in the determination of glucose [90,91]. Since that time, the reagent was been termed the Trinder reagent and has enjoyed wide use.

This chapter describes the characterization of an immobilized glucose oxidase/Trinder determination of glucose. The chemical reactions and continuous flow instrumentation involved in this study are reported in Section A. The Trinder color-forming reaction is explored in more detail in Section B. Next, experiments concerning the effect of reactor design on the assay sensitivity (Section D) and the characterization of the glucose oxidase reaction (Section C) are discussed. Finally, the sensitivity of the determination was improved by adding sodium azide to the system. The reasons for doing this are given in Section E.

- A. The Method and Instrumentation
- 1. The glucose oxidase reaction

The reaction which is catalyzed by immobilized glucose oxidase, the analytical reaction, is given below.

$$\beta$$
-D-glucose + O_2 + H_2O + δ -D-gluconolactone + H_2O_2 (4.1)

The enzyme is specific for the β -form of the substrate. Glucose oxidase reacts much more slowly with the α -form and other sugars [126]. The enzyme considered here is extracted from <u>Aspergillus niger</u> and contains two flavine adenine dinucleotide (FAD) groups per molecule [127]. The reaction involves only the fully oxidized and fully reduced forms of the enzyme in the following manner [128].

E-FAD +
$$\beta$$
-D-glucose $\stackrel{\rightarrow}{\leftarrow}$ E-FAD-glucose
E-FAD-glucose + H_2O $\stackrel{\rightarrow}{\leftarrow}$ E-FADH $_2$ + δ -D-gluconolactone
E-FADH $_2$ + O_2 \rightarrow E-FAD + H_2O_2

The mechanism is a ping-pong bi-bi type, and, consequently, the rate equation is of the following form.

$$v = k_e[E]_o/(1 + K_m^G/[Glucose] + K_m^O/[Oxygen])$$
 (4.2)

The reported kinetics constants for glucose oxidase have recently been reviewed [129]. The mean values for K_m^G , K_m^O , and k_e are 9 x10⁻² M, 6 x10⁻⁴ M, and 1.2 x10² s⁻¹ respectively. Several compounds have been found to be inhibitors: 8-hydroxyquinoline, sodium nitrate,

semicarbazide [128], α -D-glucose [130], and hydrogen peroxide [131], among others.

The glucose oxidase preparations used here were purchased from Sigma Chemical Company. Type II enzyme, obtained several years ago, was used for the studies reported in Sections A-D of this chapter. The enzymes used in the experiments described in Section E were all purchased in 1982. This distinction is important because the two lots of enzymes displayed different properties.

2. The Trinder/peroxidase reaction

Because neither the substrates or the products of the analytical reaction absorb light in the visible region, a second, color-forming reaction is required. Hydrogen peroxide is a good oxidizing agent $(H_2O_2 + 2 H^+ + 2 e^- + 2 H_2O, E^\circ = 1.77 V)$, and is usually chosen for further reaction. The reaction of hydrogen peroxide and a hydrogen donor is slow, however, so a soluble enzyme, horseradish peroxidase, is used as a catalyst. The reaction mechanism is given below [132,133].

$$E + H_2O_2 \stackrel{?}{\leftarrow} Complex I$$
 $Complex I + AH_2 \stackrel{?}{\leftarrow} Complex II + AH$
 $Complex II + AH \rightarrow E + A + 2 H_2O$

Here AH_2 represents the hydrogen donor. Excess peroxide can combine with Complex II to produce an inactive enzyme species. The substrate specificity of the free enzyme is

high; only peroxide, formic acid, and acetic acid yield complexes that are active [133]. However, the specificity of the enzyme-substrate complexes is poor. Many hydrogen donors can participate, including phenols, aromatic amines, ascorbic acid, and leucodyes.

The overall reaction in the case of the Trinder reagents is given below.

The exact coupling mechanism of the two organic compounds is not known. A possible mechanism is that each reagent first loses two electrons and two hydrogen ions to the hydrogen peroxide, forming water and a reactive intermediate. Then the intermediates instantaneously react to form the dye product. Therefore, two hydrogen peroxide molecules and, consequently, two glucose molecules are required for the production of one molecule of dye. This fact is important when the molar absorptivity of the product or the percent glucose conversion is calculated.

The peroxidase used in the following experiments was purchased in 1982 from Sigma (Type II) and contained about 200 Units/mg of solid.

3. The continuous flow manifold

The analytical and color-forming reactions occur in the manifold of a continuous flow instrument. The reagents

are added, mixed, and reacted in a flowing, gas-segmented, liquid stream. Figure 4.3 is a diagram of the reaction manifold, showing the order and rate in which the reagents are added. A peristaltic pump meters the reagents. The composition of the reagents is considered below in the order in which they are added to the flow stream.

Sample and Wash Reagents. In continuous flow methods, the samples and another liquid are alternately injected into the flowing liquid stream. This other liquid is called the "wash" solution, and in the following studies was distilled, deionized water (DDW). The wash solution minimizes sample carryover by rinsing the manifold tubing and flow cell between consecutive samples. The sample:wash timing was usually 40 seconds:20 seconds. Thus, the sample throughput was 60 samples/hour.

The samples were either hydrogen peroxide or glucose standards. A hydrogen peroxide stock solution was prepared by diluting 0.50 mL of 30% peroxide solution to 0.500 liters with DDW. This solution was standardized by reaction with acidic KI and subsequent titration with standard thiosulfate [134]. Working standards were made daily by appropriate dilution of the stock solution with DDW. The primary glucose standard was prepared by dissolving 2.000 g of anhydrous, granular α -D-glucose and 0.5 g of benzoic acid in about 750 mL of DDW contained in a 1.000 L volumetric flask. The resulting soultion was then diluted to the

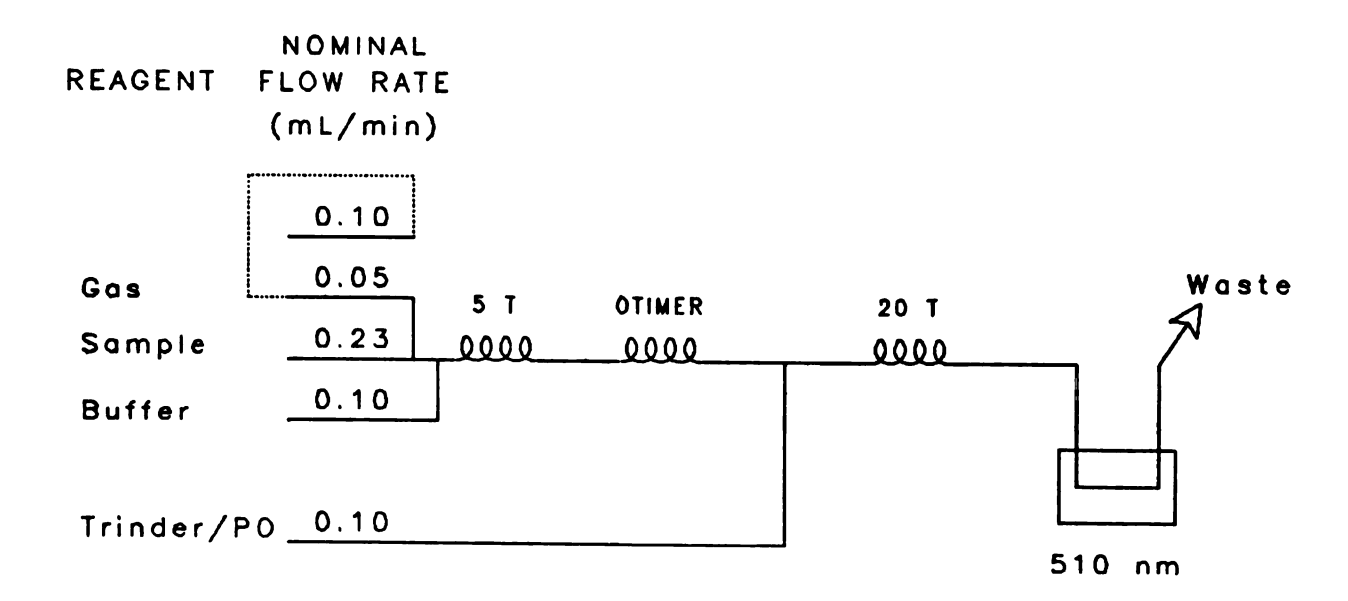


Figure 4.3. The continuous flow reaction manifold.

The pump speed setting which gave nominal flow rates was 42.

mark with DDW and allowed to stand at room temperature for 24 hours to ensure complete mutarotation. Working glucose standards were prepared by appropriate dilution of the primary standard with DDW. The hydrogen peroxide and glucose stock solutions were stored in a refrigerator at 4 °C.

Gas Segments. The sample and wash slugs were segmented with gas bubbles using dual pump tubes. The "helper" tube at a nominal flow rate of 0.10 mL/min builds up pressure in the second, smaller i.d. tube, and the bubbles are forced rapidly into the liquid stream. This procedure helps phase the segmentation with the pump roller lift-off. Phasing of the gas bubbles improves the system characteristics. Room air was used unless otherwise noted. The segmentation rate was 1.67 bubbles per second at a pump speed setting of 42.

Buffer Reagent. The next reagent added to the manifold is a buffer which provides the optimal hydrogen ion concentration for the enzymatic reactions. Potassium phosphate buffers (0.1 M) were used in these studies. The pH optimum of the chemical system was found to be 6.85. The experimental evidence is presented in Figure 4.4. Several drops of Brij-35 wetting agent were always added to the pH 6.85 buffer. This agent promoted pulseless flow through the manifold and preserved the integrity of the gas bubbles.

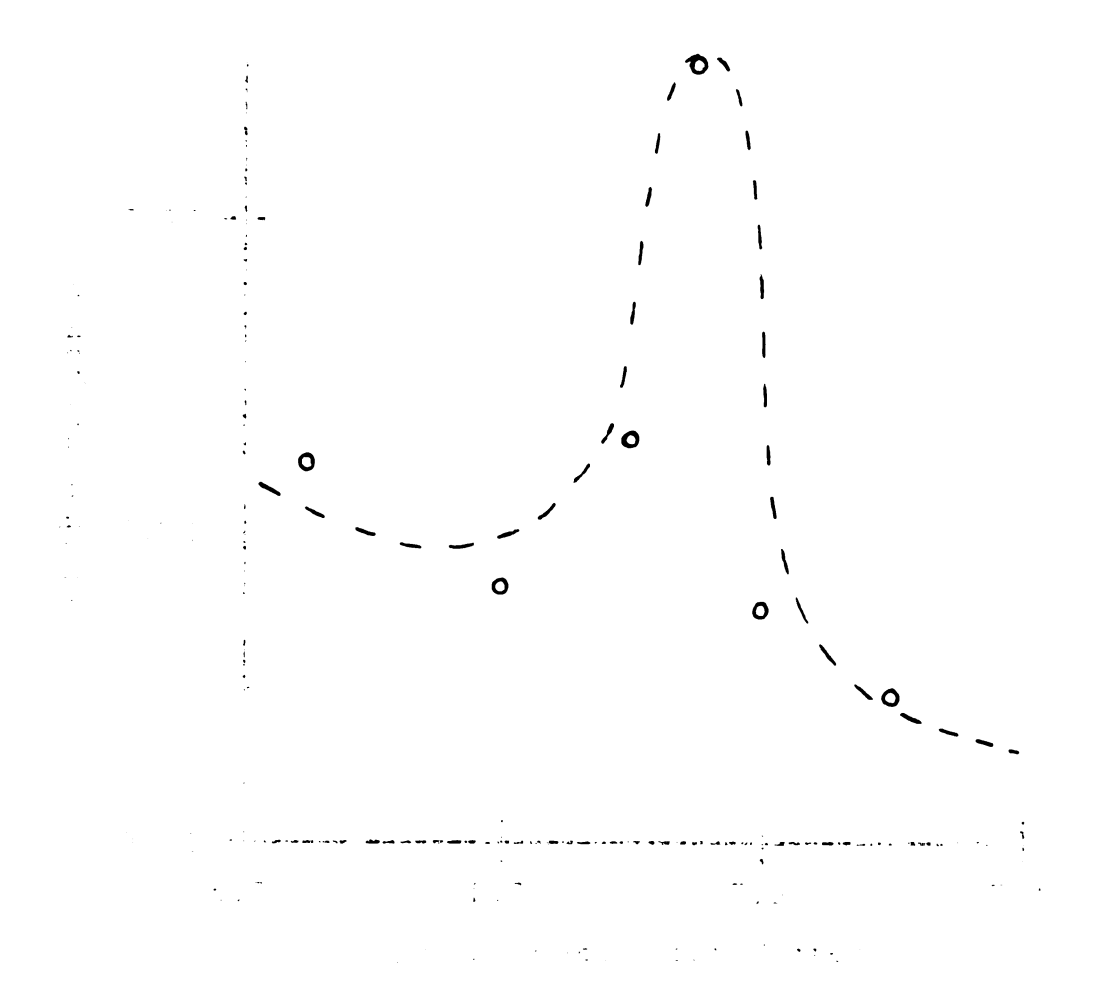


Figure 4.4. The pH dependence of the glucose assay.
A 0.1 M phosphate buffer was used to control the pH. The dotted line indicates the approximate relationship in the absence of many data points.

Glucose Oxidase Reactor. After mixing in a five-turn glass coil, the sample and buffer were directed into the immobilized enzyme reactor. The preparation of the glucose oxidase reactor was detailed in Chapter 2, Table 2.3. The analytical reaction occurred in the presence of the bound glucose oxidase. The percentage of glucose that was reacted in the enzyme loop was never more than 10%. The product, hydrogen peroxide, was swept out of the reactor by the flowing liquid stream.

Trinder/Peroxidase Reagent. Finally, the Trinder/ peroxidase reagent was added. The reagent was prepared as follows. A 10 mM stock solution of 4-aminoantipyrine (AAP) was pepared by dissolving 1.02 g of the solid (Sigma) in 0.500 L of DDW. A 10 mM stock solution of 2-hydroxy-3,5-dichlorobenzenesulfonate was prepared by dissolving 1.33 g of the solid (Research Organics) in 0.500 L of DDW. The working reagent was made by dispensing 5.00 mL of each of these stock solutions and 5 mg of peroxidase into a 50.0 mL volumetric flask and then diluting to the mark with the pH 6.85 phosphate buffer. This composite reagent was prepared daily. A 20-turn mixing coil (about 100 seconds residence time at nominal flow rates) was used at the exit end of the manifold to ensure a complete reaction between the peroxide and the Trinder reagents. The pink dye was then passed into the flow cell.

4. The continuous flow instrument

A modular single-channel continuous flow instrument, diagrammed in Figure 4.5, was used in all of the experiments. A Brinkmann IP-12 peristaltic pump, modified to accommodate sixteen rollers, was used to proportion the reagents. The pump speed setting that provided nominal flow rates was 42. This speed was used unless otherwise mentioned. The manifold was constructed from 1.0 mm i.d. glass mixing coils, injector fittings, and a 1.0 cm flow cell (0.5 mm i.d., Technicon). Sampling was performed manually.

The colorimeter was designed and built in this laboratory. The light source was a miniature tungsten-halogen lamp (Model 03000, Welch-Allyn), and the light was transmitted to the flow cell via a glass fiber optic bundle (Model EK15-12, Dolan-Jenner). Wavelength selection was accomplished with a 510 nm interference filter (Ditric Optics, bandpass = 8 nm) mounted between the exit window of the flow cell and the detector. The detection system consisted of a photodiode (Princeton Applied Research) and an operational amplifier current-to-voltage converter. A bubble-gate removed the air segments electronically [135].

The data were collected and stored on a strip-chart recorder or in RAM by a microcomputer [86]. The data stored in the microcomputer were shipped to a PDP-8/e (Digital Equipment Corporation) minicomputer following each experiment for long-term storage and computation of the

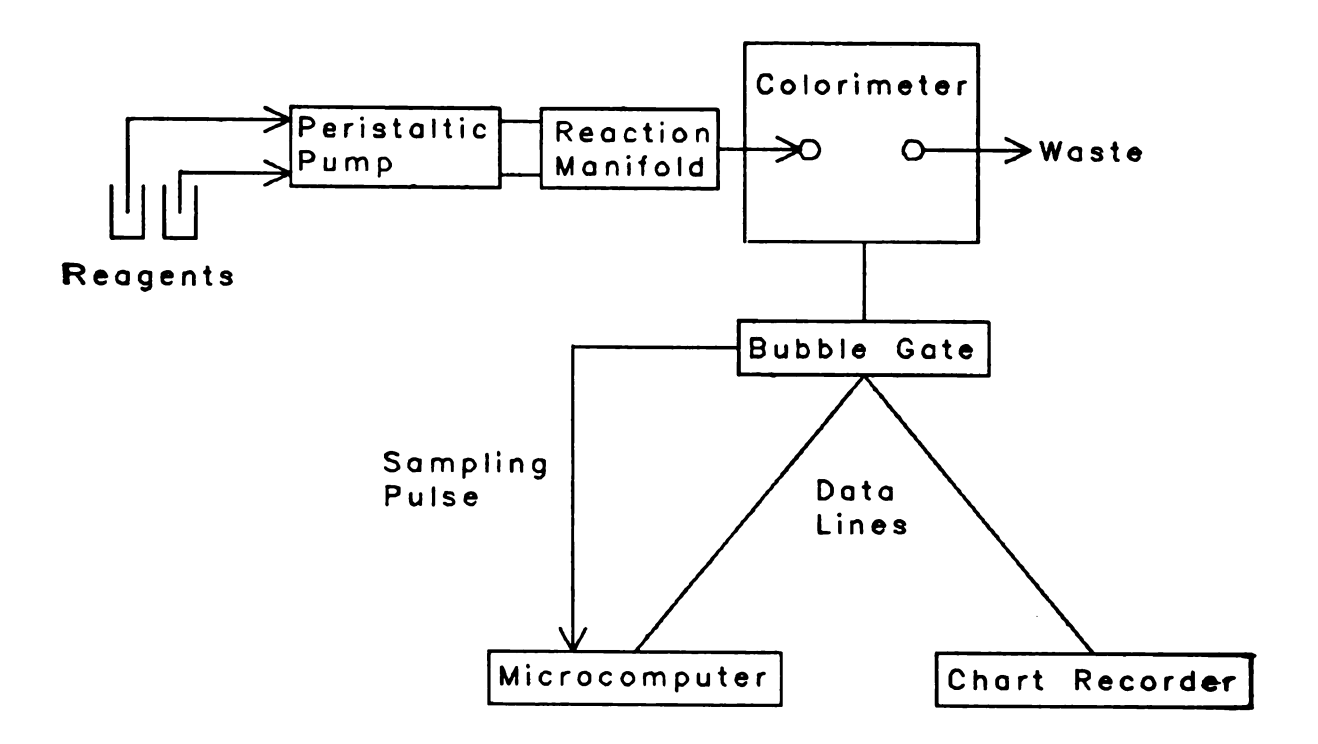


Figure 4.5. Diagram of the continuous flow instrument.

steady-state absorbance values. The data were initial sample concentrations and their associated absorbance values. In most cases, a calibration curve of absorbance versus analyte concentration was constructed for a series of standards. The slope of the calibration curve was used as a measure of the immobilized enzyme activity. A larger slope meant that the assay conditions had improved.

B. Experimental Studies of the Trinder Reaction

With coupled enzyme reactions, the rate of one of the reactions can be measured accurately (< 2% error) if the two reaction rates differ by a factor of 50 or more. Consequently, the Trinder reaction must occur at a high velocity so that the measured rate depends strictly on the glucose oxidase reaction. Another way to prevent errors is to allow the indicator reaction to go to completion. This is only possible, however, when the two reactions are separated in time, as they are in this determination. Thus, conditions were adjusted so that the color-forming reaction went to completion.

The concentrations of the Trinder reagents and the peroxidase were set as high as possible without unduly increasing the cost of the assay. An indicator reagent containing 6 mM AAP, 5 mM DCPS, and 80 Units/mL of peroxidase was prepared and used in the continuous flow manifold. Likewise, 1:5 and 1:10 dilutions of this reagent

were prepared and used. The least concentrated reagent only produced a 3% smaller instrumental response than did the most concentrated. Thus, concentrations of 1 mM AAP, 1 mM DCPS, and 20 Units/mL of peroxidase were chosen as optimal; the reaction approached completion without wasting reagents.

The optimal reaction time for the Trinder reaction was determined. With peroxide standards as the sample and the glucose oxidase reactor removed, the effect of reaction time on the instrumental response was small but noticeable. Assuming that the reaction was complete after 200 seconds, 96% of the 50 μ M $\rm H_2O_2$ sample was reacted within the first 100 seconds. Even at a pump speed setting of 56 and a 20-turn glass mixing coil in place (about a 70 second reaction time), the reaction was more than 90% complete.

Results of stopped-flow studies of the Trinder reaction, shown in Figure 4.6, revealed that reactions with peroxide solutions of 50 μ M or less were more than 90% complete in about thirty seconds. The Trinder reagent and peroxidase concentrations were the same as described in Section A. The hydrogen peroxide, 0 - 50 μ M, reacted according to pseudo-first order reaction kinetics, with a rate constant of 0.09 sec⁻¹. This confirmed that the Trinder reagents were in large excess and that the mechanism involving a single peroxide molecule, given above, is correct. In all the studies presented here, the Trinder reaction was made to

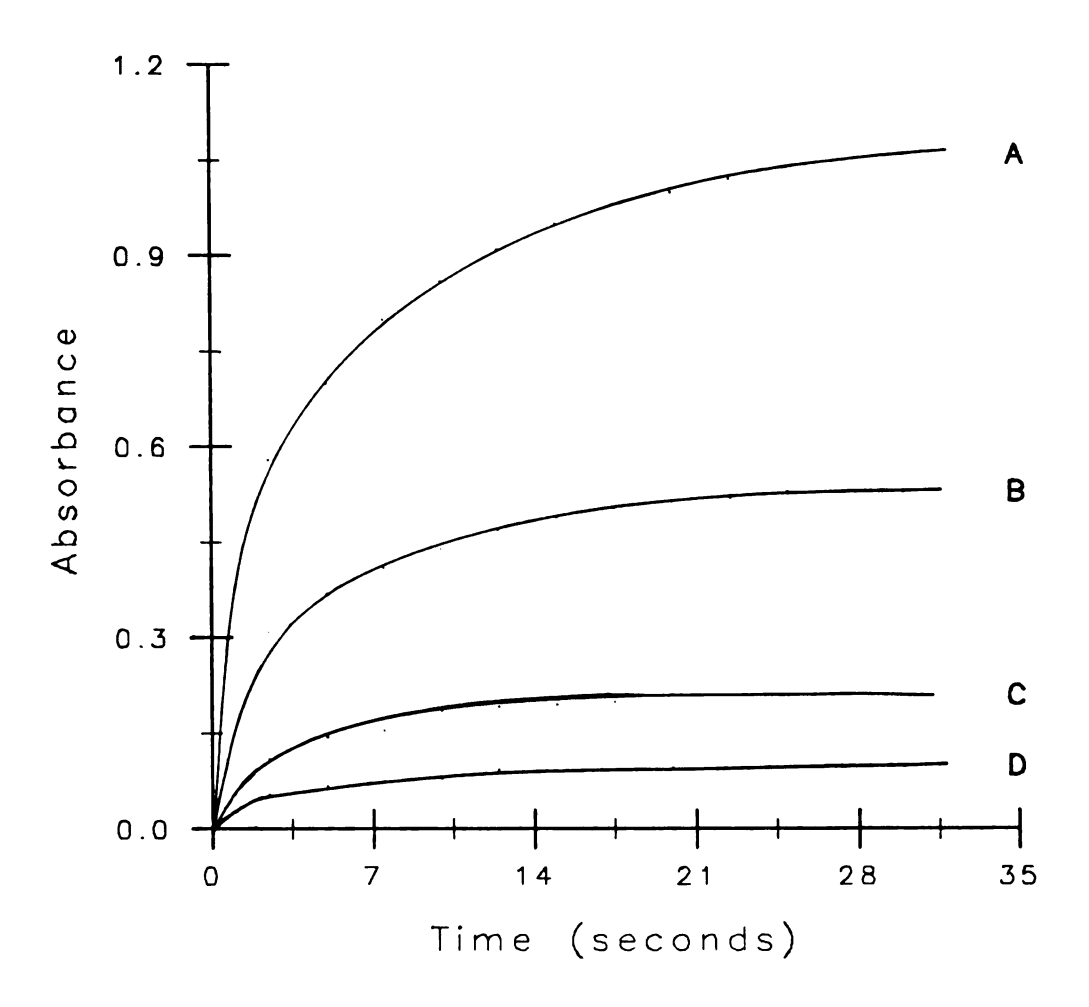


Figure 4.6. Progress curves for the reaction of hydrogen peroxide and the Trinder reagent. The peroxide concentrations were 50 μ M (A), 25 μ M (B), 10 μ M (C), and 5 μ M (D).

approach completion with the use of excess reagents and long reaction times.

The molar absorptivity of the Trinder product was determined. A series of hydrogen peroxide solutions of known concentration were tested, and the resulting steady-state absorbance values were recorded. To account for dilution in the manifold, the actual flow rates were calculated by weighing the amount of water delivered by the various pump tubes over a known period of time. The molar absorptivity at 510 nm was calculated to be $5 \pm 1 \times 10^4$ AU $\,\mathrm{M}^{-1}\,\mathrm{cm}^{-1}$. This does not compare well with the value of 1.2×10^4 AU $\,\mathrm{M}^{-1}\,\mathrm{cm}^{-1}$ reported in the literature [136]. The reason for this discrepancy is not known.

In almost all reports concerning the GO/Trinder assay, several substances are mentioned as interferences. Uric acid, ascorbic acid, gentisic acid, and L-DOPA are most often cited [94,115,136,137]. These interferences occur primarily because the peroxidase-peroxide complex does not react specifically with a single reducing agent. The severity of the problem can be lessened by performing a protein precipitation on the serum sample. A common precipitating agent for glucose assays is the Somogyi reagent [138]. A stepwise treatment with Ba(OH)₂ and then ZnSO₄ precipitates the proteins along with uric acid and other metabolites, but ascorbic acid remains in the supernatant.

Ascorbic acid, added to the CF manifold, lowered the instrumental response. Figure 4.7 reveals the effect of ascorbate on the apparent peroxidase activity. The glucose oxidase reactor was not used, and a series of peroxide standards were sampled. The loss in assay sensitivity may be due to inhibition of peroxidase, loss of peroxide, or other factors. Stopped-flow studies were performed to determine the exact nature of the ascorbate interference. Ascorbic acid absorbs light at 261 nm; its oxidized form does not [93]. By monitoring the decrease in the ascorbate concentration, it was found that hydrogen peroxide and ascorbic acid react rapidly, but only in the presence of peroxidase. Thus, ascorbate lowers the concentration of peroxide in the glucose assay. Further evidence was provided by studying the formation of the Trinder product in the presence of ascorbate. A lag phase which increases with increasing ascorbate concentration is evident in Figure 4.8. The rate constants, measured after the lag period, were nearly independent of the ascorbate concentration. facts suggest that ascorbate acts as an alternate substrate for peroxidase and, in this way, inhibits the enzyme.

The problem of removing the ascorbate interference is a difficult one. Prior oxidation to dehydroascorbic acid is possible, but this risks oxidation of the glucose. Also, remaining oxidizing agents may react with the Trinder solution. One researcher has used ascorbate oxidase to remove

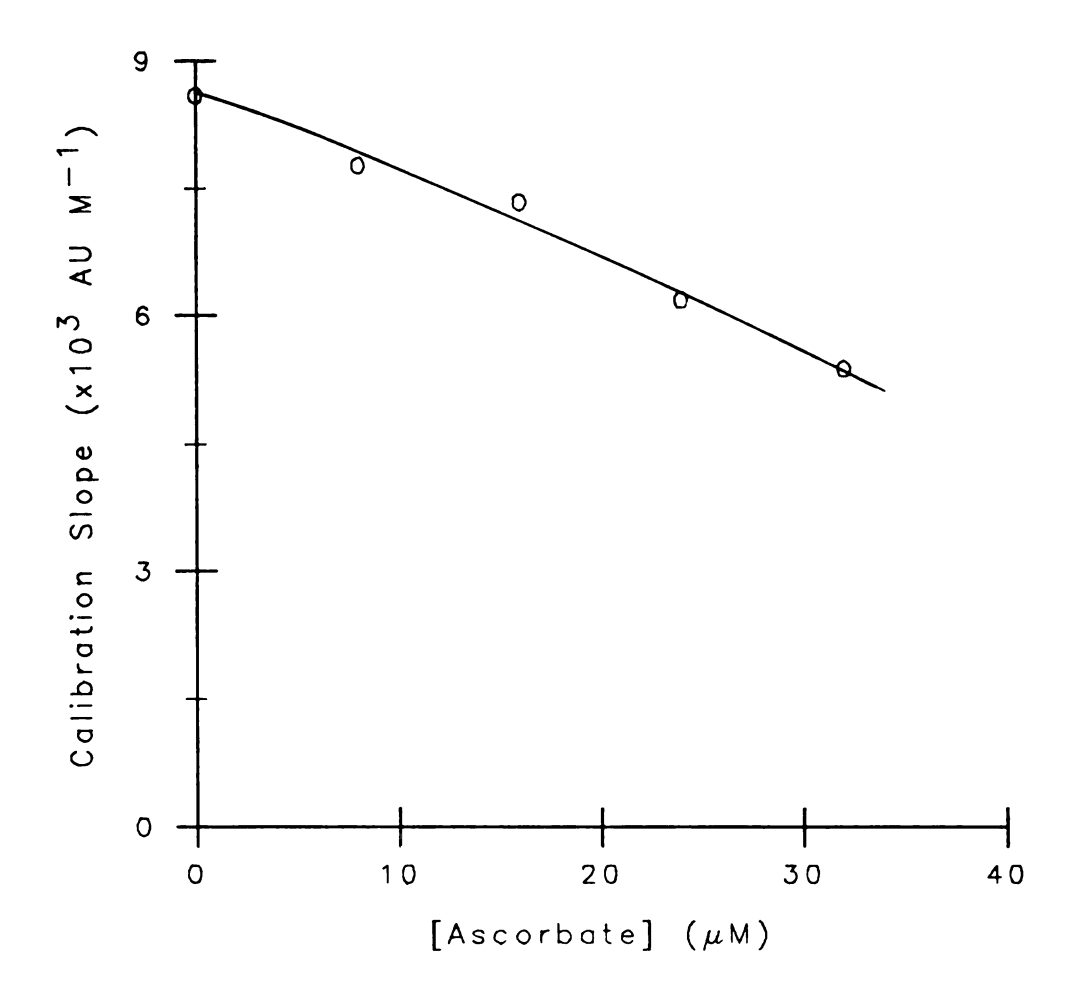


Figure 4.7. The effect of ascorbate concentration on the assay sensitivity.

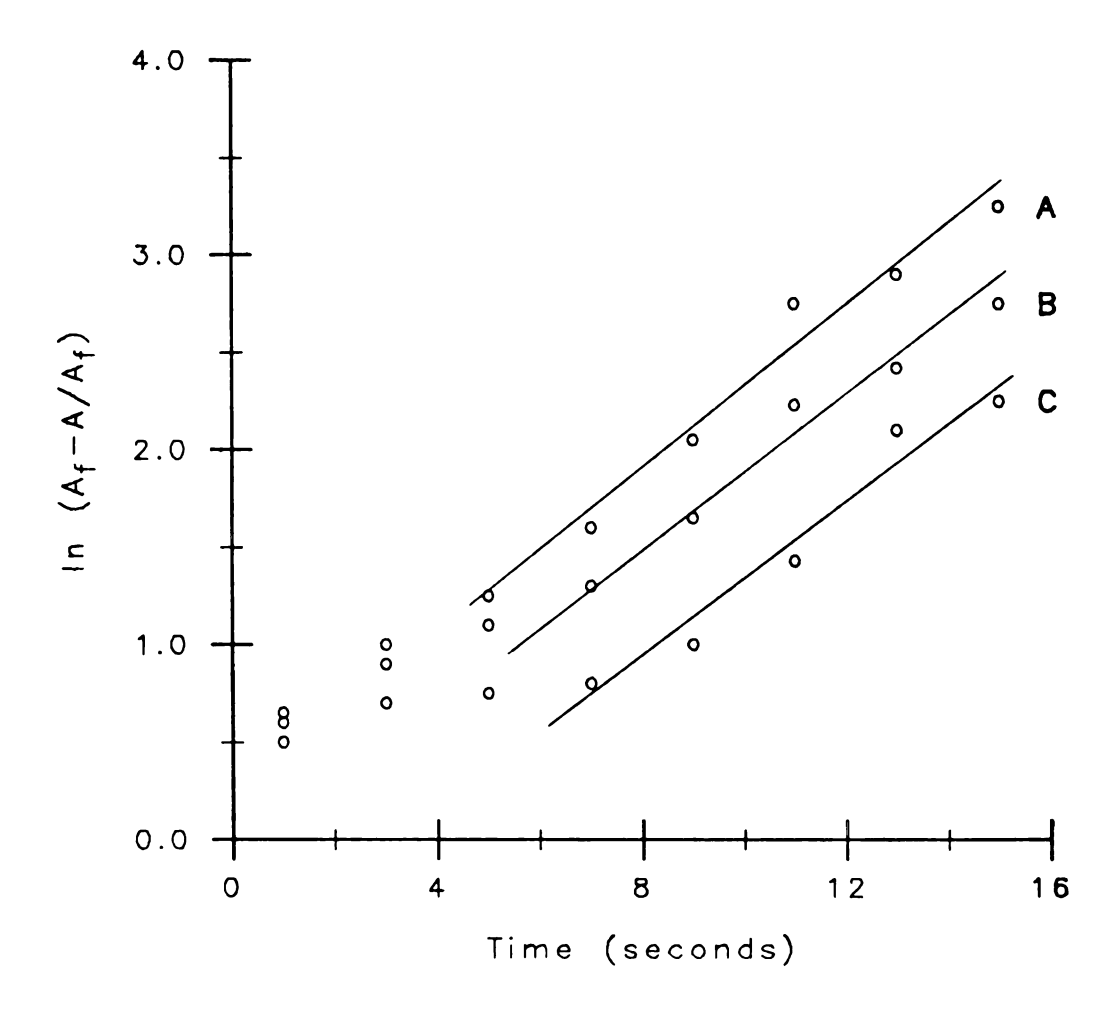


Figure 4.8. First order plots of data for the hydrogen peroxide-Trinder reaction in the presence of ascorbate. The ascorbate concentrations were 10 μM (A), 20 μM (B), and 40 μM (C). A was the absorbance at equilibrium, and A was the absorbance at any time, t.

ascorbic acid [136], but this approach is very expensive. A satisfactory solution has not been found.

- C. Reaction Characteristics
- 1. Segmentation gas composition

In analytical reaction rate determinations, a linear relationship between the rate and the analyte concentration must be established. In the case of glucose, the Trinder reaction has a negligible effect, and, thus, the reaction rate is described by equation 4.2. In order to attain a rate that is only proportional to the glucose concentration, the oxygen concentration must be larger than 20 $K_{\rm m}^{\rm O}$ or 1 x10 $^{-2}$ M, and the glucose concentration must be smaller than $K_{\rm m}^{\rm G}/20$ or 4.5 x10 $^{-3}$ M.

The concentration of glucose after dilution or dialysis of the sample is usually well below 4.5 mM. The concentration of oxygen in 0.1 M phosphate buffer saturated with air is 0.26 mM at 22 °C [139]. This value is less than the K_m^O value, and, therefore, linear calibration curves should not be possible. This is not the case, however. A large source of oxygen is provided by the air bubbles which segment the liquid stream. To prove this, the effect of segmentation gas composition on the determination was studied.

The manifold and reagents were used as described in Section A. The gases, $\rm N_2$ and $\rm O_2$, were bled from pressurized tanks and allowed to fill a large bottle. The

appropriate pump tube was placed in the bottle. Room air was the source of air. A series of glucose standards was sampled, and the resulting calibration curves are shown in Figure 4.9. When the assay is entirely dependent on dissolved oxygen, the analytical range of glucose concentrations is limited to 0.5 mM or less. The linearity improves with increasing oxygen concentration. With air segmentation, samples containing less than about 3 mM glucose can be tested; this is well within the range for blood glucose analysis.

The gas composition also affected the continuous flow peak shapes. When nitrogen gas was used, large spikes occurred at the falling edges of the peaks. See Figure 4.10. These spikes were due to air bubbles which entered the sampling system as the probe was moved between the sample and wash solutions. With the extra oxygen, the reaction could occur to a greater extent. Small spikes also occur with the use of air segments.

2. The effect of ionic strength

The ionic strength of the solution passing through the glucose oxidase reactor had little effect on the enzyme activity. The usual continuous flow manifold was used. The buffer concentration was lowered to 1.0 mM, so that the ionic strength was controlled by adding KCl to the sample and wash solutions. Chloride ion is not known to affect either of the enzymatic reactions. The ionic strength

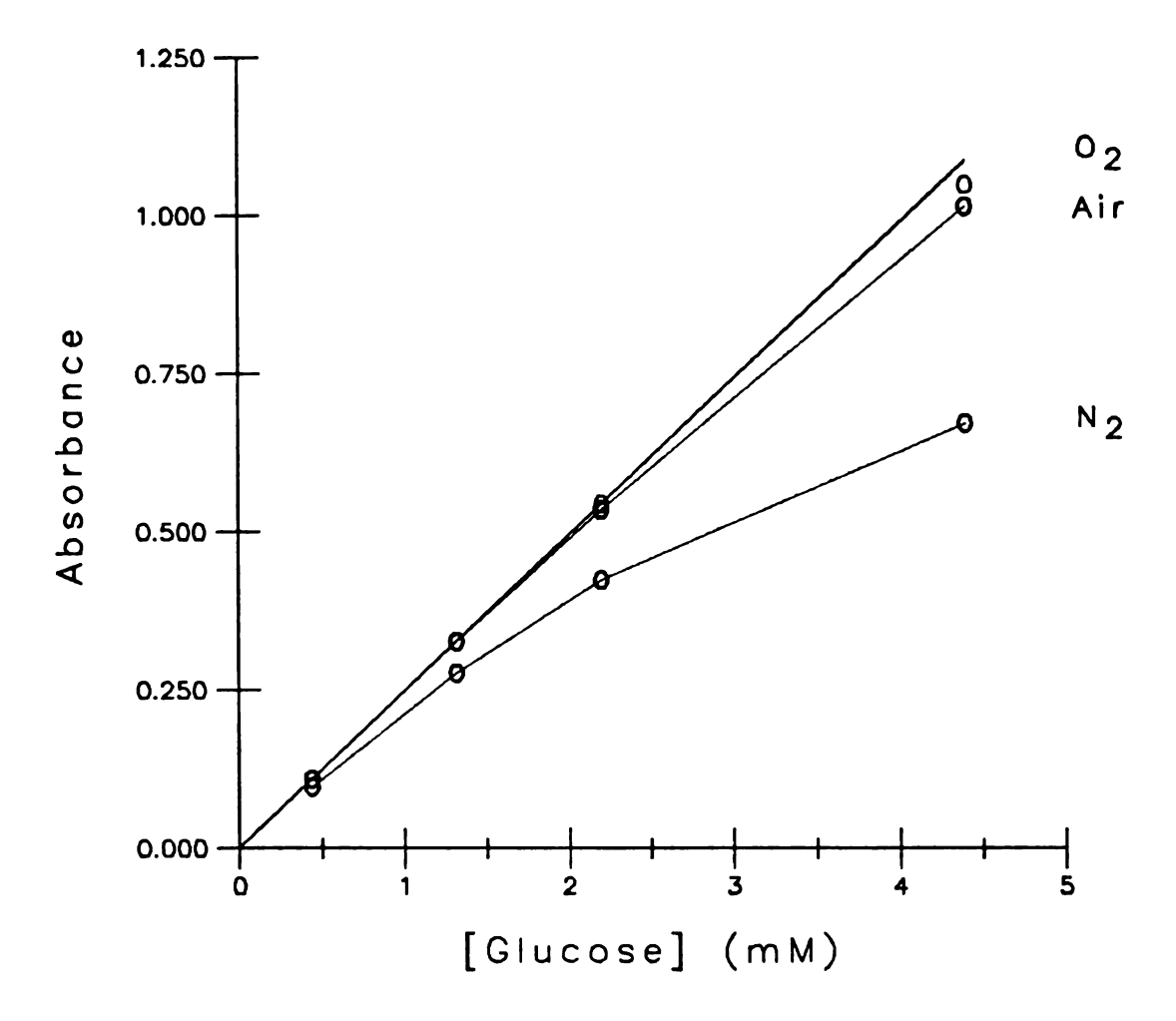


Figure 4.9. Calibration curves for a series of glucose standards using three different segmentation gases: N_2 , Air, O_2 .

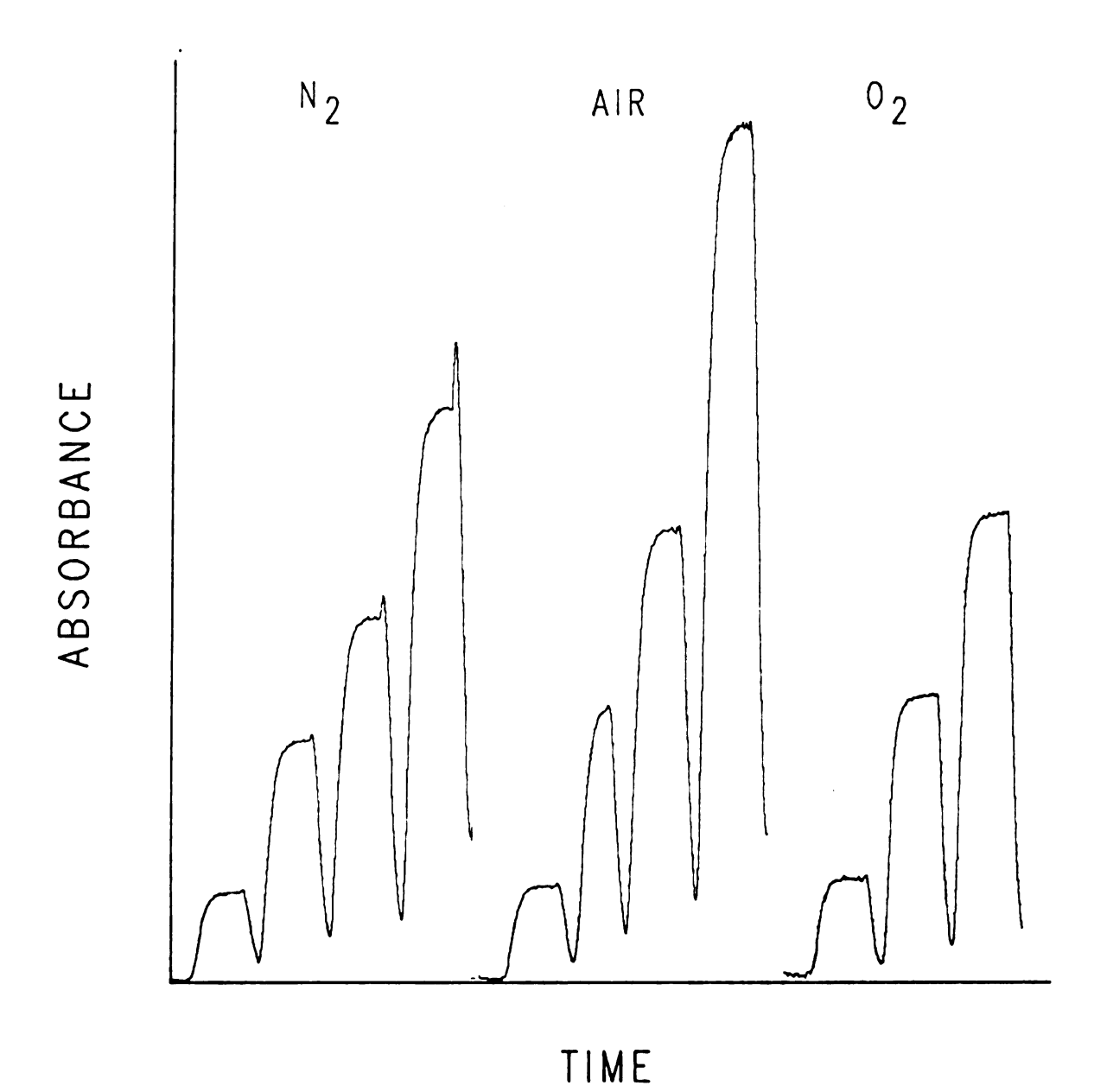


Figure 4.10. The output from the continuous flow instrument using three different segmentation gases. The glucose concentrations were 0.44 mM, 1.44 mM, 2.22 mM, and 4.44 mM. Only the first three concentrations were sampled using $\mathbf{0}_2$.

through the final mixing coil, in which the colorforming reaction occurred, was held nearly constant by
preparing the Trinder reagent in 0.1 M buffer. Consequently, the final ionic strength only varied from
0.010 M to 0.015 M.

Figure 4.11 shows an initial increase and then a slow decline in instrumental response as the ionic strength is increased. Only a small change was expected since the substrates are uncharged. However, since the carrier was positively charged, enzyme-carrier interactions may have been altered. According to equation 3.3, an increase in ionic strength should increase the K_m value and lower the reaction rate. This study shows the same general trend.

3. The specificity of glucose oxidase

The oxidation of most sugars, except β -D-glucose, is catalyzed very slowly by glucose oxidase. Nine different sugars, obtained commercially in the highest purity forms, were sampled, first with the immobilized glucose oxidase reactor in place, and then with soluble glucose oxidase added to the buffer reagent (0.2 mg/mL) and the enzyme reactor removed. The continuous flow manifold and the other reagents were the same in both experiments. Table 4.2 is a list of the results. No sugar other than β -D-glucose showed high reactivity toward glucose oxidase. The aqueous and immobilized enzyme results were remarkably similar. This indicates that the conformation of the enzyme

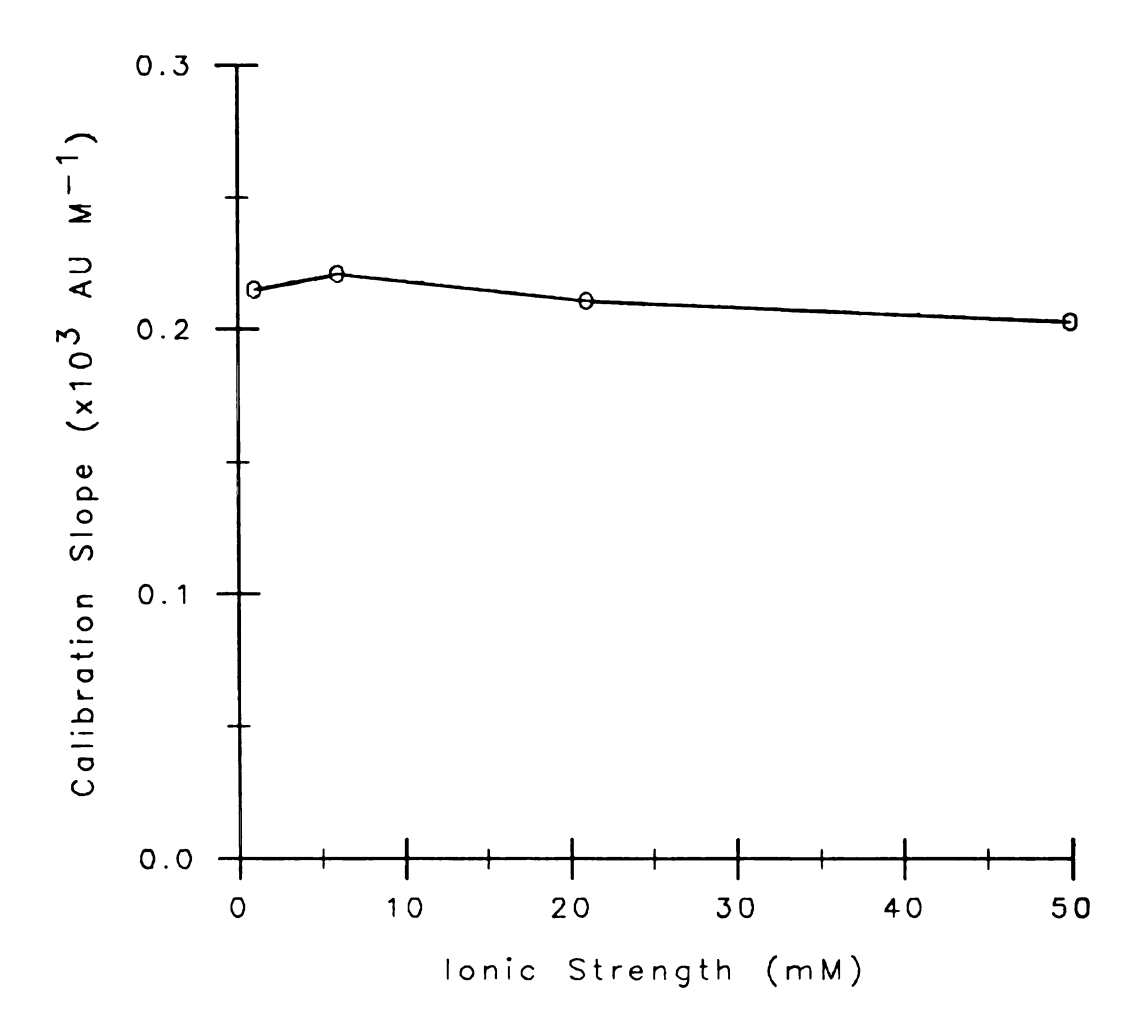


Figure 4.11. The effect of ionic strength on the glucose oxidase reaction.

Table 4.2. Specificity of Glucose Oxidase

	Relative Reactivity			
Sugar	Immobilized	Aqueous	Aqueous*	
β-D-glucose	100	100	100	
2-deoxy-D-glucose	2.5	2.4	25	
Maltose	1.1	0.95	0.19	
α-D-glucose	0.6	-	0.64	
Xylose	0.31	0.26	0.98	
Mannose	0.27	0.23	0.98	
Galactose	0.03	0.05	0.14	
Fructose	0.03	0.02	-	
Glucosamine	0.03	0.02	<0.05	
Sucrose	0.00	0.00	_	

^{* -} Values reported in the literature [126]

was not significantly altered during immobilization. Correlation of the results with an aqueous enzyme study, performed in 1952, was fair. The literature values may be inflated by impure reagents; the amount of β -D-glucose in various sugar preparations is probably much lower today.

4. Mutarotation kinetics

To replace the β -D-glucose which is converted to hydrogen peroxide, the α -form of D-glucose is converted spontaneously to the β -form. This process is termed mutarotation. The chemical equation and associated rate equation are shown below.

$$\beta$$
-D-glucose $\stackrel{\rightarrow}{\leftarrow} \alpha$ -D-glucose (4.4)

$$-d[\beta]/dt = k_1[\beta] - k_2[\alpha]$$
 (4.5)

If $[\beta]_{O}$ - $[\beta]$ is substituted for $[\alpha]$ ($[\beta]_{O}$ is the initial concentration of the β -form) and the equation integrated, the rate equation appears in the following form.

$$-\ln(1.565[\beta]/[\beta]_{0} - 1) = (k_{1}+k_{2})t$$
 (4.6)

The term, k_1+k_2 , is identified as the "mutarotation constant" [96,97].

A 4.44 mM β -D-glucose solution was prepared, and immediately the solution was sampled with the continuous flow instrument. Steady-state absorbance values were obtained for the glucose solution at intervals over a two hour period. Assuming that the α -form had a negligible

reaction rate with the immobilized glucose oxidase, first order data were calculated and plotted in Figure 4.12. The mean rate constant was determined to be 0.017 ± 0.002 min⁻¹, in good agreement with the literature value of $0.012 \, \text{min}^{-1}$ [96,97].

The specificity value for α -D-glucose was also obtained. Initially, only the β -form existed in the sample solution, and, thus, the sensitivity toward the β -form was calculated. Knowing this and that 64% of the glucose is of the β -form at equilibrium, reaction rate measurements at equilibrium allowed calculation of the α -form reactivity. The following equation was derived.

$$S_{\alpha}/S_{\beta} = 2.78(A_{\infty}/A_{0}) - 1.77$$
 (4.7)

Here S_{α} and S_{β} are the sensitivities of glucose oxidase toward the α and β forms of glucose, and A_{∞} and A_{0} are the equilibrium and initial absorbances. The reactivity of the α -form was only 0.6% of that for the β -form. Glucose oxidase shows very high specificity indeed.

The effect of glucose mutarotation on the overall reaction kinetics is small because the mutarotation rate constant is about ten times smaller than the glucose oxidase reaction rate constant. If one considers a 30 second residence time in the enzyme reactor, up to 10% of the β -D-glucose is consumed by the enzyme, while only about 0.5% of the α -form can be converted to the β -form in

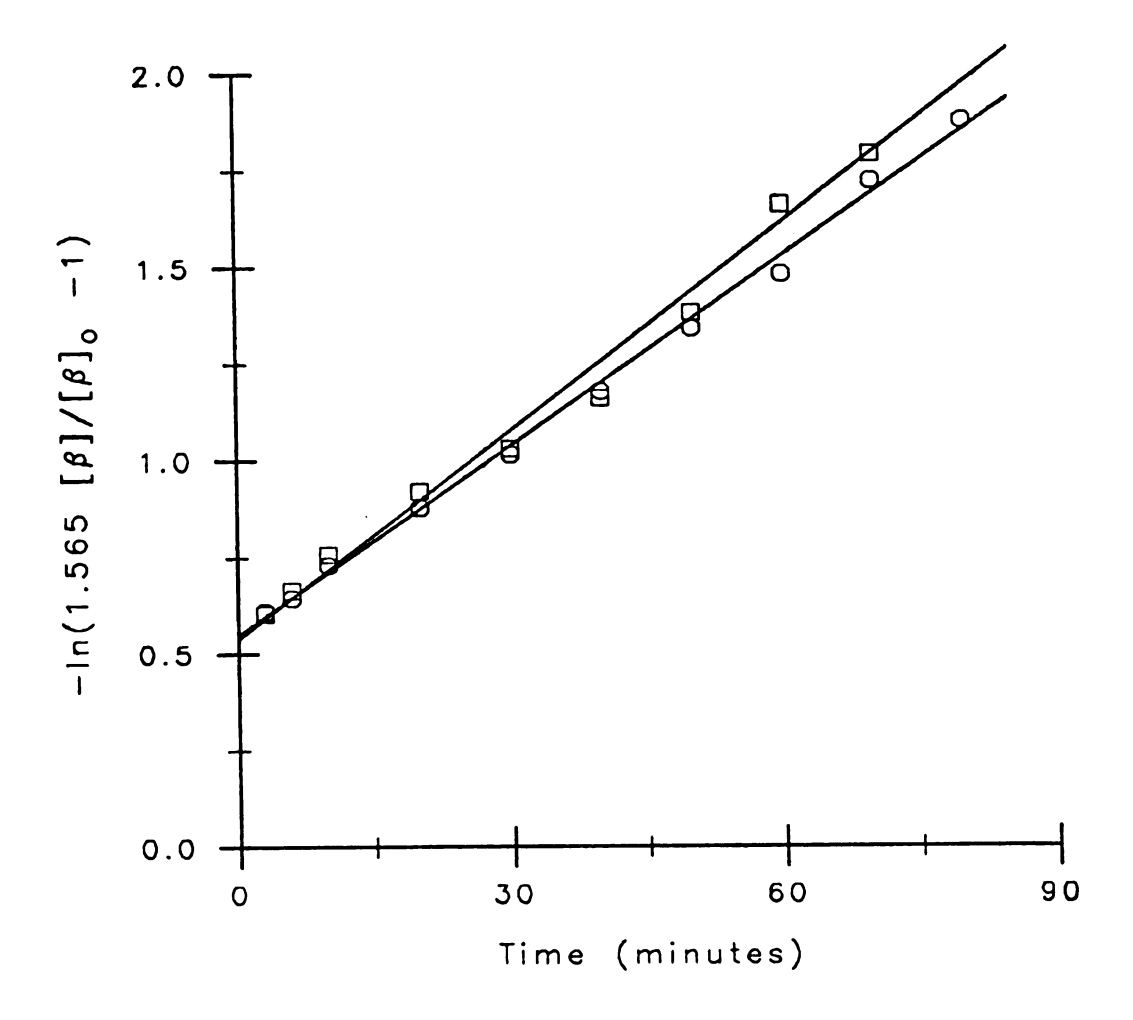


Figure 4.12. First order plot of data for the mutarotation of a 4.44 mM $\beta\text{-D-glucose}$ solution at 22 °C. The results of two independent experiments are presented. [β] is the concentration of the $\beta\text{-form}$ of D-glucose at any time, t, while [β] is the initial $\beta\text{-form}$ concentration.

the same time period. Consequently, once the standard glucose solutions have come to equilibrium, the mutaroatation process can be neglected.

- D. Reactor Design Characteristics
- 1. Coiling diameter

Immobilized enzyme reactors are usually molded into helical coils to make them easier to incorporate into a continuous flow manifold. The coiling of the reactor should also improve the radial mixing in each liquid segment [83]. The reaction rate should increase with better radial mass transport, and, thus, with more tightly wound reactors. Horvath and coworkers found that the apparent activity of trypsin immobilized inside a nylon tube improved as the coiling diameter decreased [140]. However, this effect only occurred at flow rates greater than 3 mL/min.

By improving the radial mixing, coil formation decreases sample dispersion, or the "wash" of the system.

Ideally, the rising portion of a continuous flow peak can be described by the following equation [1].

$$H(t) = H(ss)(1 - exp(-t/b))$$
 (4.8)

Here H(t) is the absorbance at any time along the peak, H(ss) is the steady-state absorbance (flat portion of the peak), t is the time, and b is a measure of the magnitude of the sample dispersion. The term, b, is called the wash

value of the system and is defined as the time required for the absorbance to change from H(t) to 0.37 H(t). Smaller b values are desirable and can result from tighter coiling of the mixing loops and enzyme reactor.

A 25 cm glucose oxidase reactor, coiled to various diameters, was inserted into the manifold, and a series of glucose standards, 0.4 to 4.4 mM, was sampled. The manifold and reagents were the same as those described in Section A. The total flow rate through the reactor was only 0.38 mL/min.

The results are presented in Figure 4.13. The reaction rate was unaffected by the changes in the reactor design. This indicates that either the reaction rate is limited by the enzyme kinetics or that radial substrate transport was not improved significantly at the low flow rate. The latter explanation is in agreement with Horvath's work [140]. The wash, however, was improved by about 30%. Thus, small coiling diameters are desirable, but the coiling process does not have to be very precise to obtain good analytical results.

2. Coil temperature

An experiment was performed to determine the effect of temperature on the apparent activity of glucose oxidase. The manifold and reagents were the same as those described in Section A. The enzyme reactor was heated by gluing the reactor into a plastic drying tube, sealing the drying tube, and then passing heated water through the tube. The water,

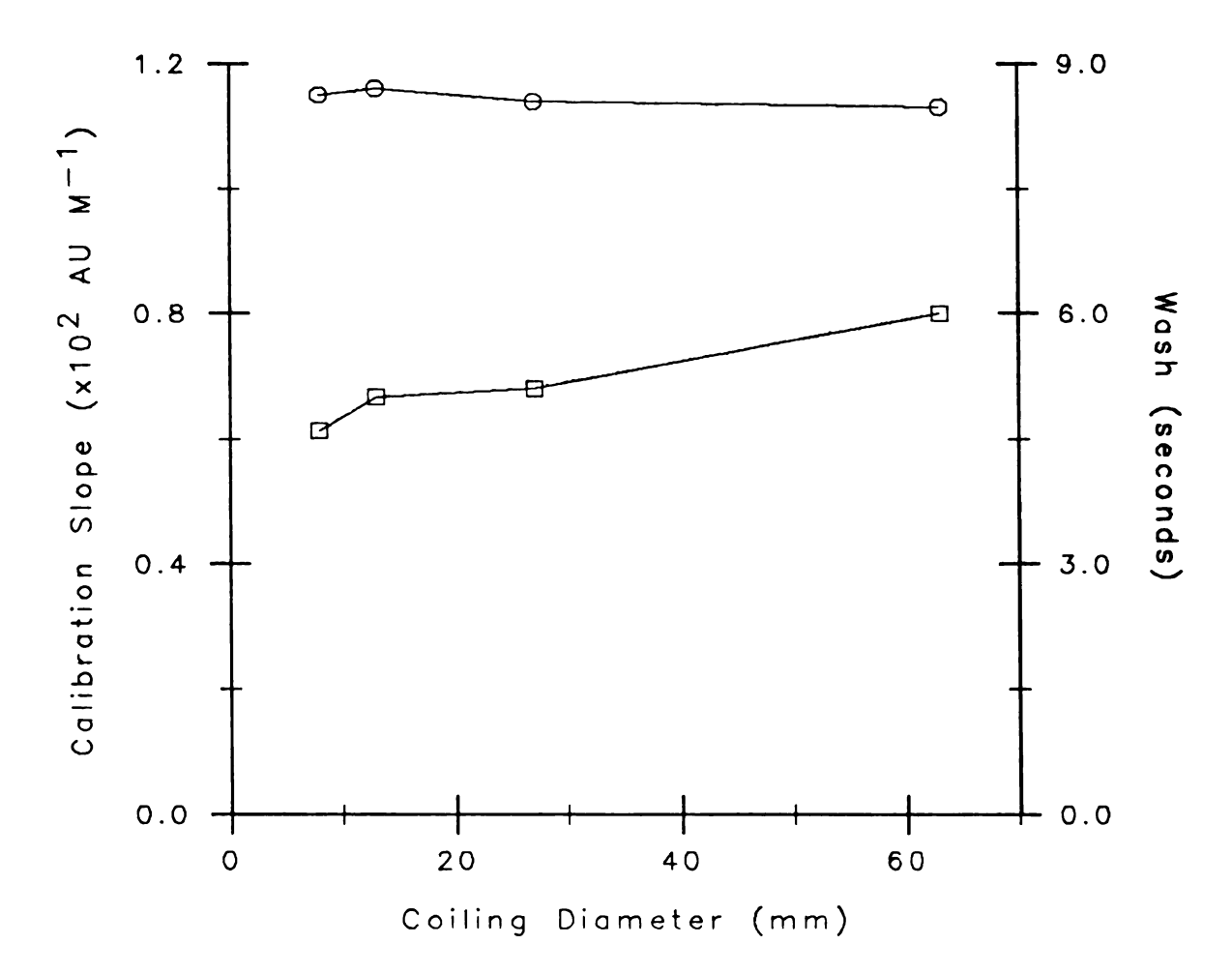


Figure 4.13. The effect of coiling diameter on the calibration slope (0) and wash (\square).

contained in a 2 liter beaker, was thermostatted using a Haake Model E52 heating bath/circulator unit. Since the color-forming reaction went nearly to completion, temperature had little effect on the Trinder reaction.

The temperature dependence of the analytical reaction is shown in Figure 4.14. The results do not conform to the Arrhenius equation. It is also interesting to note that at room temperature (22 °C) a small temperature shift can change the reaction rate by several percent. This fact could explain the fluctuations of the activity of enzyme reactors in long-term stability studies (e.g. Figure 2.5). The stability of the enzyme reactor at high temperatures was tested by heating the reactor to 41 °C, and sampling glucose standards over a one hour interval. The initial and final results were identical, which indicates that immobilized glucose oxidase is very stable with respect to temperature.

- E. The Characterization and Elimination of the Effect of Catalase
- 1. The nature of the interference

In the glucose determination described here, the hydrogen peroxide produced in the immobilized enzyme tube is reacted downstream with the Trinder/peroxidase reagent. The analytical and color-forming reactions are separated in time for two reasons. First, separation allows the reactions to be optimized individually in terms of reaction

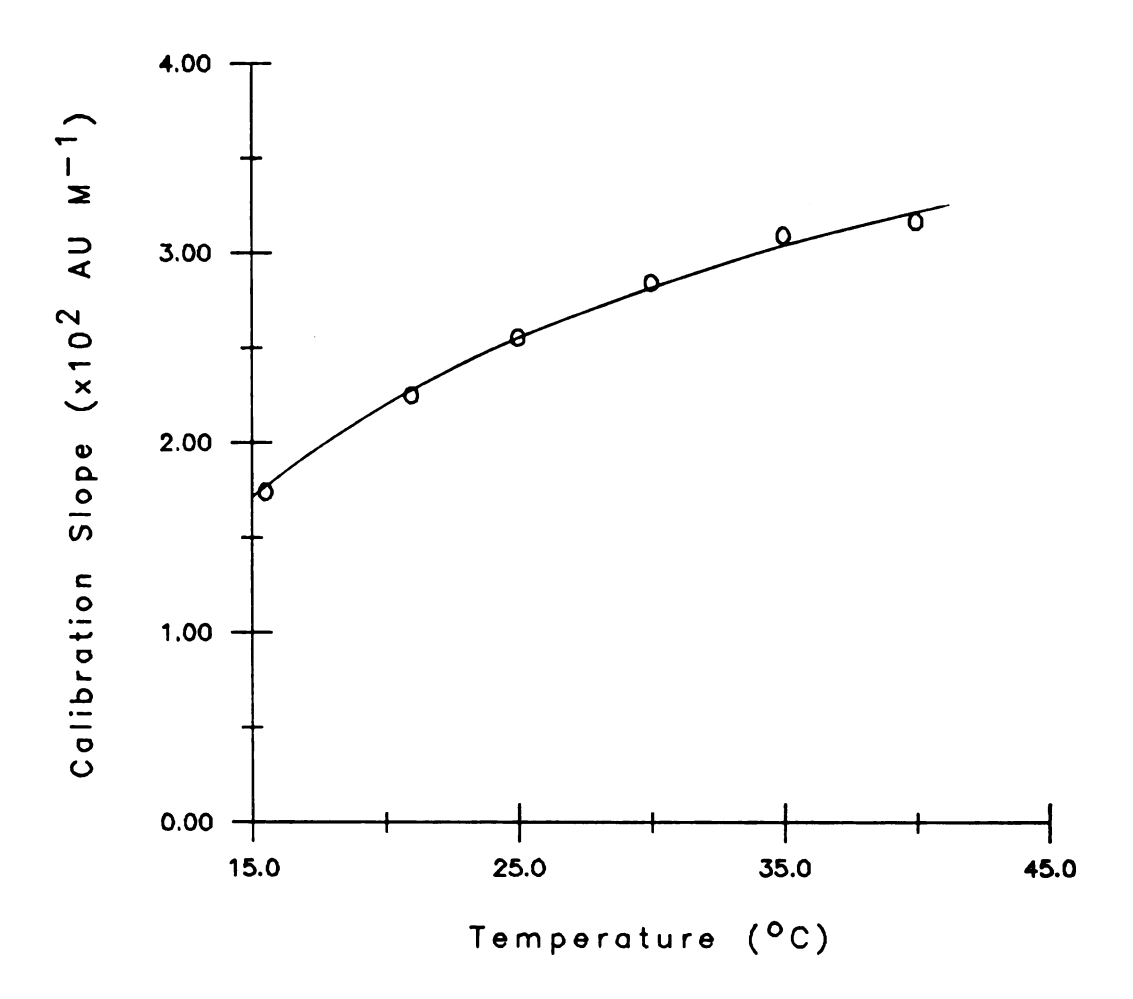


Figure 4.14. The dependence of the assay sensitivity on temperature.

time, reagent concentrations, pH, etc. In soluble enzyme methods, a compromise between the optimal values for each reaction is necessary. Second, the separation improves the wash characteristics of the system. The Trinder compounds adsorb strongly to the nylon tubing, which degrades the wash. These two factors prohibit the simultaneous reaction of glucose and peroxide inside the immobilized enzyme reactor.

Because of the separation of the two reactions, the sensitivity of the method was found to be reduced due to contamination of the glucose oxidase by catalase (E.C. 1.11.1.6) [141]. Catalase destroys hydrogen peroxide via the following mechanism [142]:

$$E + H_2O_2 \stackrel{?}{\leftarrow} Compound I$$
Compound $I + H_2O_2 \rightarrow E + O_2 + 2 H_2O_2$

where E is free catalase. Some of the hydrogen peroxide that otherwise would react to form product is destroyed inside the enzyme reactor by co-immobilized catalase. Since catalase has a specific activity of forty million units per gram [103], the small amounts found in most glucose oxidase preparations will have a large effect. If the color-forming reaction also occurred inside the reactor, then the effect of the catalase would be small since the peroxide would quickly be converted to the colored product by aqueous peroxidase. This is not the case in CF systems.

In a method proposed recently, the catalase was selectively inhibited by adding sodium azide to the system [141]. Hydrazoic acid is well known as an inhibitor of catalase [142-144]. Although the exact nature of the inhibition is still in question, it is known that hydrazoic acid reacts with Compound I to yield peroxide or other products. Thus, the addition of azide to the reaction system inhibits catalase by forming a compound with the enzyme-substrate complex.

A study of the effect of sodium azide on the coimmobilized catalase is presented here. The improvement
in the assay sensitivity with the addition of azide and
the variation in catalase content of several commercial
glucose oxidase preparations are described in detail.
Finally, suggestions for the detection and elimination of
the catalase interference are made.

2. The reagents and continuous flow instrument

The reagents were prepared as outlined in Section A. Sodium azide solutions were prepared in the following manner. A 250 mM stock solution was made by dissolving 3.25 g of NaN3 in 0.200 L of pH 6.85 phosphate buffer (0.1 M). This solution was stable for several weeks at room temperature. Working azide solutions were prepared by appropriate dilution of the stock with buffer. Five drops of Brij-35 surfactant were added to these solutions prior to use. The azide solutions were substituted for the buffer reagent

in the continuous flow manifold. The term, "azide" is used to mean sodium azide.

The concentrations of azide, hydrogen peroxide, and glucose reported here are the concentrations actually present inside the immobilized enzyme reactor, after dilution in the continuous flow manifold. The instrument was the same as outlined in Section A. The data were acquired by the computer in all the experiments, and the pump was operated at a speed setting of 56.

3. Enzyme immobilization

The catalase (Type C-10) and glucose oxidase (Types II, IX, and X) were purchased in 1982 from Sigma Chemical Co. and used without further purification. The enzymes were immobilized as outlined in Chapter 2, Table 2.3. The seven enzyme reactors used in this study were prepared with the aqueous enzyme solutions listed in Table 4.3. The listed catalase concentrations were derived from the catalase found in the glucose oxidase and from the amount of pure catalase added to the solutions -- reactors A, C, and D. The different reactor types will be referred to by letter names as listed in Table 4.3. When not in use, the reactors were filled with pH 6.85 phosphate buffer and stored at 4 °C.

4. Effect of azide on aqueous peroxidase

A series of experiments was performed to investigate the effect of azide on the color-forming reaction. In the first experiment, the immobilized enzyme reactor was removed

Table 4.3. Solutions Used to Prepare the Immobilized Enzyme Reactors

Reactor Type	GO (U/mL)	CAT (U/mL)	Sigma Type GO
A	0	3765	-
В	89	0.4	II
С	89	380	II
D	89	1880	ΙΙ
E	125	0.58	II
F	125	1200	IX
G	125	1.7	X

from the manifold, and peak heights were obtained for a 79 μ M peroxide standard. Then the experiment was repeated with increasing amounts of azide added to the buffer reagent. The results, shown in the upper curve of Figure 4.15, revealed that for azide concentrations of up to 30.3 mM the sensitivity of the assay remained constant within the limits of experimental error (about 3%). Thus, azide does not appear to inhibit peroxidase activity or interfere with the color-forming reaction.

5. Effect of azide on immobilized catalase

In the next series of experiments, the ability of azide to inhibit catalase activity was investigated. A 30 cm immobilized catalase reactor (reactor A in Table 4.3) was inserted into the manifold, and peak heights were obatined for a 79 µM peroxide standard with increasing concentrations of azide in the buffer. The results of this experiment are also shown in Figure 4.15. Without azide in the buffer, more than 99% of the peroxide was destroyed as it passed through the catalase reactor, but as the azide concentration increased, peroxide recovery improved dramatically. Even at an azide concentration of 15 mM, however, 20% of the peroxide was destroyed.

The manner in which azide inhibited catalase was investigated in the next set of experiments. Shorter catalase reactors (type A) were used in these studies so that the mean residence time of peroxide in the enzyme

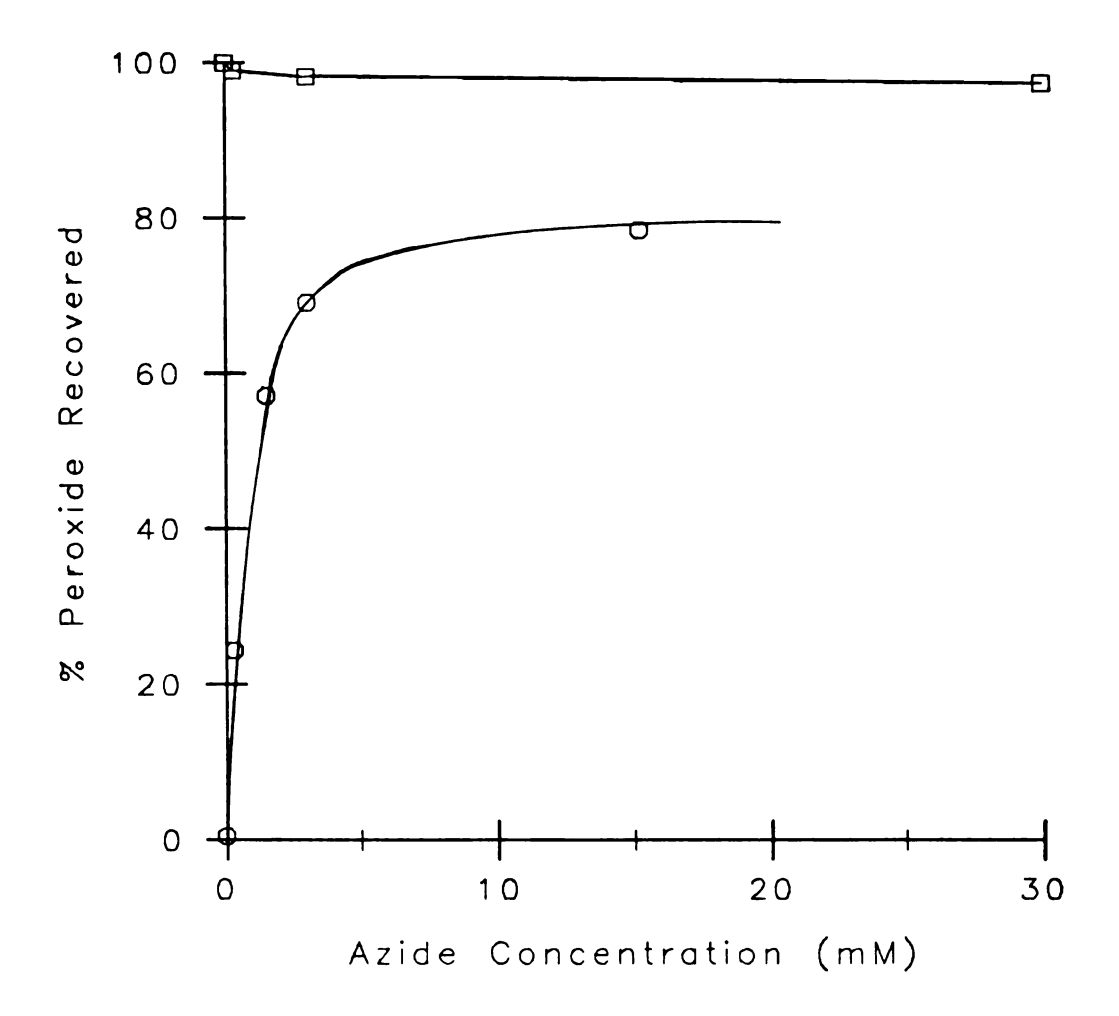


Figure 4.15. The effect of azide on the amount of hydrogen peroxide that was converted to product. A 79 μ M H₂O₂ solution was sampled without an enzyme reactor (\square) and with a 30 cm catalase reactor (0) in the manifold.

reactor was about 3.5 seconds. Under these conditions, Michaelis-Menten kinetics were applicable. A new 5 cm segment was cut from a fresh 50 cm catalase reactor and inserted into the manifold for each experiment. The differences between peak heights obtained with and without the catalase reactor in the manifold were determined for a series of hydrogen peroxide standards in the range of 20 μM - 80 μM . The decrease in steady-state absorbance with the catalase reactor in place was proportional to the catalase-induced rate of peroxide decomposition.

Figure 4.16 shows Lineweaver-Burk (L-B) plots of the results of three separate experiments. All lines intersected in a small region just below the x-axis. Dixon plots [145] of the data were hyperbolic, and replots of the L-B intercepts and slopes were non-linear. These results indicate a mixed-type noncompetitive inhibition [146]; in addition to interaction with Compound I, azide may also bind at two sites on the free enzyme. The kinetics were complicated, and more experiments would be required to completely elucidate the action of azide on immobilized catalase.

We next investigated the extent of catalase interference under non-separated reaction conditions. The Trinder/peroxidase reagent was passed through the 5 cm catalase reactor (type A). The results revealed that peroxidase successfully captured 80% of the available peroxide in the

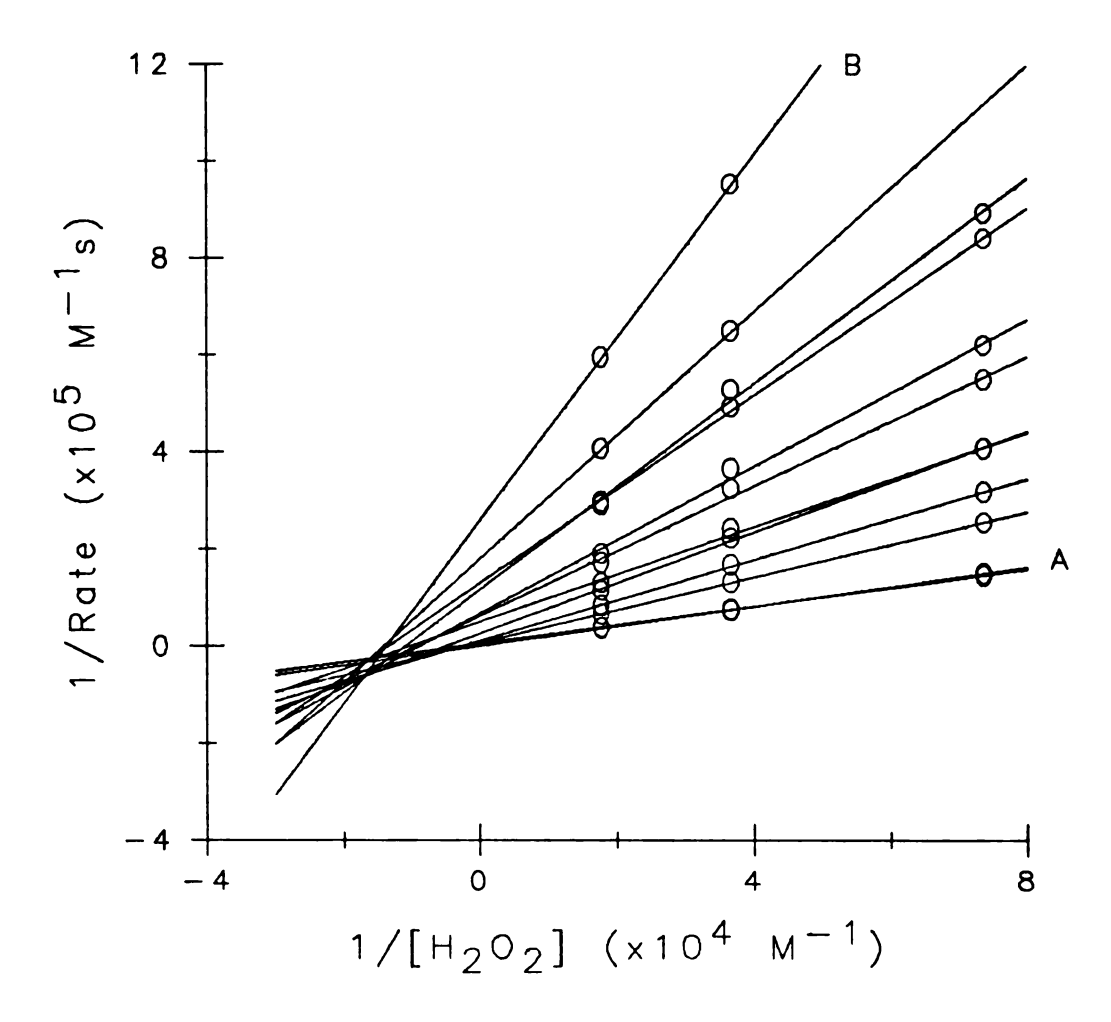


Figure 4.16. Lineweaver-Burk plot of the data which exhibited azide inhibition of immobilized catalase. The azide concentrations ranged from 0.0 (A) to 1.5 mM (B).

presence of catalase. Thus, for the small amount of catalase impurity normally found in commercial glucose oxidase preparations, the loss of peroxide from the catalase reaction in the presence of peroxidase should be negligible.

It should be noted that azide did not have an immediate effect on the immobilized catalase. The azide/buffer solution had to be passed through the reactor for about three minutes before its full effect was attained. To remove the inhibitory effect of azide, the reactor was flushed with pure buffer for five minutes. This process, however, only returned the catalase to 90% of its original activity. Thus, azide inhibition of catalase appears to be only weakly reversible, in agreement with a previous study [142].

6. Effect of azide on immobilized glucose oxidase

A preparation of glucose oxidase containing a very small amount of catalase was chosen for this study. A 50 cm glucose oxidase (GO) reactor (type B) was inserted into the CF manifold, and glucose standards in the range of 0.1 mM - 0.5 mM were used as the sample. Curve B of Figure 4.17 shows the effect of azide on the GO reactor. Azide solutions of more than 0.5 mM had a large, negative effect on glucose oxidase activity. Dixon plots of these data, Figure 4.18, show that the inhibition was purely non-competitive and that the K_T value was 18 mM.

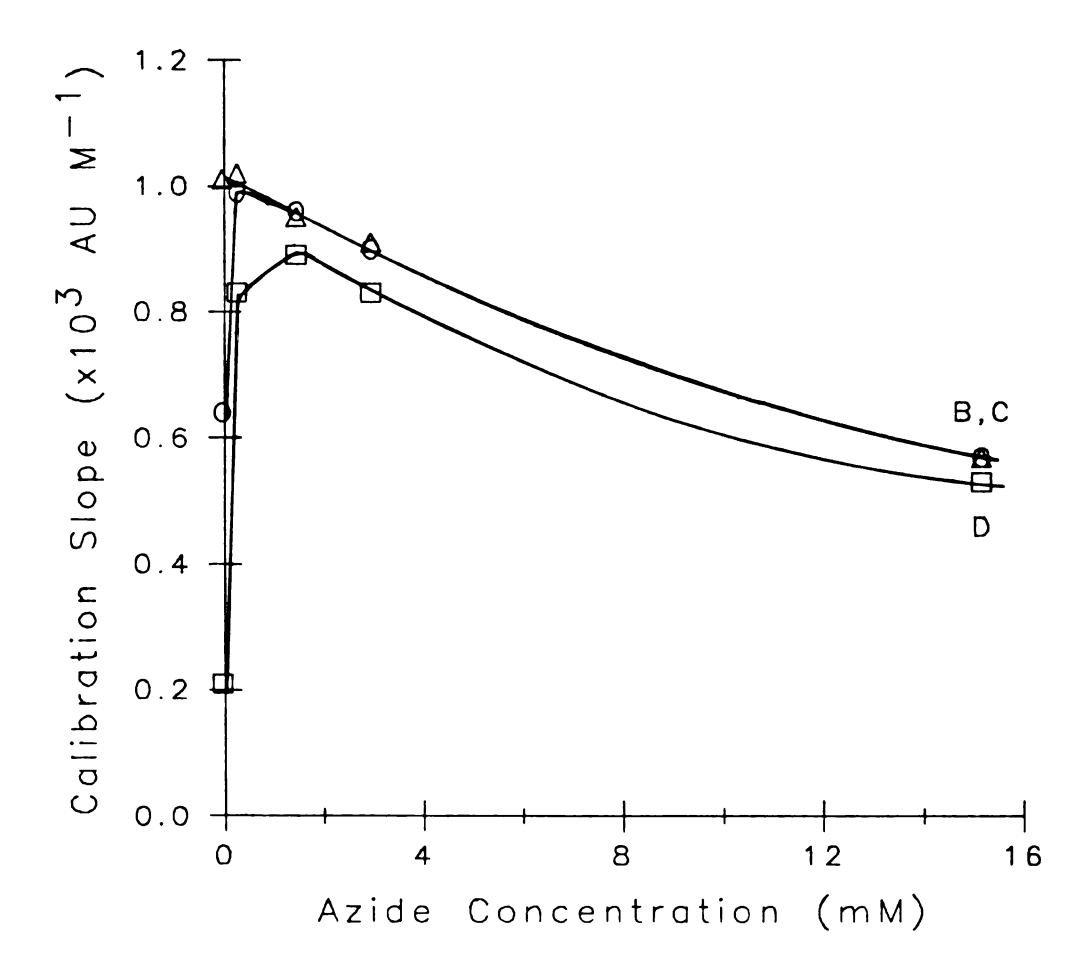


Figure 4.17. The effect of azide on three glucose oxidase reactors, type B (Δ), type C (0), and type D (\square), containing various amounts of catalase (refer to Table 4.3).

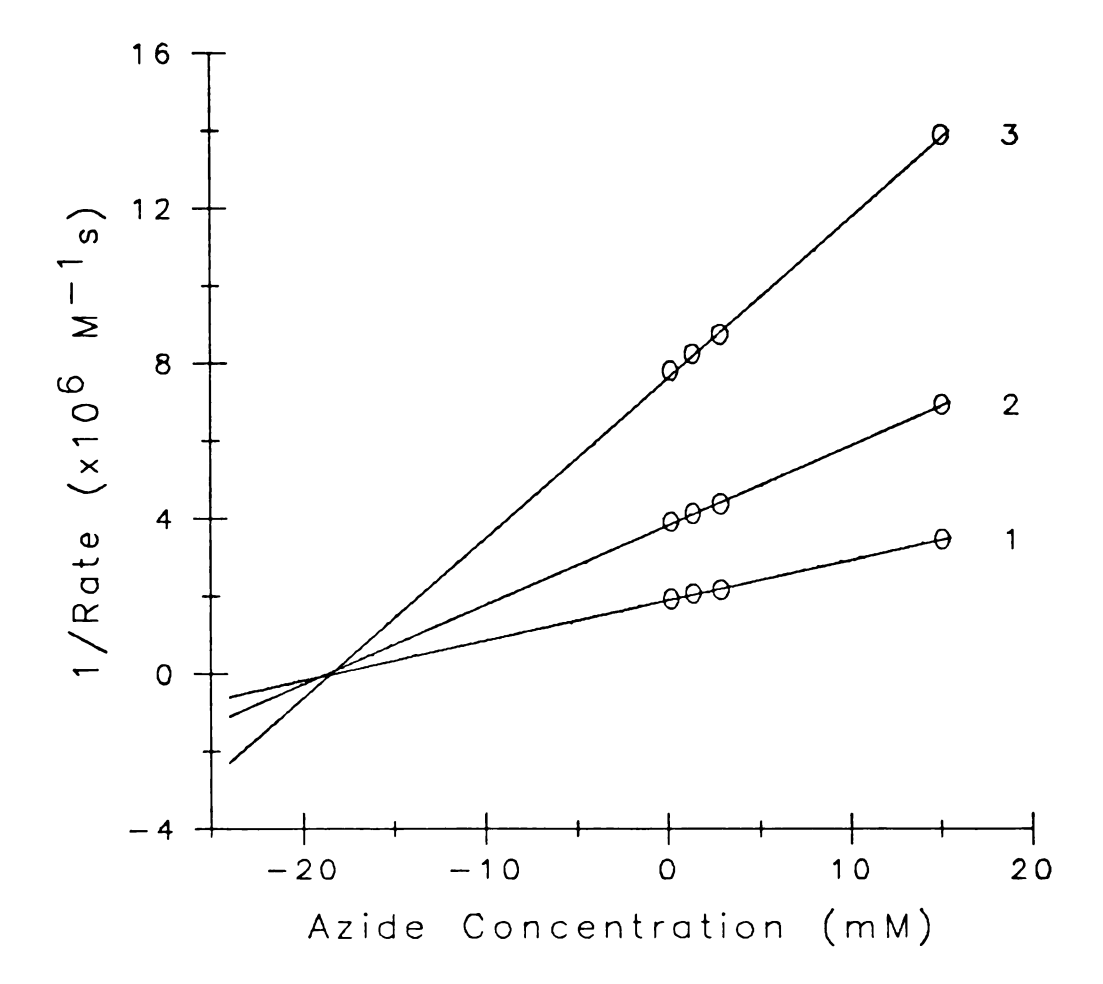


Figure 4.18. Dixon plot of data from Figure 4.17, curve B. Three glucose concentrations were used: 0.44 mM (1), 0.22 mM (2), and 0.11 mM (3).

Two other reactors were prepared from Type II glucose oxidase spiked with small (type C) and large (type D) amounts of catalase. The different concentration ranges at which azide first inhibits catalase and then glucose oxidase in these reactors can be seen in Figure 4.17. The optimal azide concentration increased as the amount of catalase in the reactor increased. The rapid rise in assay sensitivity observed as the concentration of azide in the buffer approached 1 mM is due to catalase inhibition. The more gradual decrease in assay sensitivity at higher azide concentrations is due to glucose oxidase inhibition.

We were surprised that the addition of a second enzyme to the immobilization solution had only a small effect on the bonding of the primary enzyme. At an azide concentration of 15.2 mM, at which the action of catalase is very small, the calibration slopes of all three reactors (types B,C, and D) were similar (relative standard deviation between reactors = 4%), which indicates that the amount of active glucose oxidase bonded in all three reactors was nearly the same.

7. Effect of azide on different preparations of glucose oxidase

Reactor types E, F, and G (40 cm in length) represented immobilized forms of Sigma Types II, IX, and X glucose oxidase respectively. The catalase activities of

of these preparations (Table 4.3) were very different, and the differences can be seen if one compares the points at zero azide concentration for the three curves in Figure 4.19. The calibration curves were prepared by sampling peroxide standards in the range of 10 μ M - 40 μ M. Reactor F exhibited very little activity which reflects the higher catalase activity.

Addition of azide improved the sensitivity only a small amount for reactor types G and E, while the characteristics of reactor F changed noticeably. At an azide concentration of 15.2 mM, the assay sensitivity with reactor type F in place approached that of the other two reactors. Again, the presence of a second enzyme had only a small effect on the bonding of the primary enzyme.

8. A method to determine the presence of catalase

The properties of the same enzyme preparation can vary from lot to lot. For example, some Sigma Type II glucose oxidase purchased five years ago exhibited high catalase activity [141], while a batch purchased several months ago showed negligible catalase activity. Thus, it is important to know the catalase activity in the glucose oxidase preparations to be used.

To determine whether catalase activity in a given lot of glucose oxidase is sufficient to cause problems in an immobilized enzyme glucose assay, a simple test is suggested. First, immobilize the glucose oxidase in a 50 cm or longer

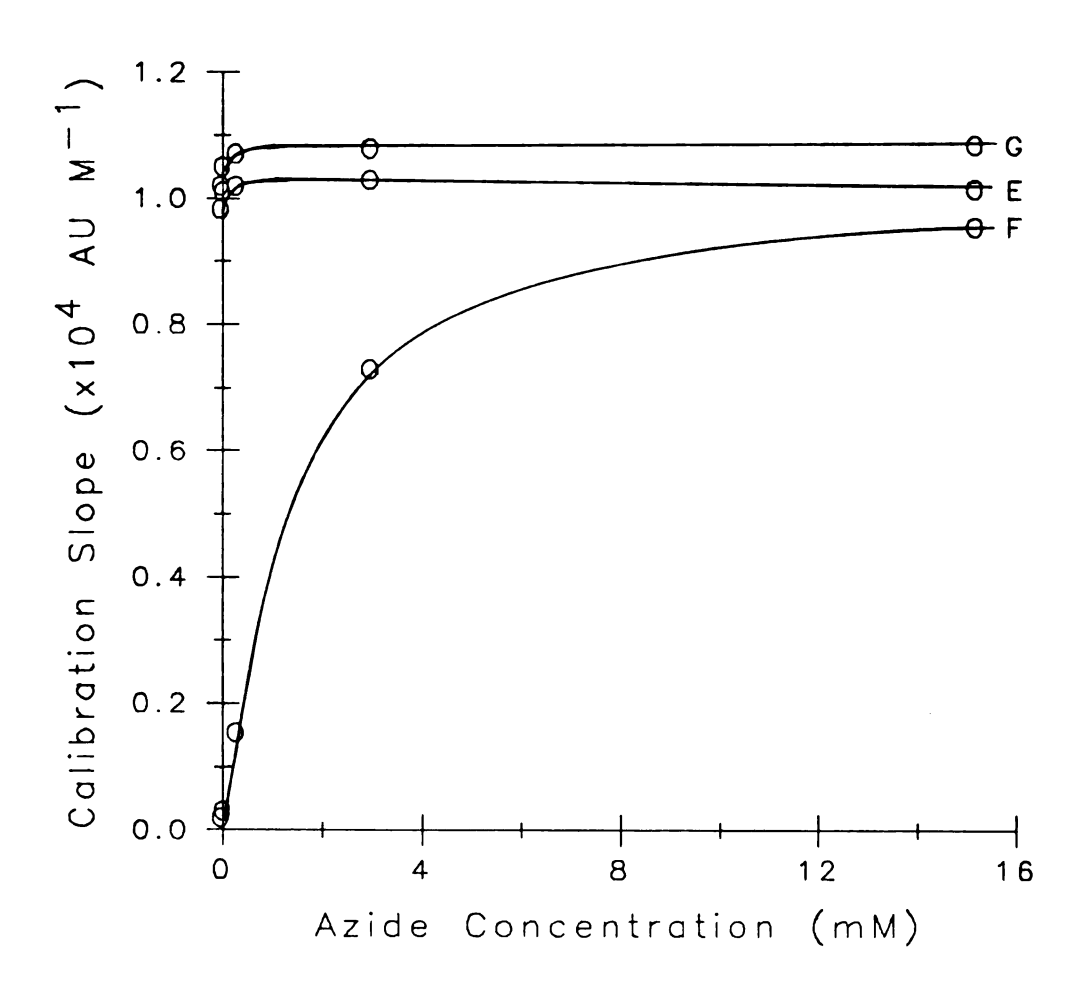


Figure 4.19. The effect of azide on three commercial preparations of glucose oxidase, reactor types G, E, and F (refer to Table 4.3).

reactor, and then cut the tube into 10 and/or 20 cm segments. Determine, with glucose as the sample, the calibration slopes with various lengths of reactor in the CF manifold. If the catalase content of the reactor is significant, a curved plot of the calibration slope versus reactor length will result. Figure 4.20 shows the results of such an experiment. As the catalase activity in the reactors increases (types B+D), the plot becomes more hyperbolic. To verify the presence of catalase, azide is added to the system so that the concentration inside the enzyme reactor is about 1 mM. If straight lines are produced, as shown in Figure 4.21, then catalase interference is confirmed. In this way, one can determine if the use of sodium azide is warranted.

9. Conclusions

The results presented here should be applicable to systems that use chromogenic agents other than the Trinder reagent. The analytical and color-forming reactions, however, must be separated in time for the effect of azide to be evident. Azide does not affect the accuracy of control serum assays. Table 4.4 shows that no significant difference was found between the results obtained with and without added azide. The sensitivity of the glucose determination is improved by the addition of sodium azide when glucose oxidase immobilized enzyme reactors, containing appreciable amounts of catalase, are used.

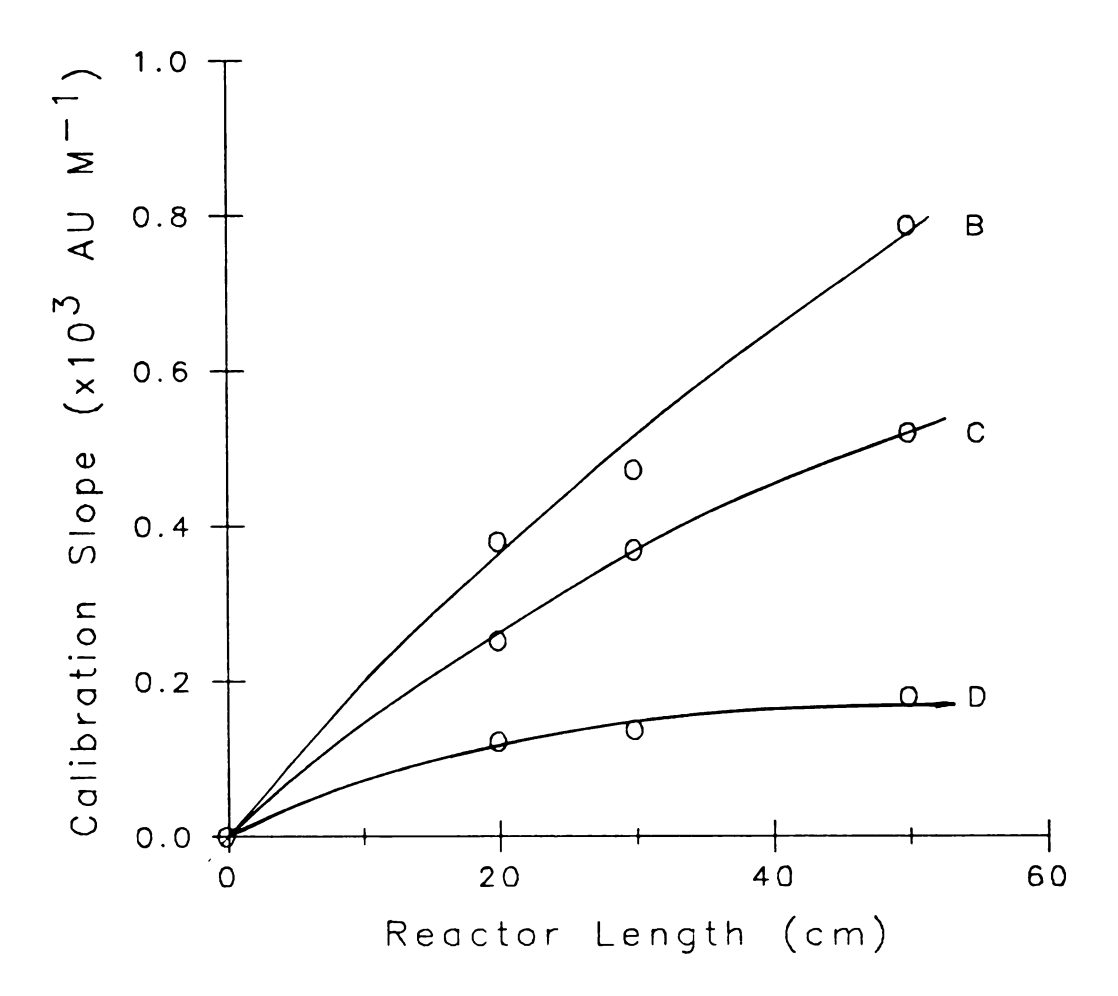


Figure 4.20. The change in calibration slope with different lengths of reactors B, C, and D (refer to Table 4.3). No azide was added.

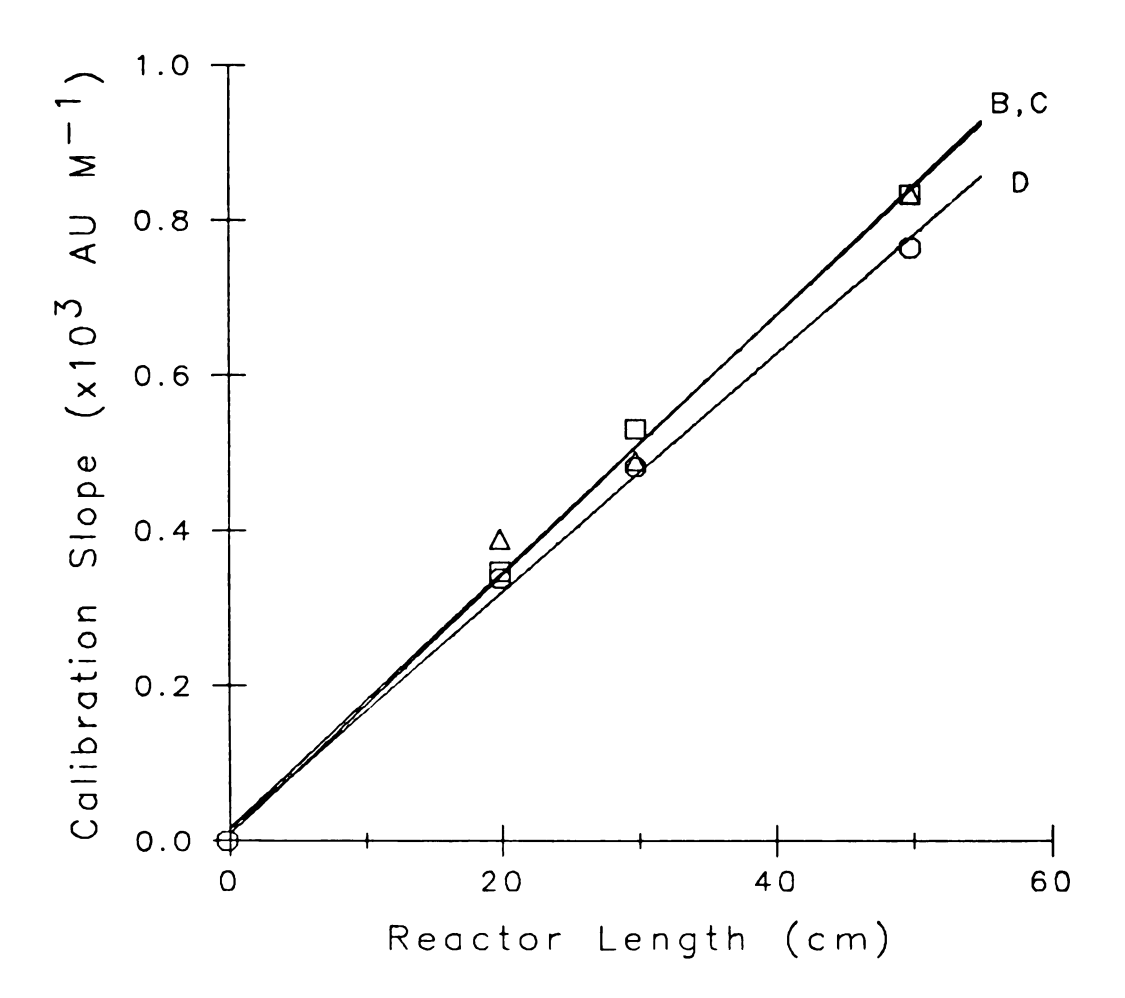


Figure 4.21. The change in calibration slope with different lengths of reactors B, C, and D (refer to Table 4.3). The reactions occurred in the presence of 0.8 mM azide.

Table 4.4. Glucose Concentrations Found in Control Sera With and Without Added Azide

Glucose Concentrations (mg/dL)

Control Serum	Expected	Found (no azide)	Found (2 mM azide)
Calibrate	165	143	153
Monitrol	95	91	95
Sigma	92	74	75

The 95% confidence limits for the experimentally determined values are $\pm\ 5\ \text{mg/dL}_{\raisebox{-1pt}{\text{\circle*{1.5}}}}$

CHAPTER 5

Enzyme Immobilization on Non-porous Glass

As shown in previous chapters, nylon serves well as a carrier for immobilized enzymes. Yet, nylon is far from perfect in many cases. Aromatic compounds tend to adsorb to the nylon, and nylon has a small surface area-to-volume ratio. Also, a charge develops on the surface during immobilization; this charge can alter the enzyme properties. Since these problems are not easily solved, the use of other carriers has been an active area of research.

Glass offers the advantages of being inert, sturdy, and readily available in a variety of forms; glass shows good wash characteristics in continuous flow manifolds. On the other hand, non-porous glass has a small surface area-to-volume ratio and has no reactive groups for direct enzyme attachment. These problems can be overcome, however, by growing "whiskers" on the glass to increase the surface area and reacting the glass with a silynating reagent to activate the surface. Coiled glass tubing for use in continuous flow instruments is somewhat expensive, but the use of straight tubing in the stopped-flow instrument presented in Chapter 3 or the use of beads packed into a tube is ideal.

The preparation and use of immobilized enzyme glass reactors are discussed in this chapter. Glucose oxidase was

again chosen as the enzyme; the reactions were discussed in Chapter 4. First, glass tubing was used in a segmented CF system. The results are presented in Section A. Then glucose oxidase was attached to non-porous glass beads for use in a flow-injection instrument. Section B includes analytical results from this novel system.

A. Immobilization of Glucose Oxidase on Glass Tubing
Borosilicate glass tubing of 1.25 mm i.d. and 30 cm
in length was bent in a U-shape for use in the segmented
continuous flow instrument. The glucose oxidase was attached
to the glass by procedures adapted from those described by
Iob and Mottola [147]. Four major steps are involved:
tube cleaning, "whisker" formation, activation, and enzyme
bonding. The details are given below.

The glass was cleaned first by filling the tube with concentrated HCl and heating it to 60 °C for 24 hours.

Next, the tube was washed with 100 mL each of distilled water and acetone. The glass was dried by passing nitrogen gas over the surface.

In the second step, the glass was etched and silica needles were formed on the inner surface of the tube. The procedure was taken from that reported by Onuska, $\underline{\text{et.al.}}$. [148]. The tube was filled with a 5% w/v (saturated) methanol solution of ammonium bifluoride, NH₄F-HF for about one hour at room temperature. The excess solution was

removed by passing a stream (1 mL/min) of nitrogen gas through the tube. The tube became milky white in coloration as the methanol was removed. A constant, but slow, stream of gas was crucial for uniform coverage of the tube with the reagent. This was the most difficult portion of the treatment. The ends of the coated tube were then sealed, and the tube was placed in a muffle furnace at 425 °C for three hours. Under these conditions, the bifluoride is decomposed to ammonia and hydrogen fluoride gas. The HF removes glass at one point and then deposits silica in the form of "whiskers" at other points on the tube. The surface area of the reactor should be increased greatly.

After cooling, the tube was opened and flushed with nitrogen gas. Activation was effected by reaction with 3-aminopropyltriethoxysilane (Sigma). The original procedure was reported for activation of porous glass beads [149,150]. A neat solution was reacted at 60 °C for 1.5 hours or a 5% v/v solution in acetone was reacted at 60 °C for 24 hours. Both procedures were hampered by the fact that the solution slowly evaporated, leaving behind a yellow gum, which often restricted solution flow through the tube. The formation of the residue needs to be remedied before this procedure can be used reliably for the activation of glass tubing. Perhaps lower reaction temperatures and times will have to be used.

The activated tube was then washed with acetone and

water and filled with a 5% v/v solution of glutaraldehyde in pH 8.0 phosphate buffer. The reaction occurred for 1.5 hours at room temperature. No change in the coloration of the tube was evident. The glucose oxidase, 10 mg/mL in pH 6.85 phosphate buffer, was next added to the tube and allowed to react for 18 hours at 4 °C. After these procedures were performed, the tube was washed with distilled, deionized water and filled with the phosphate buffer when not in use.

The results of the experiment were somewhat encouraging. The activity of the reactor was tested as described in Chapter 4. The best glass reactors had activities that were about 25% of those prepared from nylon tubing. The wash characteristics were somewhat better. Considering the small amount of time spent on this venture, the results were very good. Further testing is warranted.

B. Glucose Oxidase Bead String Reactor

In flow-injection (FI) analysis, sample dispersion and mixing between the reagents and sample are coupled. In order for complete mixing to occur, the sample dispersion must be fairly large. Consequently, sample throughput and sensitivity are sacrificed as longer residence times are employed. In 1981, van der Linden, et.al. [151,152] suggested the use of tubing packed with impervious glass beads, which have a diameter that is 60-80% of the inner

diameter of the tube; the single bead string reactor (SBSR) was born. The liquid must travel a tortuous path through the reactor. Mixing is enhanced, while dispersion is about ten times smaller than in open tubing of the same dimensions. Wide use of such packed tubes is expected in future FI research.

Since tiny, porous glass beads had been used as carriers for enzymes in the past, it was expected that larger, non-porous glass beads would also prove to be good carriers. Once immobilized on the beads, the enzyme could be packed into a tube and used in a flow-injection instrument. The advantages of immobilized enzymes and SBSRs would be combined to yield a powerful technique. Jim Litch tested this method during an undergraduate research project.

The immobilization procedure is listed in Table 5.1 and follows the same concepts as described for glass tubing. The treatment was easier to perform, since most of the reactions occurred in a beaker, and the beads were easier to handle than the tubing. The beads acquired a red color due to the reaction between the glutaraldehyde and the amine group on the glass; this is a sign of a successful activation step. A diagram of the completed reactor is shown in Figure 5.1. A large overall reaction rate is promoted by the rapid mixing and the intimate contact between the enzyme and the bulk solution.

Table 5.1. Immobilization Procedure for Glass Beads

	Step	Reagent	Time	Temp. (°C)
1.	Cleaning	Chromic Acid 6 M HCl Distilled water Acetone	15 min. 10 min. 10 min. 10 min.	23 23 23 23
		Dry with N ₂		
2.	Whisker formation	5% w/v solution of NH ₄ F-HF in methanol	1 hour	23
		Dry with N ₂		
		Apply heat	3 hours	450
3.	Silanate	2% acetone solution of 3-aminopropyl-triethoxysilane	30 min.	23
		-Decant excess		
		Apply heat	24 hours	90
4.	Enzyme	1% glutaraldehyde in pH 8.0 buffer	30 min.	23
		5 mg/mL solution of glucose oxidase in pH 6.85 buffer	24 hours	4

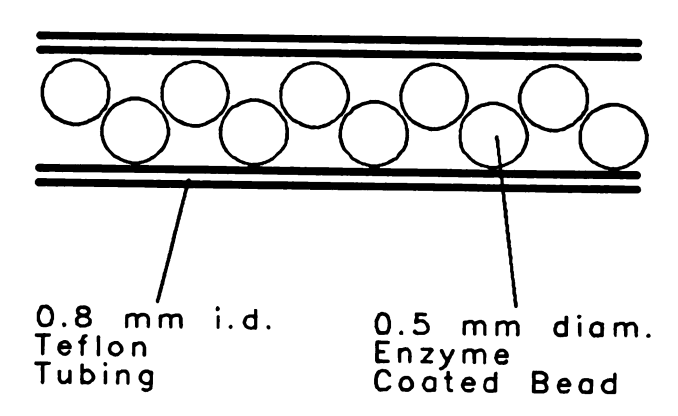


Figure 5.1. View of the immobilized enzyme single bead string reactor.

The continuous flow instrument described in Chapter 4 was modified to include a different manifold and to omit the bubble-gate. The manifold that was used is shown in Figure 5.2. A four-way slider valve (Altex), pneumatically actuated, and controlled by a ZX81 microcomputer (Sinclair) interfaced with a relay board (Byte-Back), was at the heart of the system. In position 1, the carrier stream (Trinder/peroxidase reagent) was pumped through the valve and SBSR. In position 2, the sample (glucose) was pumped into the system. The volume of glucose injected was determined by the pump speed and the time the valve spent in position 2.

Sample volume = (Pump speed)(Valve time) (5.1)

Each experiment included one cycle of the valve.

The valve times were controlled by ZX81 software so that the sample volume could be varied reproducibly over a wide range. In such systems, mixing only occurs at the leading edge of the sample zone until the valve is returned to position 1. Thus, mixing between reagents and sample in this design may differ from more common FI instruments which employ a 6-way valve and a sample loop.

The analytical and color-forming reactions occurred simultaneously inside the reactor. Results indicated that the indicator reaction was much faster than the glucose oxidase reaction. This is necessary for a useful determination. All the reagents were prepared as described in

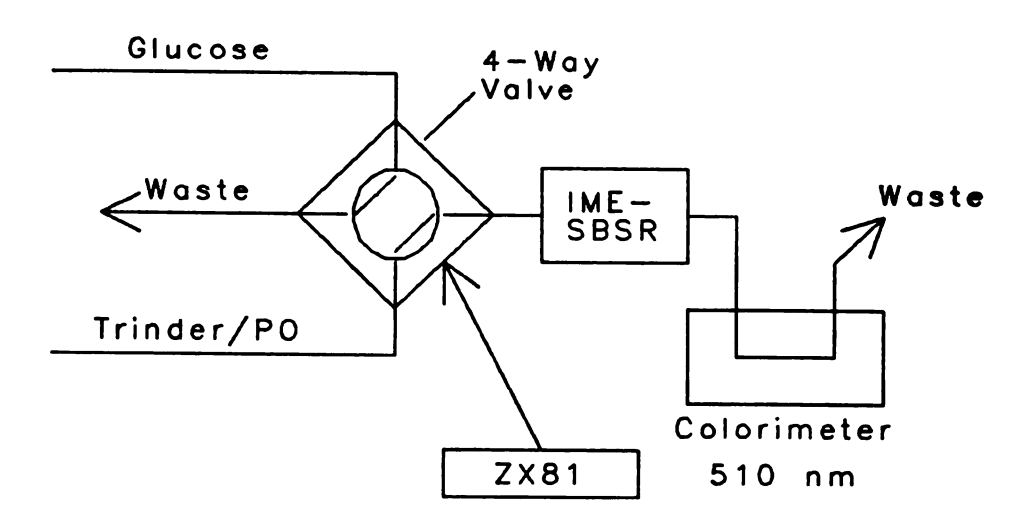


Figure 5.2. Schematic diagram of the flow-injection instrument.

Chapter 4. The reactor was 21 cm in length and had an internal diameter of 0.8 mm. If the beads take up 30% of the total reactor volume, the void volume of the reactor was about 75 μL .

The sample volume was varied at four different flow rates. When large sample volumes were used, two peaks often resulted from a single sample injection. The reason for this was incomplete mixing; the reaction occurred at both ends of the sample slug, but the reagents never reached the center of the slug. The two peaks varied as to which was the higher, but in all cases the heights were within 25% of each other. Large volumes were desirable because increased instrumental output resulted. However, if the sample volume was too large double peaks occurred. The optimal sample volume for the system was found by plotting the volume between the double peaks versus the sample volume. The x-intercept, the point where only a single peak is produced, should be the optimal volume. Figure 5.3 shows the interesting results. The curves for the four pump speed settings all follow nearly the same line. This is evidence that mixing in a SBSR is independent of flow rate and residence time. The optimal volume was about 45 μ L. In practice, however, sample volumes up to 65 µL did not give perceptible double peaks.

Four glucose standards were each sampled for five

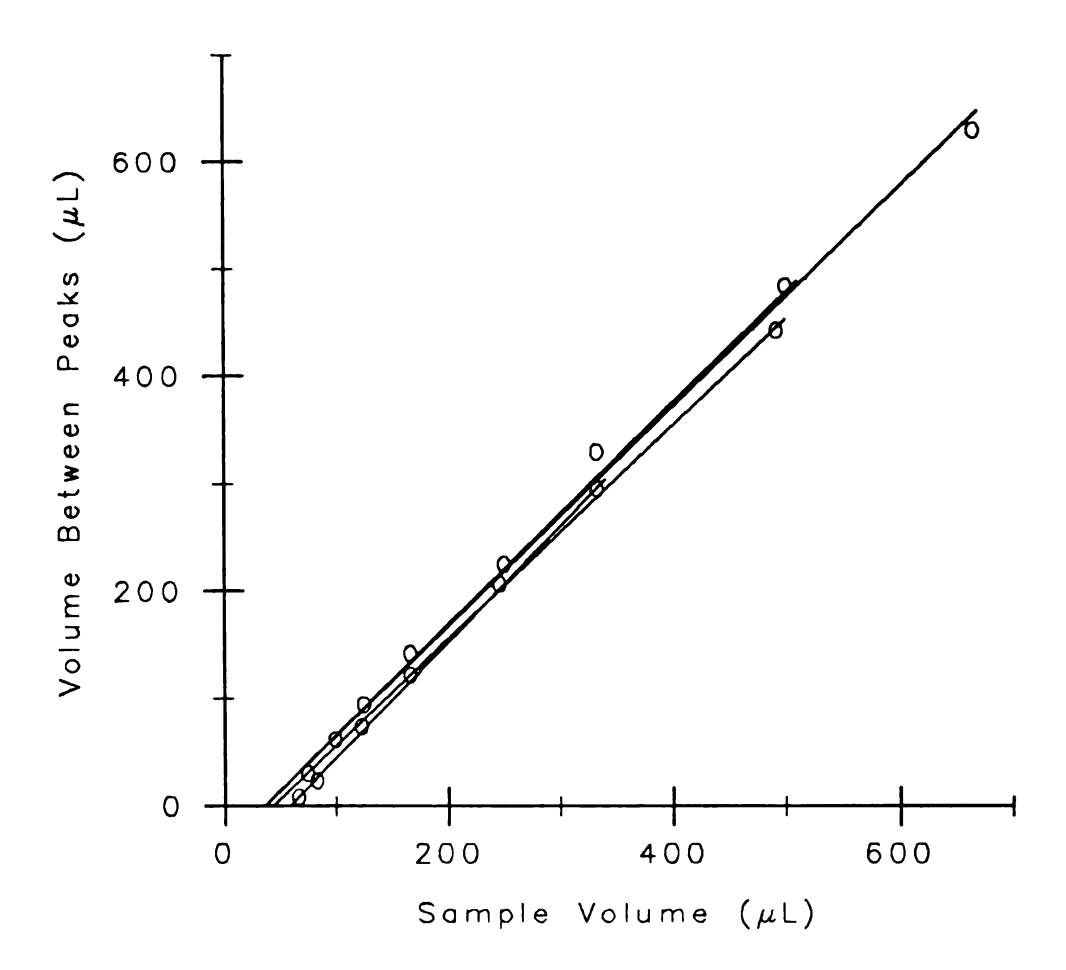


Figure 5.3. The degree of incomplete mixing at various sample volumes. Four pump speeds were used: 8.3, 12.3, 25.0, and 33.3 $\mu L/sec.$

seconds at a flow rate of 12.3 μ L/sec. The residence time in the enzyme reactor was about 6 seconds. The instrumental output is shown in Figure 5.4. The average relative standard deviation of the results was less than 2%. A calibration curve is shown in Figure 5.5. The results were very good; the correlation coefficient was 0.99994. The use of this method for the determination of glucose looks promising. With further optimization, the sample throughput should be increased from the current value of 60 samples/hour. Many other substrates could be determined in this way, using other enzymes.

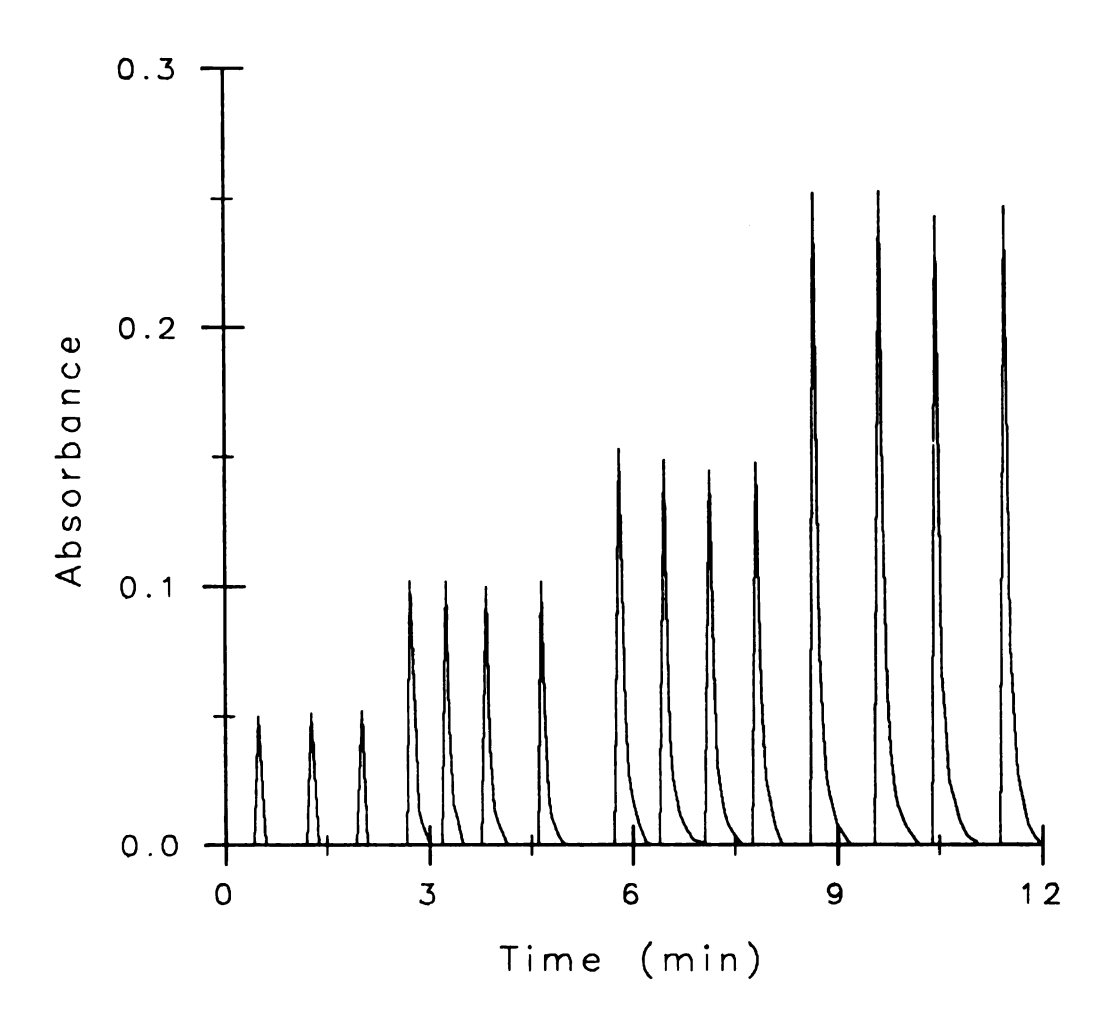


Figure 5.4. Flow-injection instrumental response.
The four glucose concentrations were:
0.44 (A), 0.88 (B), 1.33 (C), and 2.22 (D) mM.

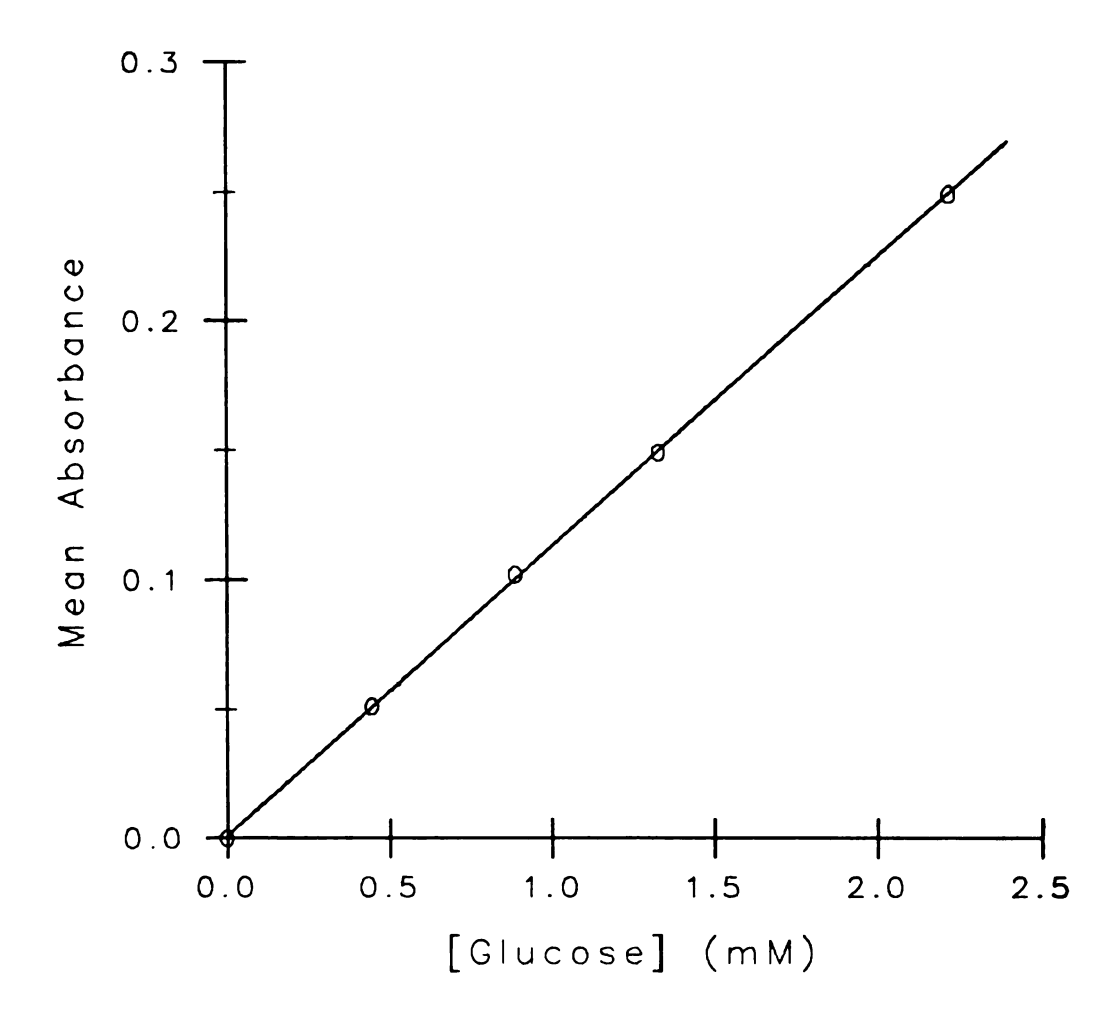


Figure 5.5. Calibration curve for the flow-injection determination of glucose.

CHAPTER 6

Future Plans

The use of open-tubular immobilized enzyme reactors in flowing systems continues to grow, and more research is needed to characterize such systems. A few of my ideas for future research in this area are presented below. I plan to continue some portions of my doctoral research, and, hopefully, others at Michigan State will spend their time working with immobilized enzymes.

- 1) Fast immobilization procedure for nylon. The current procedure for bonding enzymes to nylon takes about 1.5 days. The duration of the procedure might be shortened without adversely affecting the enzyme atachment. A three-hour or less immobilization treatment would be advantageous for undergraduate research and teaching laboratory experiments. It is known that most of the enzyme bonds to the activiated nylon within the first ten minutes of reaction. Thus, the reduction of the procedure in terms of time is feasible.
- 2) Properties of bi-enzyme systems. Many determinations involve two or more enzyme-catalyzed reactions. It would be helpful to know how each enzyme affects the attachment of the other. The studies presented in Chapter 4, Section E, suggested that the secondary enzyme, catalase, did not significantly disturb the bonding of the primary enzyme,

glucose oxidase. The properties of bi-enzyme systems should be studied in more detail.

- 3) Properties of immobilized enzymes in continuous flow systems. Immobilized glucose oxidase reactors have been fully characterized for use in a continuous flow instrument. Other enzymes could be incorporated into the CF manifold, and their properties could be studied. After several enzyme systems have been tested in this fashion, general conclusions about the characteristics of OTIMERs in continuous flow systems can be drawn.
- 4) Fundamental studies of the influence of molecular diffusion on immobilized enzyme kinetics. The stopped-flow instrument described in Chapter 3 may prove to be a very powerful tool in probing the interaction of diffusion and immobilized enzyme kinetics. By changing the reactor parameters and measuring the reaction rates, a mathematical description of such systems should be possible to derive. Subsequently, the inherent enzyme properties could be calculated from the measured apparent properties. This project deserves a lot of attention.
- 5) Immobilized enzyme bead string reactor. Very fast and sensitive clinical determinations may be possible with the use of enzyme-coated glass beads packed into a Teflon tube. Flow-injection determinations using such reactors show

great promise and can be expanded for use with highly active enzymes, other than glucose oxidase. The experimental design would be similar to that described in Chapter 5.



APPENDIX A

Derivation of Diffusion-control Rate Equation

Model: 1) Circular tube of radius, r

- 2) Substrate reacts at the reactor wall very fast to form product.
- 3) A radial concentration gradient in substrate and product is established.
- 4) Substrate diffuses toward reactor wall.
- 5) Product diffusing away from reactor wall.

[S] = [S]_b for 0<x<r at t=0,
where x is the distance from the</pre> Initial condition:

center of the reactor.

Boundary condition: [S] = 0 for x=r at t>0.

Diffusion equation: $\partial[S]/\partial t = D(\partial^2[S]/\partial x^2 + (\partial[S]/\partial x)/x)$

Final result: [P] = $[S]_b(1-4\sum_{s=1}^{3}(\exp(-Dtj_s^2/r^2))/j_s^2)$

APPENDIX B

Derivation of the Absorbance of a Solution with a Radial Concentration Gradient

- Model: 1) Reaction solution is axially uniform.
 - 2) The concentration gradient is radially symmetric.
 - 3) The concentration gradient does not change with time (steady-state conditions).
 - 4) The gradient is linear (d[P]/dx = constant).
 - 5) The product is the absorbing species.
 - 6) Light traverses the reactor parallel to the axis.

Considering a slice of solution from the center of the tube to the reactor wall:

Absorbance = $\varepsilon L[P]$

$$[P] = \left(\int_{0}^{\sigma} ([P]_{w} - ([P]_{w} - [P]_{b})x/\sigma \right) dx + \int_{0}^{r} [P]_{b} dx / r$$

where x is the distance from the center of the reactor, σ is the diffusion layer thickness, and where r is the reactor radius.

Integrating the above equation and combing terms:

[P] =
$$\sigma/2r([P]_w-[P]_b) + [P]_b$$

Thus, Absorbance = $\varepsilon L([P]_b + \sigma/2r([P]_w-[P]_b))$

Case 1: No enzyme reaction (common absorbance measurement)

$$[P]_{w} = [P]_{b}$$
 and Absorbance = $\varepsilon L[P]_{b}$

Case 2: Start of enzyme reaction

$$[P]_{h} = 0$$
 and Absorbance = $\varepsilon L[P]_{w}(\sigma/2r)$



LIST OF REFERENCES

- 1. W.B. Furman, editor, Continuous Flow Analysis: Theory and Practice, Marcel Dekker, NY (1976).
- 2. L.R. Snyder, J. Levine, R. Stoy, and A. Conetta, Anal. Chem. 48, 942A (1976).
- 3. L.R. Snyder, J. Chromatog. 125, 287 (1976).
- 4. J. Ruzicka and E.H. Hansen, Chemtech 9, 756 (1979).
- 5. J. Ruzicka and E.H. Hansen, Flow Injection Analysis, John Wiley and Sons, NY (1981).
- 6. D. Betteridge, Anal. Chem. 50, 832A (1978).
- 7. B. Chance, J. Franklin Inst. 229, 455 (1940).
- 8. S.R. Crouch, F.J. Holler, P.K. Notz, and P.M. Beckwith, Appl. Spec. Rev. <u>13</u>, 165 (1977).
- 9. E.T. Gray and H.J. Workman, J. Chem. Ed. 57, 752 (1980).
- 10. P.W. Carr and L.D. Bowers, <u>Immobilized Enzymes in Analytical and Clinical Chemistry</u>, John Wiley and Sons, NY (1980).
- 11. M.D. Trevan, <u>Immobilized</u> <u>Enzymes</u>, John Wiley and Sons, NY (1980).
- 12. I. Chibata, editor, <u>Immobilized Enzymes</u>, <u>Research and Development</u>, John Wiley and Sons, NY (1980).
- 13. T.M.S. Chang, <u>Immobilized Enzymes</u> and <u>Proteins</u>, Volumes 1 and 2, Plenum Press, NY (1977)
- 14. L.B. Wingard, E. Katchalski-Katzir, and L. Goldstein, editors, Applied Biochemistry and Bioengineering, Volume 1, Academic Press, NY (1976).
- 15. H.H. Weetall, editor, <u>Immobilized Enzymes</u>, <u>Antigens</u>, <u>Antibodies</u>, <u>and Peptides</u>, <u>Marcel Dekker</u>, NY (1975).

- 16. R.A. Messing, editor, <u>Immobilized Enzymes</u> for <u>Industrial Reactors</u>, Academic Press, NY (1975).
- 17. M. Salmona, C. Saronio, and S. Garattini, <u>Insolubilized Enzymes</u>, Raven Press, NY (1974).
- 18. O. Zaborsky, <u>Immobilized</u> <u>Enzymes</u>, CRC Press, Cleveland (1973).
- 19. S. Aiba, A.E. Humphrey, and N.F. Millis, <u>Biochemical</u> Engineering, Academic Press, NY (1973), pp 393-416.
- 20. L.B. Wingard, Enzyme Engineering, John Wiley and Sons, NY (1972), pp 177-400.
- 21. L.D. Bowers, Trends Anal. Chem. 1, 191 (1982).
- 22. L.D. Bowers and P.W. Carr, Adv. Biochem. Eng. <u>15</u>, 89 (1980).
- 23. L.D. Bowers and P.W. Carr, Anal. Chem. 48, 544A (1976).
- 24. H.H. Weetall, Anal. Chem. 46,602A (1974).
- 25. L.B. Wingard, Adv. Biochem. Eng. 2, 1 (1972).
- 26. G.G. Birch, N. Blakebrough, and K.J. Parker, <u>Enzymes</u> and <u>Food</u> <u>Processing</u>, Applied Science Publishers, London (1981).
- 27. L.B. Wingard, E. Katchalski-Katzir, and L. Goldstein, Applied Biochemistry and Bioengineering, Volume 2, Academic Press, NY (1979).
- 28. S. Kindel, Technology 1, 62 (1981).
- 29. K.J. Skinner, Chem. Eng. News, August 18,1975, 22.
- 30. C.R. Martin, Trends Anal. Chem. 1, 175 (1982).
- 31. G.G. Guilbault and M.H. Sadar, Acc. Chem. Res. 12, 344 (1979).
- 32. G.G. Guilbault and M.H. Sadar, Proc. Analyt. Div. Chem. Soc., October 1977, 302.
- 33. W.J. Blaedel and R.C. Engstrom, Anal. Chem. 52, 1691 (1980).

- 34. F. Scheller and D. Pfeiffer, Anal. Chim. Acta 117, 383 (1980).
- 35. W.J. Blaedel and J. Wang, Anal. Chem. 52, 1426 (1980).
- 36. R.M. Ianniello and A.M. Yacynych, Anal. Chim. Acta 131, 123 (1981).
- 37. R. Renneberg, D. Pfeiffer, F. Scheller, and M. Janchen, Anal. Chim. Acta 134, 359 (1982).
- 38. E.L. Gulberg and G.D. Christian, Anal. Chim. Acta 123, 125 (1981).
- 39. W. Hinsch and P.V. Sundaram, Fres. Z. Anal. Chem. 309, 25 (1981).
- 40. M. Mascini and G. Palleschi, Anal. Chim. Acta 136, 69 (1982).
- 41. W. Hinsch, W.-D. Edersbach, and P.V. Sundaram, Clin. Chim. Acta 104, 95 (1980).
- 42. W. Hinsch and P.V. Sundaram, Clin. Chim. Acta 104, 87 (1980).
- 43. B. Danielsson, B. Mattiasson, and K. Mosbach, Pure Appl. Chem. 51, 1443 (1979).
- 44. C. Spink, CRC Critical Rev. Anal. Chem. 9, 1 (1980).
- 45. R.S. Schifreen, D.A. Hanna, L.D. Bowers, and P.W. Carr, Anal. Chem. 49, 1929 (1977).
- 46. A.O. Lindberg, Anal. Chim. Acta 131, 133 (1981).
- 47. A.S. Attiyat and G.D. Christian 105, 154 (1980).
- 48. C.-H. Kiang, S.S. Kuan, and G.G. Guilbault, Anal. Chem. 50, 1319 (1978).
- 49. J.-C. Kaun, S.S. Kuan, and G.G. Guilbault, Anal. Chim. Acta 100, 229 (1978).
- 50. P.V. Sundaram and S. Jarayaman, Clin. Chim. Acta 94, 309 (1979).
- 51. O.R. Zaborsky and J. Ogletree, Biochem. Biophys. Res. Comm. 61, 210 (1974).

- 52. D.J. Inmann and W.E. Hornby, Biochem. J. $\underline{129}$, 255 (1972).
- 53. D.L. Morris, J. Campbell, and W.E. Hornby, Biochem. J. 147, 539 (1975).
- 54. P.V. Sundaram, Biochem. J. 183, 445 (1979).
- 55. P.V. Sundaram and D.K. Apps, Biochem. J. <u>161</u>, 441 (1977).
- 56. P.V. Sundaram and M.P. Igloi, Clin. Chim. Acta 94, 295 (1979).
- 57. F.N. Onyezili and A.C. Onitiri, Anal. Biochem. 113, 203 (1981).
- 58. G.A. Noy, A. Buckle, and K. Alberti, Clin. Chim. Acta 89, 135 (1978).
- 59. F.N. Onyezili and A.C. Onitiri, Anal. Biochem. 117, 121 (1981).
- 60. J. Campbell, W.E. Hornby, and D.L. Morris, Biochim. Biophys. Acta 384, 307 (1975).
- 61. V. Toome, S. DeBernardo, K. Manhart, and M. Weigele, Anal. Lett. $\underline{7}$, 437 (1974).
- 62. W.-T. Law and S.R. Crouch, Anal. Lett. $\underline{13}$, 1115 (1980).
- 63. O. Warburg and W. Christian, Biochem. Z. 310, 384 (1941).
- 64. P.D. Boyer, editor, The Enzymes, Academic Press, NY.
- 65. M. Dixon and E.C. Webb, <u>Enzymes</u>, Academic Press, NY (1964).
- 66. J.B. Sumner and G.F. Somers, Chemistry and Methods of Enzymes, Academic Press, NY (1953).
- 67. K.J. Laidler and P.S. Bunting, The Chemical Kinetics of Enzyme Action, Clarendon Press, Oxford, England (1973), p 398.
- 68. E.W. Wharton, E.M. Crook, and K. Brocklehurst, Eur. J. Biochem. 6, 572 (1968).

- 69. W.E. Hornby, M.D. Lilly, and E.M. Crook, Biochem. J. 98, 420 (1966).
- 70. J.-M. Engasser and C. Horvath, Applied Biochemistry and Bioengineering, Volume 1, Academic Press, NY (1976), pp 146-149.
- 71. G.P. Royer, <u>Immobilized Enzymes</u>, <u>Antigens</u>, <u>Antibodies</u>, and Peptides, Marcel Dekker, NY (1975), pp 66-68.
- 72. J.-M. Engasser and P.Hisland, Biochem. J. $\underline{173}$, 314 (1978).
- 73. J.-M. Engasser, P.R. Coulet, and D.C. Gautheron, J. Biol. Chem. 252, 7919 (1977).
- 74. I.C. Cho and H. Swaisgood, Biochim. Biophys. Acta 334, 243 (1974).
- 75. P. Nitisewojo and H.O. Hultin, Eur. J. Biochem. 67, 87 (1976).
- 76. N.L. Smith and H.M. Lenhoff, Anal. Biochem. <u>61</u>, 392 (1974).
- 77. K.J. Laidler and P.S. Bunting, Meth. Enzymol. $\underline{64}$, 227 (1980).
- 78. T. Kobayashi and K.J. Laidler, Biotech. Bioeng. 16, 99 (1974).
- 79. N.J. Daka and K.J. Laidler, Can. J. Biochem. $\underline{56}$, 774 (1978).
- 80. N.J. Daka and K.J. Laidler, Biochim. Biophys. Acta 612, 305 (1980).
- 81. Advances in Automated Analysis, Technicon International Congress 1976, Volume 1, Mediad Inc., Tarrytown, NY (1977).
- 82. L.R. Snyder and H.J. Adler, Anal. Chem. 48, 1017 (1976).
- 83. L.R. Snyder and H.J. Adler, Anal. Chem. 48, 1022 (1976).
- 84. S. Morgenstern, Advances in Automated Analysis, Volume 1, Therman Assoc., Miami (1971), p 85.

- 85. M.D. Joseph, D.J. Kasprazak, and S.R. Crouch, Clin. Chem. 23, 1033 (1977).
- 86. D.R. Christmann, S.R. Crouch, and A. Timnick, Anal. Chem. 53, 276 (1981).
- 87. P.D. Boyer, editor, The Enzymes, Volume XI, Academic Press, NY (1975), pp 289-292.
- 88. J.R. Florini and C.S. Vestling, Biochim. Biophys. Acta 25, 575 (1957).
- 89. H.L. Pardue, Advances in Analytical Chemistry and Instrumentation, Volume 7, John Wiley and Sons, NY (1968), pp 141-207.
- 90. P. Trinder, Ann. Clin. Biochem. 6, 24 (1969).
- 91. D. Barham and P. Trinder, Analyst 97, 142 (1972).
- 92. N.W. Tietz, <u>Fundamentals</u> of <u>Clinical</u> <u>Chemistry</u>, W.B. Saunders, Philadelphia (1976), p 1213.
- 93. R.H. White-Stevens, Clin. Chem. 28, 578 (1982).
- 94. J.A. Lott and K. Turner, Clin. Chem. $\underline{21}$, 1754 (1975).
- 95. N.W. Tietz, editor, <u>Fundamentals of Clinical Chemistry</u>, W.B. Saunders, Philadelphia (1976), pp 234-263.
- 96. F. Gram, J.A. Hveding, and A. Reine, Acta Chem. Scand. <u>27</u>, 616 (1973).
- 97. E.N. Drake and C.E. Brown, J. Chem. Ed. 54, 124 (1977).
- 98. J. Okuda and I. Miwa, Anal. Biochem. 39, 387 (1971).
- 99. A.S. Kaston and R. Brandt, Anal. Biochem. $\underline{6}$, 461 (1963).
- 100. P.V. Sundaram, B. Blumemberg, and W. Hinsch, Clin. Chem. 25, 1436 (1979).
- 101. L.P. Leon, M. Sansur, L.R. Snyder, and C. Horvath, Clin. Chem. 23, 1556 (1977).
- 102. L. Gorton and K.A. Bhatti, Anal. Chim. Acta $\underline{105}$, 43 (1979).

- 103. Sigma Chemical Company Catalog, 1982 edition.
- 104. D.L. Williams, A.R. Doig, and A. Korosi, Anal. Chem. 42, 118 (1970).
- 105. M. Koyama, Y. Sato, M. Aizawa, and S. Suzuki, Anal. Chim. Acta 116, 307 (1980).
- 106. T. Osaki, Biotech. Bioeng. 22, 1287 (1980).
- 107. G.J. Lubrano and G.G. Guilbault, Anal. Chim. Acta 97, 229 (1978).
- 108. B. Watson, D.N. Stifel, and F.E. Semersky, Anal. Chim. Acta $\underline{106}$, 233 (1979).
- 109. G. Sittampalam and G.S. Wilson, J. Chem. Ed. $\underline{59}$, 70 (1982).
- 110. D.C. Williams, G.F. Huff, and W.R. Seitz, Clin. Chem. 22, 372 (1976).
- 111. J.N. Miller, B.F. Rocks, and D.T. Burns, Anal. Chim. Acta 93, 353 (1977).
- 112. L.B. McGowan, B.J. Kirst, and G.L. LaRowe, Anal. Chim. Acta 117, 363 (1980).
- 113. F. Heinz and T.W. Beuhausen, J. Clin. Chem. Clin. Biochem. 19, 977 (1981).
- 114. R. Chirillo, G. Caenaro, B. Pavan, and A. Pin, Clin. Chem. 25, 1744 (1979).
- 115. J. Ziegenhorn, U. Neumann, A. Hagen, W. Bablok, and K. Stinshoff, J. Clin. Chem. Clin. Biochem. <u>15</u>, 13 (1977).
- 116. American Research Products Company, bulletin.
- 117. L.G. Morin and J. Prox, Clin. Chem. $\underline{19}$, 959 (1973).
- 118. R.H. White-Stevens and L.R. Stover, Clin. Chem. 28, 589 (1982).
- 119. N. Gochman and J.M. Schmitz, Clin. Chem. <u>18</u>, 943 (1972).

- 120. L.P. Leon, S. Narayanan, R. Dellenbach, and C. Horvath, Clin. Chem. 22, 1017 (1976).
- 121. A.T. Romano, Clin. Chem. 19, 1152 (1973).
- 122. C. Matsubura, K. Ishii, and K. Takamura, Microchem. J. 26, 242 (1981).
- 123. K. Tamaoku, Y. Murao, K. Akiura, and Y. Ohkura, Anal. Chim. Acta 136, 121 (1982).
- 124. I. Seigo, Eisei Kensa 28, 760 (1979).
- 125. J.D. Artiss, R.J. Thibert, J.M. McIntosh, and B. Zak, Microchem. J. 26, 487 (1981).
- 126. D. Keilin and E.F. Hartree, Biochem. 50, 331 (1952).
- 127. D. Keilin and E.F. Hartree, Biochem. 42, 221 (1948).
- 128. R. Bentley, Meth. Enzymol. 1, 340 (1955).
- 129. V. Linek, P. Benes, J. Sinkule, O. Holecek, and V. Maly, Biotech. Bioeng. 22, 2515 (1980).
- 130. S. Gondo, T. Osaki, and M. Morishita, J. Mol. Cat. 12, 365 (1981).
- 131. P.F. Greenfield, J.R. Kittrell, and R.L. Laurence, Anal. Biochem. 65, 109 (1975).
- 132. B.C. Saunders, A.G. Holmes-Siedle, and B.P. Stark, <u>Peroxidase</u>, Butterworths, Washington, D.C. (1964).
- 133. A.C. Maehly, Meth. Enzymol. 2, 801 (1955).
- 134. I.M. Kolthoff, E.B. Sandell, E.J. Meehan, and S. Bruchenstein, Quantitative Chemical Analysis, The MacMillan Co., NY (1969), p 854.
- 135. C.J. Patton, M. Rabb, and S.R. Crouch, Anal. Chem. 54, 1113 (1982).
- 136. S. Klose, M. Sholtz, E. Munz, and R. Portenhauser, Clin. Chem. 24, 250 (1978).
- 137. F. Zoppi and D. Fenili, Clin. Chem. $\underline{26}$, 1229 (1980).

- 138. N.W. Teitz, editor, <u>Fundamentals of Clinical Chemistry</u>, W.B. Saunders, Philadelphia (1976) p 254.
- 139. Y. Malpiece, M. Sharan, J.-N. Barbotin, P. Personne, and D. Thomas, J. Biol. Chem. 225, 6883 (1980).
- 140. C. Horvath, B.A. Solomon, and J.-M. Engasser, Ind. Eng. Chem. Fundam. 12, 431 (1973).
- 141. R.Q. Thompson, C.J. Patton, and S.R. Crouch, Clin. Chem. 28, 556 (1982).
- 142. G.R. Schonbaum and B. Chance, The Enzymes, Volume 13, Academic Press, NY (1976), pp 363-408.
- 143. D. Keilin and P. Nicholls, Biochim. Biophys. Acta 29, 302 (1958).
- 144. P. Nicholls and G.R. Schonbaum, <u>The Enzymes</u>, Volume 8, Academic Press, NY (1963), pp 147-225.
- 145. M. Dixon, Biochem. J. 55, 170 (1953).
- 146. I.H. Segel, Enzyme Kinetics, John Wiley and Sons, NY (1975), pp 170-203.
- 147. A. Iob and H.A. Motolla, Clin. Chem. 27, 195 (1981).
- 148. F.I. Onuska, M.E. Comba, T. Bistricki, and R.J. Wilkinson, J. Chrom. 142, 117 (1977).
- 149. H.H. Weetall, Science 166, 616 (1969).
- 150. P.J. Robinson, P. Dunnill, and M.D. Lilly, Biochim. Biophys. Acta 242, 659 (1971).
- 151. W.E. van der Linden, Trends Anal. Chem. $\underline{1}$, 188 (1982).
- 152. J.M. Reijn, W.E. van der Linden, and H. Poppe, Anal. Chim. Acta <u>123</u>, 229 (1981).

